People's Democratic Republic of Algeria
Ministry of Higher Education and Scientific Research

Ahmed Zabana University of Relizane
Faculty of Natural and Life Sciences
Department of Biological Sciences

PhD THESIS LMD, 3rd Cycle

Field: Biological Sciences

Speciality: Applied Biochemistry

Thesis title

Phytochemical exploration of halophytic plants and valorization for the formulation of a bioinsecticide

Presented and publicly defended by
Ms. *TABOURI Mounira*

Before the jury members composed of

President	Mr. BENAISSA Miloud	MCA	University of Relizane
Supervisor	Mr. DJELLOULI Mustapha	MCA	University of Relizane
Co-Supervisor	Ms. BELKHEIR Khadidja	MCA	University of Relizane
Examiner	Mr. BENABDERRAHMANE Mokhtar	Pr	University of Sidi Bel Abbès
Examiner	Mr. BENSAHLA TALET Lotfi	Pr	University of Oran
Examiner	Ms. OUCIF Hanane	MCA	University of Relizane

University year
2025-2026

Dedication

In the name of Allah, the Most Gracious, the Most Merciful.

I dedicate this humble work to the most precious people in my life, with all my love and gratitude.

To my beloved father, ***Abed****, and my dearest mother,* ***Yamina,*** *the greatest blessings in my life. Their unconditional love, endless sacrifices, sincere prayers, and constant support have been the light that guided my journey. No words can fully express the depth of my gratitude and love for them.*

To my beloved sisters and brother, ***Samira, Marwa, and Abdellah****, always present with love, care, and encouragement.*

To my dear fiancé, ***Bendjebbar Abdelaziz,*** *my source of strength, support, and motivation, whose patience, encouragement, and belief in me have made this journey easier and more meaningful.*

To my respected uncle and aunts, ***Abdelkader, El Hadj, Zoubida, Kheira, and Fatima****, with deep respect and gratitude.*

To the families ***Tabouri, Benadjemia, and Bendjebbar****, in appreciation of their kindness, support, and sincere wishes.*

Mounira….



Acknowledgements

First and foremost, I would like to express my deepest gratitude and sincere appreciation to my supervisor, Mr. **DJELLOULI Mustapha**, and my co-supervisor, Mrs. **BELKHEIR Khadija**, Associate Professors (Class A) at the University of Relizane, for accepting to supervise this work. I am particularly grateful for their availability, invaluable guidance, continuous support, despite their numerous academic and professional responsibilities and the confidence they placed in me throughout this study.

I would also like to extend my sincere thanks to the honorable members of the jury

Mr. **BENAISSA Miloud**, MCA at Relizane University

Ms. **OUCIF Hanane**, MCA at Relizane University

Mr. **BENABDERRAHMANE Mokhtar**, Pr at Sidi Bel Abbès University

Mr. **BENSAHLA TALET Lotfi**, Pr at Oran University

for kindly accepting to examine and evaluate this work.

My sincere gratitude is extended to Mr. **ELANDALLOUSSI Elhadj**, Head of the Laboratory of Environment and Sustainable Development, University of Relizane.

My sincere gratitude is extended to Professor **NEMMICHE Saïd**, Abdelhamid Ibn Badis University, Mostaganem, for his valuable scientific support and encouragement.

I would like to express my heartfelt thanks to Mrs. **MOSCOSO-RUIZ Inmaculada**, Mrs. **CEA-PAVEZ, Inés** and Mr. **VERARDO Vito** from the CIDAF, Spain, for their collaboration and scientific contribution.

Special thanks are due to Mr. **BENOTMANE Kamel**, Ph.D. student at Relizane University, for his valuable assistance and support in carrying out this work.

I would also like to thank Mrs. **LAREF** Nora, at the University of Relizane,

My sincere appreciation is also extended to Mrs. **SEBAHI Kheira**, and Mr**. NAHAL Omar** for their administrative assistance and for facilitating the completion of the procedures related to this work.

I would like also to express my sincere gratitude to all the members of the **Doctoral Promotion 2022/2023**, especially **MERABTI Aicha** and **DAHOUN Meriem**

Finally, I would like to thank everyone who contributed, directly or indirectly, to the completion of this study and supported me throughout this academic journey.

Abstract

This study aimed to investigate the phytochemical profile and evaluate the antioxidant and insecticidal activities of leaf methanolic extracts from three Algerian halophytes: *Atriplex halimus*, *Limbarda crithmoides*, and *Suaeda fruticosa*.

Phytochemical screening was conducted to detect major secondary metabolites, along with the quantification of total phenolic, flavonoid, and tannin contents using the Folin–Ciocalteu, aluminum chloride, and vanillin assays, respectively. ATR-FTIR spectroscopy was used to identify functional groups, while HPLC-ESI-QTOF-MS analysis provided a detailed characterization of the phytochemical constituents. Antioxidant activity was evaluated using DPPH, ABTS, and FRAP assays. Insecticidal activity was assessed through direct contact bioassays at four concentrations (25, 50, 100, and 200 mg/mL) against *Tribolium confusum*, as well as repellency and plant powder toxicity tests. Finally, molecular docking studies targeting acetylcholinesterase (AChE) were performed to identify potential bioactive compounds responsible for the observed biocidal effects.

The phytochemical screening results revealed the presence of major bioactive constituents in all extracts, while FTIR analysis confirmed their characteristic functional groups. *S. fruticosa* exhibited the highest levels of total phenolics and tannins (119.33 ± 7.24 mg GAE/g DW and 4.51 ± 0.09 mg CE/g DW, respectively), whereas *A. halimus* showed the highest flavonoid content (73.07 ± 0.19 mg QE/g DW), and *L. crithmoides* recorded the lowest values.

These results were consistent with the observed antioxidant and insecticidal activities. Indeed, *S. fruticosa* showed the strongest antioxidant activity, with the lowest IC_{50} values for DPPH (0.48 ± 0.001 mg/mL) and ABTS (1.03 ± 0.006 mg/mL), as well as the highest FRAP value (2130.96 ± 2.55 µmol Fe^{2+}/g DW), followed by *A. halimus* and *L. crithmoides*. Similarly, insecticidal assays revealed the lowest LC_{50} value (50.03 ± 12.65 mg/mL after 96 h of treatment) compared with *A. halimus* (84.73 ± 0.00 mg/mL) and *L. crithmoides* (88.86 ± 17.52 mg/mL).

HPLC-ESI-QTOF-MS analysis in negative ion mode led to the identification of 24, 27, and 29 bioactive constituents in *A. halimus*, *L. crithmoides*, and *S. fruticosa*, respectively, including compounds such as kaempferol 3-O-rutinoside-7-O-glucoside, naringin, feruloyltyramine, rutin, dicaffeoylquinic acid, quercetin 3-O-glucoside, chlorogenic acid, and 3-O-feruloylquinic acid. Molecular docking studies further showed that these compounds exhibited strong binding affinity toward insect acetylcholinesterase (AChE).

Keywords: Halophytes, *Atriplex halimus*, *Limbarda crithmoides*, *Suaeda fruticosa*, phytochemical profile, antioxidant activity, insecticidal activity, *Tribolium confusum.*

ملخص

هدفت هذه الدراسة إلى استكشاف الملف الكيميائي النباتي وتقييم النشاط المضاد للأكسدة والنشاط المبيد للحشرات للمستخلصات الميثانولية لأوراق ثلاثة نباتات ملحية جزائرية، وهي *Atriplex halimus, Limbarda crithmoides,* *Sueada fruticosa.*

أُجري الفحص الكيميائي النباتي للكشف عن أهم المستقلبات الثانوية، إلى جانب تقدير المحتويات الكلية للفينولات والفلافونويدات والتانينات باستخدام اختبارات فولين–سيوكالتو، وكلوريد الألومنيوم، والفانيلين، على التوالي. كما استُخدمت تقنية التحليل الطيفي بالأشعة تحت الحمراء بتحويل فورييه باستخدام الانعكاس الكلي الموهّن (ATR-FTIR) لتحديد المجموعات الوظيفية، في حين أتاح التحليل باستخدام كروماتوغرافيا السائل عالية الأداء المقترنة بمطياف الكتلة ذي التأين بالرش الكهربائي ومحلل زمن الطيران (HPLC-ESI-QTOF-MS) توصيفًا تفصيليًا للمكونات الكيميائية النباتية. وقُيّم النشاط المضاد للأكسدة باستخدام اختبارات DPPH و ABTSو .FRAPأما النشاط المبيد للحشرات، فقد جرى تقييمه من خلال اختبارات التلامس المباشر عند أربعة تراكيز (25 و50 و100 و200 ملغ/مل) ضد حشرة *Tribolium confusum*، بالإضافة إلى اختبارات الطرد واختبارات السمية باستخدام مسحوق النباتات. وأخيرًا، أُجريت دراسات الالتحام الجزيئي، مستهدفةً إنزيم أستيل كولين إستيراز(AChE) ، بهدف تحديد المركبات النشطة بيولوجيًا المحتملة والمسؤولة عن التأثيرات الإبادية الملحوظة.

أظهرت نتائج الفحص الكيميائي النباتي وجود مكونات رئيسية نشطة بيولوجيًا في جميع المستخلصات، في حين أكد تحليل ATR-FTIR وجود المجموعات الوظيفية المميزة لها. وسجّل نبات *S. fruticosa* أعلى محتوى كلي من الفينولات والتانينات، بلغ 119.33 ± 7.24 ملغ مكافئ حمض الغاليك/غرام من الوزن الجاف (mg GAE/g DW) و4.51 ± 0.09 ملغ مكافئ الكاتيشين/غرام من الوزن الجاف(mg CE/g DW) ، على التوالي. في المقابل، أظهر نبات *A. halimus*أعلى محتوى من الفلافونويدات، بلغ 73.07 ± 0.19 ملغ مكافئ الكيرسيتين/غرام من الوزن الجاف (mg QE/g DW)، بينما سجّل نبات *L. crithmoides* أدنى القيم.

وتوافقت هذه النتائج مع الأنشطة المضادة للأكسدة والمبيدة للحشرات التي لوحظت. إذ أظهر نبات *S. fruticosa* أقوى نشاط مضاد للأكسدة، مسجلًا أدنى قيم التركيز المثبط بنسبة 50 (IC_{50}) %في اختباري DPPH وABTS، حيث بلغت 0.48 ± 0.001 ملغ/مل و1.03 ± 0.006 ملغ/مل، على التوالي، بالإضافة إلى تسجيله أعلى قيمة في اختبارFRAP ، بلغت 2130.96 ± 2.55 ميكرومول من الحديد الثنائي/(Fe^{2+}) غرام من الوزن الجاف. وجاء بعده كل من *A. halimus* و *L. crithmoides*. وبالمثل، أظهرت اختبارات النشاط المبيد للحشرات أن مستخلص *S. fruticosa* سجّل أدنى قيمة للتركيز القاتل لنصف الأفراد المختبرة(LC_{50}) ، بلغت 50.03 ± 12.65 ملغ/مل بعد 96 ساعة من المعالجة، مقارنةً بـ84.73 ± 0.00 ملغ/مل لمستخلص A. halimus و88.86 ± 17.52 ملغ/مل لمستخلص*L. crithmoides.*

أدى تحليل HPLC-ESI-QTOF-MS في نمط التأين السالب إلى تحديد 24 و27 و29 مركبًا نشطًا بيولوجيًا في كل من *A. halimus* و*L. crithmoides* و*S. fruticosa*، على التوالي. وشملت هذه المركبات كايمبفيرول 3-O-روتينوزيد-7-O-غلوكوزيد(kaempferol 3-O-rutinoside-7-O-glucoside) ، والنارينجين(naringin) ، والفيرولويل تيرامين (feruloyltyramine)، والروتين(rutin) ، وحمض ثنائي الكافيويل الكينيك(dicaffeoylquinic acid) ، والكيرسيتين 3-O-غلوكوزيد(quercetin 3-O-glucoside) ، وحمض الكلوروجينيك(chlorogenic acid) ، وحمض 3-O-فيرولويل الكينيك (3 .O-feruloylquinic acid-كما أظهرت دراسات الالتحام الجزيئي أن هذه المركبات تتمتع بألفة ارتباط قوية تجاه إنزيم أستيل كولين إستيراز (AChE) لدى الحشرات.

الكلمات المفتاحية: النباتات الملحية، *Atriplex halimus*، *Limbarda crithmoides*، *Suaeda fruticosa*، الملف الكيميائي النباتي، النشاط المضاد للأكسدة، النشاط المبيد للحشرات، *Tribolium confusum.*

Résumé

Cette étude visait à examiner le profil phytochimique et à évaluer les activités antioxydante et insecticide des extraits méthanoliques de feuilles de trois halophytes algériennes : *Atriplex halimus*, *Limbarda crithmoides* et *Suaeda fruticosa*.

Un criblage phytochimique a été réalisé afin de détecter les principaux métabolites secondaires, ainsi qu'une quantification des teneurs totales en composés phénoliques, en flavonoïdes et en tanins, à l'aide des méthodes de Folin–Ciocalteu, du chlorure d'aluminium et de la vanilline, respectivement. La spectroscopie ATR-FTIR a été utilisée pour identifier les groupes fonctionnels, tandis que l'analyse HPLC-ESI-QTOF-MS a permis une caractérisation détaillée des constituants phytochimiques. L'activité antioxydante a été évaluée à l'aide des tests DPPH, ABTS et FRAP. L'activité insecticide a été étudiée au moyen de bioessais par contact direct à quatre concentrations (25, 50, 100 et 200 mg/mL) contre *Tribolium confusum*, ainsi que par des tests de répulsion et de toxicité de la poudre végétale. Enfin, des études de docking moléculaire ciblant l'acétylcholinestérase (AChE) ont été réalisées afin d'identifier les composés bioactifs potentiels responsables des effets biocides observés.

Les résultats du criblage phytochimique ont révélé la présence de principaux constituants bioactifs dans tous les extraits, tandis que l'analyse FTIR a confirmé leurs groupes fonctionnels caractéristiques. *S. fruticosa* a présenté les teneurs les plus élevées en composés phénoliques totaux et en tanins (119.33 ± 7.24 mg EAG/g MS et 4.51 ± 0.09 mg EC/g MS, respectivement), tandis que *A. halimus* a montré la teneur la plus élevée en flavonoïdes (73.07 ± 0.19 mg EQ/g MS), et que *L. crithmoides* a enregistré les valeurs les plus faibles.

Ces résultats concordaient avec les activités antioxydantes et insecticides observées. En effet, *S. fruticosa* a présenté la plus forte activité antioxydante, avec les valeurs d'IC_{50} les plus faibles pour les tests DPPH (0.48 ± 0.001 mg/mL) et ABTS (1,03 ± 0,006 mg/mL), ainsi que la valeur FRAP la plus élevée (2130.96 ± 2.55 µmol Fe^{2+}/g MS), suivie par *A. halimus* et *L. crithmoides*. De même, les essais insecticides ont révélé la valeur de CL_{50} la plus faible (50.03 ± 12.65 mg/mL après 96 h de traitement), comparativement à *A. halimus* (84.73 ± 0.00 mg/mL) et à *L. crithmoides* (88.86 ± 17.52 mg/mL).

L'analyse HPLC-ESI-QTOF-MS en mode d'ionisation négative a permis d'identifier 24, 27 et 29 constituants bioactifs chez *A. halimus*, *L. crithmoides* et *S. fruticosa*, respectivement, parmi lesquels figurent notamment le kaempférol 3-O-rutinoside-7-O-glucoside, la naringine, la féruloyltyramine, la rutine, l'acide dicaffeoylquinique, la quercétine 3-O-glucoside, l'acide chlorogénique et l'acide 3-O-féruloylquinique. Les études de docking moléculaire ont également montré que ces composés présentaient une forte affinité de liaison envers l'acétylcholinestérase (AChE) des insectes.

Mots-clés : Halophytes, *Atriplex halimus*, *Limbarda crithmoides*, *Suaeda fruticosa*, profil phytochimique, activité antioxydante, activité insecticide, *Tribolium confusum*.

Contents

Dedication
Acknowledgements
Résumé
Abstract
ملخص
List of abbreviations
List of figures
List of tables
List of equations
Introduction 1

Part I: Bibliographic review

Chapter 1: Overview of wheat and its insect pest

I. Presentation of the host plant "wheat" 5
1. Definition and origin 5
2. Systematic position 5
3. Morphological description of the grain 6
4. Chemical composition 7
5. Production and importance 7
5.1. In the World 7
5.2. In Algeria 9
6. Grain storage methods 9
6.1. Underground Storage (matmoura) 9
6.2. Storage in Bags 10
6.3. Storage in bulk 10
6.4. Storage in warehouse 10
6.5. Storage in silo 11
6.6. Advanced storage methods 11
7. Wheat Deterioration Factors 11
II. Presentation of *Tribolium confusum* 13
1. Description 13
2. Systematic Position 14
3. Origin and geographical distribution 14
4. Description of the different developmental stages 14
4.1. Egg 14
4.2. Larva 14
4.3. Pupa 15
4.4. Adult 15
5. Biology 15
6. Sex Determination 16
7. Feeding habits 16
8. Importance and damages 17
9. Control methods 17
9.1. Preventive management 17
9.2. Curative management 18
9.2.1. Physical control 18
9.2.1.1. Cold treatment 18
9.2.1.2. Heat treatment 18
9.2.1.3. Inert atmosphere storage 18

9.2.2. Chemical control 18
9.2.3. Biotechnological control 18
9.2.4. Biological control 19
9.2.4.1. Natural enemies 19
9.2.4.2. Plants 19

Chapter 2: Overview of halophytes

I. Presentation of halophytes 21
1. Definition 21
2. Worldwide geographical distribution and habitat 21
3. Classification 22
4. Mechanisms of adaptation to saline environments 22
4.1. Morphological adaptations 22
4.2. Anatomical adaptations 23
4.3. Physiological adaptations 23
5. Phytochemical compositions 23
6. Potential applications 23
6.1. Phytoremediation of saline and polluted soils 23
6.2. Food security in arid and saline regions 23
6.3. Environmental conservation and ecosystem services 24
6.4. Medicinal compounds and essential oil production 24
6.5. Bioenergy and biofuel production 24
II. Presentation of the studied halophytes 25
1. *Atriplex halimus* 25
1.1. Morphological description 25
1.2. Taxonomic classification 26
1.3. Geographical distribution 27
1.4. Uses 27
2. *Limbarda crithmoides* 27
2.1. Morphological description 27
2.2. Taxonomic classification 28
2.3. Geographical distribution 29
2.4. Uses 29
3. *Suaeda fruticosa* 30
3.1. Morphological description 30
3.2. Taxonomic classification 31
3.3. Geographical distribution 31
3.4. Uses 31

Chapter 3: Presentation of phenolic compounds

1. Definition 33
2. Classification 33
2.1. Simple phenolic compounds 33
2.1.1. Phenolic acid 34
2.1.1.1. Hydroxybenzoic acid 34
2.1.1.2. Hydroxycinnamic acid 34
2.2. Polyphenols 35
2.2.1. Flavonoids 35
2.2.1.1. Flavones 35
2.2.1.2. Flavonols 36
2.2.1.3. Flavanones 36
2.2.1.4. Isoflavones 36

2.2.1.5. Neoflavonoids 36
2.2.1.6. Flavanols 36
2.2.1.7. Anthocyanidins 37
2.2.2. Tannins 37
2.2.3. Stilbenes 38
2.2.4. Lignans 38
3. Biosynthesis 39
4. Extraction methods 40
4.1. Conventional extraction methods 40
4.2. Non-conventional extraction methods 41
5. Quantification methods 41
6. Functional properties and health benefits 42
7. Mechanisms underlying antioxidant and insecticidal activities 43
7.1. Antioxidant mechanisms 43
7.2. Insecticidal mechanisms 44
7.2.1. Oxidative stress and cellular damage 44
7.2.2. Neurotoxicity and disruption of nervous system function 44
7.2.3. Digestive system disruption and antifeedant activity 45
7.2.4. Growth inhibition and reproductive suppression 45

Part II: Materials and methods

I. Materials 47
1. Plant material 47
2. Animal material 48
3. Chemicals and reagents 48
II. Methods 48
1. Study Sites 48
2. Extracts Preparation 49
3. Phytochemical investigation of plant extracts 50
3.1. Qualitative phytochemical screening 50
3.2. Quantitative phytochemical analysis 51
3.2.1. Total phenolic content (TPC) 51
3.2.2 Total flavonoid content (TFC) 52
3.2.3. Total tannin content (TTC) 53
3.3. ATR-FTIR analysis 54
3.4. Identification of bioactive compounds using HPLC-ESI-QTOF-MS analysis 54
4. Evaluation of biological activities *in vitro* 55
4.1. Antioxidant Activity assessment 55
4.1.1. DPPH radical scavenging assay 55
4.1.2. ABTS radical scavenging activity 56
4.1.3. Ferric reducing antioxidant power (FRAP) method 57
4.2. Insecticidal activity 58
4.2.1. Insect breeding 58
4.2.2. Repellency test 58
4.2.3. Contact toxicity test 59
4.2.4. Oral toxicity bioassay using plant powders 60
5. Validation of extract safety on wheat seed germination 61
6. Insecticidal activity *in silico* 62
6.1. Protein preparation 62
6.2. Ligand preparation 62

6.3. Molecular docking procedure 63
6.4. Validation of docking results 63
7. Statistical analysis 64

Part III: Results and discussion

1. Extraction yield 66
2. Phytochemical characterization of plant extracts 67
2.1. Phytochemical screening 67
2.2. Total phenolic, flavonoid and tannin contents 68
2.3. ATR-FTIR analysis 70
2.4. HPLC-ESI-QTOF-MS results 74
3. Biological activities *in vitro* 80
3.1. Antioxidant activity 80
3.2. Insecticidal activity 82
3.2.1. Repellent effect 82
3.2.2. Contact effect 83
3.2.3. Powder plant effect 86
4. Effect of plant extracts on wheat germination 89
5. Insecticidal activity *in silico* (molecular docking) 90
Conclusion 101
References 104
Annexes 122

List of abbreviations

°C : Degree Celsius
µg: Microgram
µL: Microlitre
***A. halimus*:** *Atriplex halimus* L.
ABTS:2,2′-Azino-bis(3-ethylbenzothiazoline-6-sulfonic acid)
$AlCl_3$: Aluminium chloride
ATR-FTIR: Attenuated Total Reflectance–Fourier Transform Infrared Spectroscopy
DPPH: 2,2-Diphenyl-1-picrylhydrazyl
FAO: Food and Agriculture Organization
FRAP: Ferric Reducing Antioxidant Power
HPLC-ESI-QTOF-MS: High-Performance Liquid Chromatography–Electrospray Ionization–Quadrupole Time-of-Flight Mass Spectrometry
IC_{50}: Half-Maximal Inhibitory Concentration
***L. crithmoides*:** *Limbarda crithmoides*
L: Liter
LC_{50}: Median Lethal Concentration
m/z: Mass-to-Charge Ratio
MeOH: Methanol
mg AAE/g DW : Milligrams of Ascorbic Acid Equivalents per gram of Dry Weight
mg Fe^{2+}/g DW: Milligrams of Ferrous Ion Equivalents per gram of Dry Weight
mg GAE/g DW: Milligrams of Gallic Acid Equivalents per gram of Dry Weight
mg QE/g DW: Milligrams of Quercetin Equivalents per gram of Dry Weight
mg CAE/g DW: Milligrams of Catechin Equivalents per gram of Dry Weight
mg: Milligram
min: Minute
mL: Millilitre
MS: Mass Spectrometry
Mt: Million tonnes
RT: Retention Time
***S. fruticosa*:** *Suaeda fruticosa*
SD: Standard Deviation
TFC: Total Flavonoid Content
TPC : Total Phenolic Content
TPTZ : 2,4,6-Tris(2-pyridyl)-s-triazine
***T.confusum* :** *Tribolium confusum* Jacquelin du Val

List of figures

Figure 01. Grain wheat anatomy 6
Figure 02. Chemical constituents in different parts of wheat grain 7
Figure 03. Global cereal production (2016–2026) 8
Figure 04. Traditional underground grain silo (Matmoura) 10
Figure 05. Adult *T. confusum* **A:** Dorsal view; **B:** Ventral view 13
Figure 06. External morphology of *T. confusum* 13
Figure 07. Morphology of the developmental stages of *T. confusum*. **A:** Egg; **B**: Larva; **C:** Pupa; **D:** Adult 15
Figure 08. Sexual differentiation at the pupal stage of *T. confusum* **(A:** female; **B:** male**)** 16
Figure 09. Damage caused by *T. confusum* on stored products **A:** Wheat flour (**1**: uninfested flour; **2**: flour infested by *T. confusum*). **B**: Wheat grains 17
Figure 10. Global distribution of halophyte habitats in relation to soil types 21
Figure 11. Potential uses of some halophyte species 24
Figure 12. Morphology of *A. halimus* **A:** Roots, **B:** Stems, **C:** Leaves, **D:** Flowers, **E:** Seeds 25
Figure 13. Morphological comparison of the two subspecies of *A. halimus*: *A. halimus* subsp. *schweinfurthii* (left) and *A. halimus* subsp. *halimus* (right) in the Region of Murcia (Spain) 26
Figure 14. Morphology of *L. crithmoides* **A:** Roots, **B:** Stems, **C:** Leaves, **D:** Flowers, **E:** Fruit 28
Figure 15. Morphology of *S. fruticosa* **A:** Flowering branch, **B:** Male flower, **C:** Stamen, **D:** Fruit, **E:** Seed, **F:** Seed (longitudinal section) 30
Figure 16. General structure of simple phenolic compounds 33
Figure 17. Main subclasses of phenolic acids and their representative compounds 34
Figure 18. General structure of flavonoids 35
Figure 19. Chemical structures of flavonoid subclasses: **(A)** Flavones; **(B)** Flavonols; **(C)** Flavanones; **(D)** Isoflavonoids; **(E)** Neoflavonoids; **(F)** Flavanols; **(G)** Anthocyanidins 37
Figure 20. Main chemical structures of tannins 38
Figure 21. General structure of stilbenes 38
Figure 22. General structure of lignans 39
Figure 23. Biosynthetic pathway of phenolic compounds 40
Figure 24. Conventional and non-conventional extraction approaches for phenolic compounds 41

Figure 25. Potential health effects of phenolic compounds on human health and disease. 43
Figure 26. Antioxidant mechanism of phenolic compounds through reactive oxygen species (ROS) scavenging 44
Figure 27. Mode of action of phenolic compounds (flavonoids) in insect larvae and adults 45
Figure 28. Map showing sample collection locations: **(1)** *A. halimus*; **(2)** *L.crithmoides*; **(3)** *S. fruticosa* 47
Figure29. Different stages of methanolic extraction using the maceration method 49
Figure 30. Gallic acid calibration curve for total phenolic content determination 52
Figure 31. Quercetin standard calibration curve for total flavonoids content determination 53
Figure 32. Catechin standard calibration curve for total tannins content determination. 53
Figure 33. HPLC-ESI-QTOF-MS system 55
Figure 34. Ascorbic acid calibration curve for the DPPH radical scavenging assay 56
Figure 35. Ascorbic acid calibration curve for the ABTS radical scavenging assay 57
Figure 36. Calibration curve of ferrous ammonium sulfate for the FRAP reducing power assay 57
Figure 37. Mass rearing of *T. confusum* 58
Figure 38. Repellency test for different doses of plant extracts compared with the control 59
Figure 39. Contact bioassays of extract against *T.confusum* 60
Figure 40. Toxic potentials of plant powders on survival of *T. confusum* 61
Figure 41. Wheat seed germination test 62
Figure 42. ATR-FTIR Spectrum of different extracts **(A):** *A. halimus*, **(B):** *L. crithmoides*, **(C):** *S. fruticosa* 73
Figure 43. Base peak chromatogram of different extracts **(A):** *A. halimus*, **(B)**: *L. crithmoides*, **(C):** *S. fruticosa* obtained by HPLC-ESI-QTOF-MS 79
Figure 44. Mortality of *T. confusum* exposed by direct contact to different concentrations of methanolic extracts: **(A):** *A. halimus*, **(B):** *L. crithmoides*, **(C):** *S. fruticosa* 84
Figure 45. Mortality of *T. confusum* fed diets supplemented with different concentrations of plant powder **(A):** *A. halimus*, **(B):** *L. crithmoides*,**(C):** *S. fruticosa* 87

Figure 46. Effect of plant extracts at the highest tested concentration (200 mg/mL) on the germination of stored wheat grains. 89

Figure 47. 2D (left) and 3D (right) intermolecular interactions of the four top-scoring compounds from the *A. halimus* extract within the active site of acetylcholinesterase (AChE): **(A)** Feruloyltyramine, **(B)** Quercetin dihydrate, **(C)** Caffeic acid 3-sulfate, and **(D)** Protocatechuic acid 4-glucoside 92

Figure 48. 2D (left) and 3D (right) intermolecular interactions of the four top-scoring compounds from the *L. crithmoides* extract within the active site of acetylcholinesterase (AChE)**: (A)** Cynarine**, (B)** Quercetin 3-O-glucoside**, (C)** Chlorogenic acid, and (**D)** 3-O-Feruloylquinic acid 95

Figure 49. 2D (left) and 3D (right) intermolecular interactions of the four top-scoring compounds from the *S. fruticosa* extract within the active site of acetylcholinesterase (AChE): **(A)** Kaempferol 3-*O*-rutinoside 7-*O*-glucoside, **(B)** Naringin, **(C)** Rutin, **(D)** Isorhamnetin 98

List of tables

Table 01. Global wheat production, utilization, and stocks (2022–2027) 8

Table 02. Algerian cereal production. 9

Table 03. Major biological agents affecting stored wheat quality and their impacts 12

Table 04. Classification of halophytes 22

Table 05. Botanical classification of *Atriplex halimus* 26

Table 06. Botanical classification of *L.crithmoides* 28

Table 07. Botanical classification of *S. fruticosa* 31

Table 08. Site geography, collection dates and altitude of studied plants. 47

Table 09. Preliminary phytochemical screening of the plant extracts. 50

Table 10. Yields extract results expressed as percentage. 66

Table 11. Phytochemical screening of the three different solvent extracts from the studied halophyte species 67

Table 12. Total phenolic, flavonoids and tannins content in the studied plant extracts 69

Table 13. Wavenumber ranges and corresponding functional groups identified by ATR-FTIR in methanolic plant extracts. 72

Table 14. Compounds identified in the methanolic extract of *A. halimus* by HPLC-ESI-QTOF-MS analysis. 74

Table 15. Identified compounds in the methanolic extract of *L. crithmoides* by HPLC-ESI-QTOF-MS analysis. 76

Table 16. Identified compounds in methanolic extract of *S. fruticosa* by HPLC-ESI-QTOF-MS analysis. 77

Table 17. DPPH, ABTS radical scavenging activity, and ferric reducing antioxidant power of plant extracts 80

Table 18. Repellency effect of methanolic extracts against *T. confusum* adults. 82

Table 19. LC_{50} values of plant extracts against *T. confusum* adults at 4 times intervals 85

Table 20. Molecular docking results of the major polyphenols identified in *A.halimus* extract with insect acetylcholinesterase (AChE) protein 91

Table 21. Molecular docking results of the major polyphenols identified in *L. crithmoides* extract with insect acetylcholinesterase (AChE) protein. 93

Table 22. Molecular docking results of the major polyphenols identified in.*S. fruticosa* extract with insect acetylcholinesterase (AChE) protein. 96

List of equations

Equation 01. Percentage of yield extraction 49
Equation 02. Percentage of DPPH radical inhibition. 55
Equation 03. Percentage of ABTS radical inhibition**.** 56
Equation 04. Percentage repellency (PR %) of plant extracts against *T. confusum* 59
Equation 05. Mortality rate of *T. confusum* adults by contact bioassay 60
Equation 06. The germination rate (%) 61

Introduction

Cereals have constituted a fundamental component of the human diet since ancient times and remain of major strategic importance for both human nutrition and animal feeding. Moreover, cereal cultivation has significantly contributed to the rise and development of several civilizations, with rice being central to Asian societies, maize to pre-Columbian civilizations, and wheat to the Mediterranean region and the Near East **(Bakroune et *al*., 2024)**.

Global cereal production is estimated at 3,043 million tonnes in 2025, representing a 6.1% increase compared with 2024, while global wheat production is projected to reach 839 Mt **(FAO, 2026)**. In Algeria, cereals constitute the backbone of the food system, with imports expected to reach 14.6 Mt during the 2025/2026 marketing season **(FAO, 2026)**.

Despite their considerable economic importance, cereal crops remain highly susceptible to infestation and contamination by a wide range of pests and pathogens, including rodents, viruses, bacteria, fungi, and insect pests, throughout the production chain, from pre-harvest and harvesting to transportation, storage, processing, and distribution **(Benhamada et *al*., 2024)**.

Insect pests are among the earliest colonizers of stored grains and constitute one of the principal factors responsible for the deterioration of grain quality during storage. They cause damage by feeding on grains, contaminating them with their developmental residues and excreta, and facilitating the spread of associated microflora. More than 100 insect species have been reported to infest stored cereals, with beetles representing the predominant group, followed by moths and psocids **(Rajendran, 2003)**.

Among these pests, *Tribolium confusum* Jacquelin du Val is one of the important secondary pests of stored products. It feeds mainly on broken kernels, grain embryos, and flour dust, causing significant quality deterioration and rendering the products unfit for consumption **(Ziaee and Ganji, 2016)**.

The application of chemical pesticides for the control of this pest contributes to improved agricultural productivity and enhanced food security. However, their prolonged use is associated with serious concerns regarding human health and environmental contamination **(Zhou et *al*., 2025)**.

Consequently, the search for novel phytopesticides as environmentally friendly and low-toxicity alternatives has become imperative **(Moutassem et *al*., 2024)**. In this regard, previous research has demonstrated the potential of halophytic plants as sources of bio-

insecticidal agents, mainly due to their diverse bioactive compounds **(Soliman et *al*., 2005; Soummane et *al*., 2011)**.

Atriplex halimus L. and *Suaeda fruticosa* Forssk. ex J.F. Gmel are two halophytic medicinal plants belonging to the Chenopodiaceae (Amaranthaceae) family, widely distributed in arid and semi-arid regions of the Mediterranean basin **(Walker et *al*., 2014; Saleem et *al*., 2021)**. They are known for a wide range of biological properties, including antioxidant, antimicrobial, antifungal, anti-inflammatory, anticancer, and antidiabetic activities **(Suthar and Solanki, 2022; Roubi et *al*., 2023)**.

Similarly, *Limbarda crithmoides* (L.) Dumort. (syn. *Inula crithmoides*), commonly known as "golden samphire," is another Mediterranean halophyte of the Asteraceae family, rich in secondary metabolites such as phenolic compounds, flavonoids, alkaloids, tannins, and polysaccharides **(Bokri et *al*., 2023)**. These bioactive constituents are associated with multiple biological activities, notably antioxidant, anti-inflammatory, antidiabetic, antifungal, antibacterial, and antitumor effects **(Brzović et *al*., 2025)**.

Although these halophytes have been extensively investigated for their medicinal potential, information regarding their insecticidal activity against stored-product pests remains limited. Therefore, this study was carried out to explore the phytochemical profiles of these halophytes and to assess their biological activities through *in vitro* and *in silico* approaches, with a particular focus on antioxidant and insecticidal properties, in order to develop alternative control strategies against *Tribolium confusum* using methanolic extracts.

This thesis is organized into three main parts. **Part I** presents the bibliographic review and is divided into three chapters; Chapter 1 provides an overview of wheat and *Tribolium confusum*, Chapter 2 focuses on halophytes and the selected plant species investigated in this work, and Chapter 3 reviews phenolic compounds. **Part II** describes the materials and methods, detailing the experimental procedures and analytical approaches employed throughout the study. **Part III** presents the results and discusses their scientific significance. Finally, the thesis concludes with a general conclusion summarizing the main findings, followed by recommendations and perspectives for future research.

Part I: Bibliographic review

Chapter 1: Overview of wheat and its insect pest

I. Presentation of the host plant "wheat"

1. Definition and origin

Wheat is the third most widely produced cereal crop in the world after maize and rice, while occupying the largest cultivated area. It is a major crop for global food security and is extensively used for human consumption in the form of bread, pasta, pastries, couscous, pizza, and other agro-industrial products. Wheat domestication began approximately 12,000 years ago during the early Holocene in the Fertile Crescent, a region encompassing parts of present-day Iraq, Iran, Jordan, Lebanon, Palestine, Syria, and Turkey. This process marked a key milestone of the Neolithic Revolution and the transition to a sedentary lifestyle. Domestication involved significant morphological, physiological, and genetic changes, collectively known as the "domestication syndrome." The earliest cultivated forms were diploid einkorn (AA) and tetraploid emmer (AABB), originating mainly from southeastern Turkey. Subsequent hybridization and evolutionary processes led to the emergence of hexaploid wheat (AABBDD), which currently dominates global production. Its spread across Europe, Asia, and Africa resulted in a wide diversity of locally adapted varieties suited to different agroecological conditions **(Khalid et *al*., 2023; Katamadze et *al*., 2023)**.

2. Systematic position

According to **(Naville, 2005; Khalid et *al*., 2023)**, the taxonomy of wheat is established as follows:

Kingdom: Plantae

Super division: Spermatophyta

Division: Magnoliophyta

Class: Liliopsida (Monocotyledon)

Subclass: Commelinidae

Order: Cyperales

Family: Poaceae/Gramineae

Genus: *Triticum* (wheat)

The genus *Triticum* includes about 5000 wheat species cultivated worldwide. The most important is *Triticum aestivum* (common or bread wheat), a hexaploid species that represents the major global wheat production. Durum wheat (*Triticum turgidum* var. *durum*), a tetraploid species, is widely grown in hot and dry regions, particularly around the Mediterranean basin, and is mainly used for pasta production. Other wheat species, such as einkorn (*Triticum monococcum* var. *monococcum*), emmer (*Triticum turgidum* var.

dicoccum), and spelt (*Triticum aestivum* var. *spelta*), are cultivated on smaller areas, often for traditional uses or niche health-food markets **(Shewry and Hey, 2015; Feldman and Levy, 2023)**.

3. Morphological description of the grain

The wheat grain (caryopsis) is a single-seeded fruit in which the seed and fruit coat are fused, making them inseparable at maturity. It is generally oval in shape, but its form can vary from nearly spherical to elongated or flattened depending on the genotype and environmental conditions. The grain usually measures about 5–9 mm in length and 3–4 mm in diameter and shows a characteristic longitudinal ventral crease where it was attached to the floral tissues. Its color ranges from whitish to brownish, and slight morphological differences may occur depending on the grain's position on the spike and growing conditions **(Šramková et *al*., 2009; Wang et *al*., 2021)**.

Inside the grain, the outer layers (pericarp, testa, and nucellar epidermis) represent about 8% of its structure. The embryo, which forms about 3% of the grain, contains the embryonic axis responsible for germination and a single cotyledon called the scutellum, which stores nutrients. The endosperm makes up nearly 90% of the grain and is divided into two parts: the starchy endosperm, rich in starch and storage proteins, and the aleurone layer, which contains proteins, oils, minerals, and dietary fiber **(Wang et *al*., 2021; Gooding and Shewry, 2022)**.

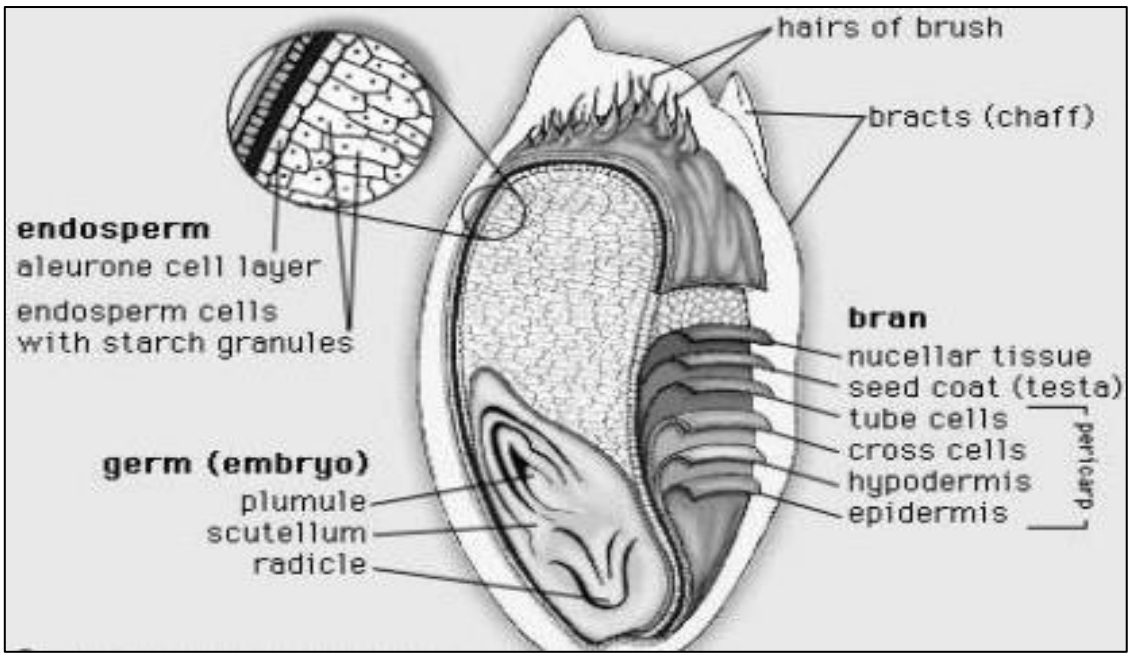


Figure 01. Grain wheat anatomy **(Šramková et *al*., 2009)**.

4. Chemical composition

The wheat grain has a chemical composition dominated by carbohydrates (approximately 80–85% of dry matter), the majority of which is starch (~80% of total carbohydrates), serving as the main energy reserve in the endosperm. Proteins account for about 10–15%, mainly represented by glutenin and gliadin, which are responsible for gluten formation. Lipids are present in low amounts (1–3%) and are mainly concentrated in the germ. Dietary fiber (about 2–3%) originates primarily from the outer layers of the grain (bran), while minerals (1.5–2%) include iron, zinc, magnesium, and phosphorus. The grain also contains B-group vitamins (B1, B2, B3, and B6), mainly located in the peripheral tissues. This composition makes wheat a highly important cereal for human nutrition due to its balanced energy and structural contributions **(Shewry and Hey, 2015)**.

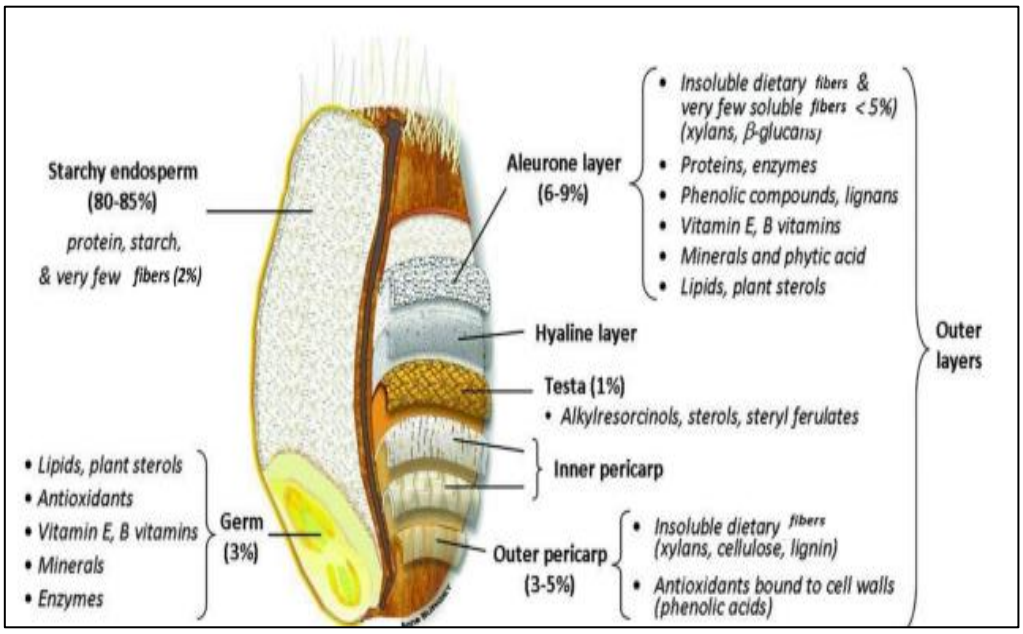


Figure 02. Chemical constituents in different parts of wheat grain **(Khalid et *al*., 2023)**.

5. Production and importance

5.1. In the World

Global cereal production in 2025 is estimated at 3.043 million tonnes, representing a 6.1% increase compared with 2024, mainly driven by higher maize production. World cereal utilization in 2025/2026 is projected to reach 2,952 Mt, up 2.7% from 2024/2025, owing to increased consumption of maize and rice. Global cereal stocks are expected to rise to 952.2 Mt, an increase of 9.5%, supported by larger wheat, maize, and rice reserves. World cereal

trade in 2025/2026 is forecast at 508.6 Mt, up 4.8% from the previous season, mainly due to a strong recovery in wheat and coarse grain trade **(FAO, 2026)**.



Figure 03. Global cereal production (2016–2026) **(FAO, 2026)**.

Among cereals, wheat remains one of the most strategically important commodities due to its large-scale production and essential role in global food security. The wheat market shows a generally stable trend with a slight increase in output, rising from about 792 Mt in 2023/24 to around 842.5 Mt in 2025/26. Global wheat consumption and ending stocks also increase steadily, with consumption rising from 778.3 to 806.1 Mt and stocks reaching 348.6 million tonnes compared with 320.0 Mt previously, supporting a more balanced global supply situation **(FAO, 2026)**.

Table 01. Global wheat production, utilization, and stocks (2022–2027).

Indicator	2022/23	2023/24	2024/25	2025/26 (Estimate)	2026/27 (Forecast)
Production (million tonnes)	807.1	792.3	798.2	842.6	810.9
Supply (million tonnes)	1099.2	1112.3	1116.7	1156.1	1157.7
Utilization (million tonnes)	778.3	794.4	794.0	804.0	806.1
Trade (million tonnes)	201.5	210.2	193.0	205.9	199.1
Ending Stocks (million tonnes)	320.0	318.5	313.5	346.8	348.6
World stock-to-use ratio (%)	40.3	40.1	39.0	43.0	42.5
Major exporters' stock-to-disappearance ratio[5] (%)	22.3	20.6	19.4	25.1	23.6

5.2. In Algeria

According to **(FAO, 2025)** statistics, cereal crops occupy a strategic position in Algeria's food system and national economy. Algerian cereal production in 2025 is estimated at 4.2 million tonnes, similar to the previous year and well above the drought-affected output recorded in 2021. Wheat is the dominant cereal crop, contributing nearly 3 Mt and representing the largest share of total cereal production **(FAO, 2025)**.

Table 02. Algerian cereal production.

Cereal	2020–2024 Average (thousand tonnes)	2024 (thousand tonnes)	2025 Estimate (thousand tonnes)	Change 2024/2025 (%)
Wheat	2755	3000	3000	0.0
Barley	944	1,000	1,150	15.0
Oats	85	105	86	−18.1
Others	12	13	12	−7.7
Total	3796	4118	4248	3.2

6. Grain storage methods

6.1. Underground Storage (matmoura)

Traditional grain storage in Algeria, particularly in the high plateaus, is carried out using underground silos known as matmoura. These structures consist of simple cylindrical or rectangular pits dug in dry, stable soils, usually clay-rich, where the groundwater level is sufficiently low. They are typically located near farms or in secure areas. Their storage capacity varies but is generally limited to a few cubic meters **(Benhamada and Idoui, 2020)**.

This technique is used in several countries around the world, including Morocco, Spain, Somalia, Yemen, and India, where different forms and shapes of underground grain pits are employed depending on local environmental conditions, available materials, and traditional practices **(Pasqualone, 2025)**.

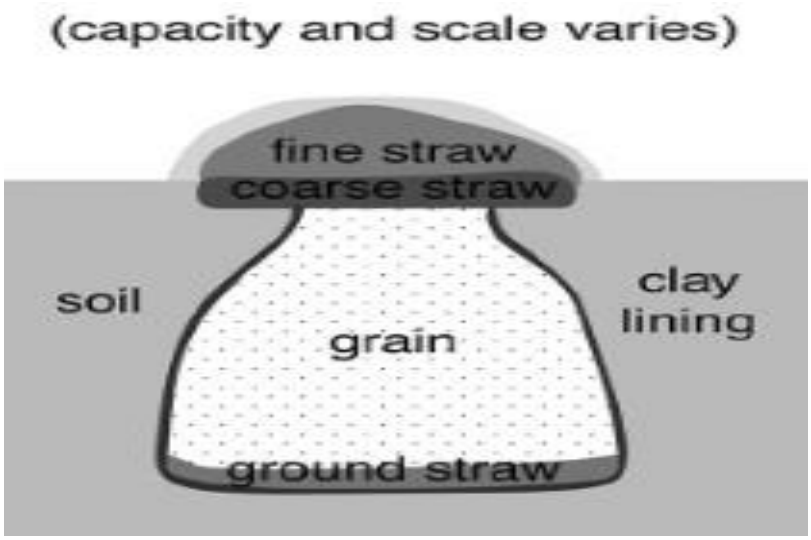


Figure 04. Traditional underground grain silo (Matmoura) **(Bevan et *al*., 2024)**.

6.2. Storage in Bags

Cereal grains can be stored in bags made of jute or polypropylene, particularly when intended for seed purposes. The bags are generally stacked in warehouses, sheds, or other storage facilities. This storage method is often considered a temporary solution. However, during periods of high production or when large-capacity storage facilities become saturated, the use of bag storage in auxiliary buildings becomes necessary to ensure the preservation of harvested grains **(Rajendran, 2003)**.

6.3. Storage in bulk

Storing grains in open warehouses is a method in which cereals are kept in bulk without airtight confinement. In this type of structure, the grains are left exposed to open air in open-sided, usually metal-framed warehouses, which allows for large storage capacity and easy handling. However, this direct exposure to the environment may increase risks related to contamination **(Cruz et *al*., 1988)**.

6.4. Storage in warehouse

A warehouse is a structure designed for the storage and physical protection of grains, whether in bulk or in bags. It may also contain equipment and materials for packaging, processing bagged grain, and controlling pests. The selection of a warehouse site should take into account factors such as topography, soil characteristics, accessibility, building orientation, and proximity to residential areas. This storage system allows cereals and cereal products to be kept either in bulk piles or in sacks **(Pekmez, 2016)**.

6.5. Storage in silo

Silos are an efficient system for grain storage, allowing large quantities to be kept in bulk while optimizing space and reducing handling and packaging costs. They also facilitate mechanical operations and help control grain temperature through aeration, which limits overheating during storage. Different types and capacities of silos exist to meet various storage needs. These structures are commonly built using materials such as concrete, brick, or assembled metal sheets **(Benhamada et *al*., 2024)**.

6.6. Advanced storage methods

Modern grain storage methods are based on advanced technologies designed to improve preservation and reduce both qualitative and quantitative losses. Among these, aeration is a widely used non-chemical technique that involves the forced circulation of ambient or conditioned air through the grain mass in order to lower temperature and reduce moisture, thereby limiting insect development, especially during winter periods. Refrigerated storage aims to maintain temperatures below 18 °C during summer by cooling the air before it is introduced into silos, which helps to slow biological activity, although it requires higher initial investment. Modified and controlled atmosphere technologies rely on the use of gases to replace chemical fumigants, effectively controlling insect pests while preserving grain quality without leaving residues. Finally, hermetic storage is based on the respiration of organisms within the grain, which creates an oxygen-depleted and carbon dioxide-rich environment **(Pekmez, 2016)**.

7. Wheat Deterioration Factors

Various pest organisms contribute to the deterioration of stored grains, including insects and mites among invertebrates, birds and rodents among vertebrates, and microorganisms such as fungi, yeasts, and bacteria. The combined activity of these organisms within the storage ecosystem adversely affects grain quality, resulting in losses in quantity, and nutritional value **(Rajendran, 2003)**.

According to **(Rajendran, 2003)**, the major wheat pests, their species, and their associated damage are summarized in **Table 03.**

Table 03. Major biological agents affecting stored wheat quality and their impacts

Pest	Species	Associated Effects on Stored Wheat
Insects	Beetles: *Sitophilus spp* (*oryzae*, *zeamais*, *granaries*) *Trogoderma granarium*, *Rhyzopertha dominica*, *Tribolium castaneum*, *Tribolium confusum*,	- Direct feeding on grains causing quantitative losses and germ damage - Contamination of grains with excreta, dead insects, and fragments - Heating of grain mass and creation of moisture–temperature hotspots - Spread of storage fungi and deterioration of grain quality - Reduction of nutritional value and sugars in infested grains - Decrease in market value leading to rejection of grains - Egg-laying damage and grain dust formation by boring insects
	Moths:*Sitotroga cerealella* *Plodia interpunctella*	
	Psocids: *Liposcelis spp*	
Mites	*Acarus siro* *Tyrophagus putrescentiae* *Pyemotes* spp,and *Cheyletus* spp.	- Consumption of the grain germ causing quality loss - Dissemination of storage fungi and bacteria in stored grains - Production of unpleasant characteristic odor - Causing dermatitis and allergic reactions in humans - Development in damp, moldy grain under low temperatures
Storage Fungi	*Alternaria*, *Cladosporium*, *Fusarium, Drechsclora spp* *Aspergillus spp* *Penicillium spp.* *Rhizopus spp.* *Mucor spp.* *Nigrospora spp.*	- Infection of high-moisture grains by field fungi before storage - Development of storage fungi at low moisture causing discoloration, heating, and off-odors - Growth of yeasts under low oxygen and high grain moisture conditions - Activation of bacteria leading to severe grain degradation - Destruction of grain germ and reduction of baking and nutritional quality - Production of mycotoxins harmful to human health
Rodents	*Mus musculus* *Rattus norvegicus* *Rattus rattu*	- Direct consumption and contamination of grains by urine, feces, hair, and body fragments. - Disease transmission to humans (plague, typhus, leptospirosis) - Damage to storage structures and equipment (wood, bags….)
Birds	*Columba livia* *Passer domesticus*	- Direct loss of grains through consumption - Grain contamination through droppings (feces) and feathers - Spread of insects and microorganisms in stored grain stocks

II. Presentation of *Tribolium confusum*

1. Description

Tribolium confusum is a beetle species belonging to the family Tenebrionidae and is widely recognized as a pest of stored food products, particularly flour and cereal grains. This holometabolous insect undergoes complete metamorphosis. The adult is a small reddish-brown beetle measuring approximately 4 mm in length. Its body is flat, elongated, and shiny. The antennae end in a well-developed club, and the eyes are located laterally on the head without any prominent projection above them **(Zohry, 2017)**.



Figure 05. Adult *T. confusum* **A:** Dorsal view; **B:** Ventral view **(Original, 2025)**.



Figure 06. External morphology of *T. confusum* **(Original, 2025)**.

2. Systematic Position

According to **(Gretia, 2009)**, *T. confusum* occupies the following taxonomic position:

Kingdom: Animalia

Phylum: Arthropoda

Class: Insecta

Order: Coleoptera

Suborder: Polyphaga

Family: Tenebrionidae

Subfamily: Ulominae

Genus: *Tribolium*

Species: *Tribolium confusum* (Jacquelin du Val, 1868)

3. Origin and geographical distribution

The confused flour beetle, *T. confusum* is believed to be of African origin. However, the transport of food commodities by humans has enabled its extensive dispersal, resulting in a nearly worldwide distribution, especially in temperate and cooler regions. The species was first recorded in Europe in 1900 in Czechoslovakia and is commonly associated with stored cereal products, occurring wherever cereals are stored as whole grains or flour **(Dawson, 1977)**.

4. Description of the different developmental stages

4.1. Egg

The egg is oblong and whitish, almost transparent, microscopic, with a smooth surface covered by a sticky substance that allows it to adhere to the infested commodity.it measures on average 0.6 × 0.3 mm **(Lepesme, 1944)**.

4.2. Larva

The larva is white, vermiform, and reaches up to 1.4 mm in length, moving freely within the infested commodity. It develops through several instars. The final-instar larva is cylindrical in shape, measuring about 7 mm in length and 0.8 mm in width, and is pale yellow in colour. Its body is nearly glabrous, covered with sparse setae, and bears legs ending with two pairs of small corniculi. It terminates with two pairs of urogomphi **(Delobel and Tran, 1993)**.

4.3. Pupa

The pupa has a white color, the abdominal segments are laterally expanded into rectangular plates with crenulated margins, and the insect is immobile and unable to move **(Balachowsky, 1936)**.

4.4. Adult

The adult is a small reddish-brown insect measuring between 3 and 4 mm in length. Its body is flat, elongated, and slightly parallel-sided. The elytra are elongated and rounded at the posterior end, bearing regular rows of punctures separated by very fine intervals. The elytral suture is weakly carinate. The legs are curved, and the hind tarsi are composed of four segments. The anterior angles of the pronotum are not prominent, and its punctation is sparse. The interocular space is very short, approximately 1.5 times the width of the eye, while the canthus of the cheeks is distinctly protruding above the eyes. The antennal club is composed of three well-defined segments **(Steffan, 1978)**.

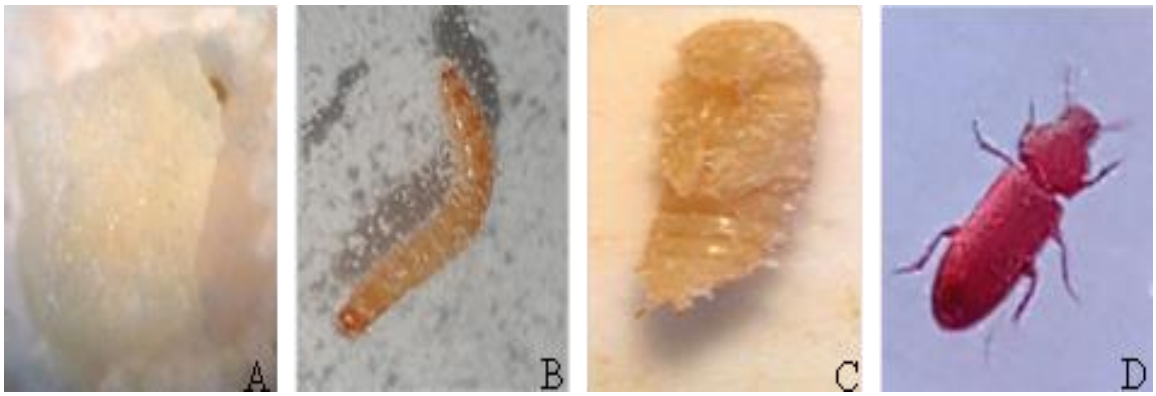


Figure 07. Morphology of the developmental stages of *T. confusum*
A: Egg; **B:** Larva; **C:** Pupa; **D:** Adult **(Original, 2025)**.

5. Biology

The first mating occurs approximately two days after adult emergence, and copulation lasts between 3 and 15 minutes. After mating, eggs are laid either individually or in clusters, often within grains already infested by other primary pests or on the surface of contaminated substrates. During its lifetime, the female can lay between 500 and 1,000 eggs. They hatch after 5 to 12 days, giving rise to a newly emerged (neonate) larva. The larva develops through several instars, the number of which varies from 5 to 12 depending on environmental conditions such as temperature, relative humidity, and food quality. During these larval instars, the insect moves freely within the infested commodity and eventually pupates within

it. The pupa is white and immobile. It represents a non-feeding stage during which the transformation into the adult takes place. Adult emergence occurs approximately six days after pupation. The total life cycle duration is about 24 to 26 days under optimal conditions **(Lepesme, 1944)**.

6. Sex Determination

In *T. confusum*, sex can be distinguished at the pupal stage based on morphological characteristics visible on the ventral side of the terminal abdominal region. Female pupae exhibit two distinct genital papillae located above the pair of dark brown, sharply pointed urogomphi. In contrast, male pupae possess a single median protuberance that appears slightly depressed. These sexually dimorphic features provide a reliable means of differentiating males from females prior to adult emergence **(Brown et *al*., 2009; Shukla and Palli, 2012)**.

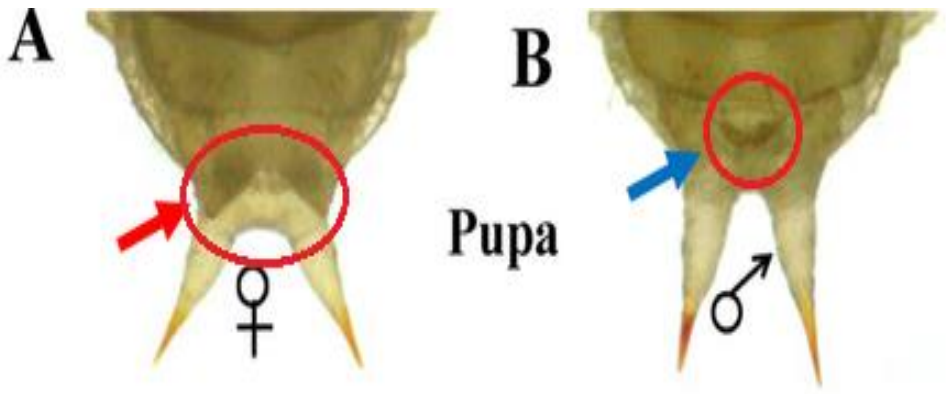


Figure 08. Sexual differentiation at the pupal stage of *T. confusum* **(A:** female; **B:** male**)** **(Shukla and Palli, 2012)**.

7. Feeding habits

T. confusum is a highly polyphagous pest species, recorded on nearly 200 types of products, including cereal commodities (flour, oat flakes, bran, and grains), spices, chocolate, and dried fruits. It may also infest animal-derived materials such as bones and other protein-rich products **(Lepesme, 1944)**.

This species is primarily attracted to starch-rich and powdered substrates. It is considered a secondary clethrophagous insect, as it mainly feeds on already damaged grains and fragments, often following the activity of primary pests such as weevils, whose damage it further extends. In addition, cannibalistic behavior has been observed, with individuals capable of consuming their own eggs and pupae **(Steffan, 1978)**.

8. Importance and damages

T. confusum causes various types of damage to stored products, including contamination with insect fragments, exuviae, and feces, as well as the development of unpleasant odors and changes in color and smell due to benzoquinone secretions. Infestation also induces important physical and chemical alterations in cereals. Physical damage is mainly characterized by grain degradation, powdering, and loss of structural integrity resulting from feeding activity, while chemical changes involve a reduction in essential nutrients such as carbohydrates, proteins, lipids, vitamins, and minerals, along with alterations in volatile compounds that affect product quality. Consequently, these combined effects lead to a decline in nutritional value, favor mold development, and lead to consumer rejection, resulting in economic losses **(Wulandari et *al*., 2025)**.



Figure 09. Damage caused by *T. confusum* on stored products
A: Wheat flour (**1**: uninfested flour; **2**: flour infested by *T. confusum*). **B**: Wheat grains **(Original, 2025)**.

9. Control methods

9.1. Preventive management

Preventive management is based on the strict application of sanitary measures involving transport equipment, storage facilities, handling installations, and harvesting machinery. Several preventive practices can be implemented before and after storage. Prior to storage, warehouses should be thoroughly cleaned, and grains must be adequately dried to maintain low moisture content **(Bush et *al*., 2006)**.

9.2. Curative management

9.2.1. Physical control

9.2.1.1. Cold treatment

Low temperatures inhibit insect development and reproduction. At temperatures below 8°C, larval penetration into grains is prevented, and prolonged exposure to sub-zero temperatures can lead to high mortality **(Fields, 1992)**.

9.2.1.2. Heat treatment

High temperatures (around 55°C) can rapidly eliminate adult insects without affecting grain germination. Moderate temperatures (around 34°C) reduce survival and cause developmental abnormalities in insects **(Fields, 1992)**.

9.2.1.3. Inert atmosphere storage

Reducing oxygen levels using gases such as CO_2 or N_2 creates lethal conditions for insects. When oxygen is lowered to below 1%, insect survival becomes impossible, effectively controlling infestations **(Navarro, 2006)**.

9.2.2. Chemical control

Two types of treatments are commonly employed for the control of stored-product insects. The first involves the application of contact insecticides directly to moving grains during handling operations, particularly organophosphates and pyrethroids, which are known for the persistence of their residues. The second is fumigation, an effective method that ensures rapid and complete eradication of insect pests, especially in cases of severe infestation or prior to commercial transactions and export **(Fleurat-Lessard, 2002)**.

9.2.3. Biotechnological control

This control technique relies on the use of synthetic pheromones that disrupt the reproductive behavior of insects by preventing mating. It also includes growth regulators (IGRs) that interfere with normal insect development. These substances cause physiological abnormalities and significantly reduce reproduction. In the long term, they contribute to a decrease in pest populations **(Tunaz and Uygun, 2004)**.

9.2.4. Biological control

9.2.4.1. Natural enemies

The natural enemies of stored-product insects mainly include predators such as *Xylocoris flavipes* and *Teretriosoma nigrescens*, as well as parasitoids such as those of the genus *Trichogramma* and *Laelius pedatus*, which contribute to the natural regulation of pest populations. These organisms act either through direct predation or parasitism, thereby reducing the development and survival of harmful insects in storage environments. Their effectiveness depends on their mode of action and their adaptation to different host species **(Schöller et *al*., 1997)**.

9.2.4.2. Plants

The use of plant-derived natural substances as bioinsecticides is an effective alternative for reducing the toxicity of chemical insecticides in grain protection. These bioproducts include aqueous and organic extracts, vegetable oils, essential oils, and plant powders. Essential oils (EOs) and plant extracts contain bioactive natural compounds that can be safely used in pest and disease control due to their rapid biodegradability in the environment. In addition, the development of insect resistance to conventional insecticides has encouraged the exploration of plant-based molecules capable of affecting different pest stages through contact, ingestion, and inhalation **(Lahlali et *al*., 2022)**.

Chapter 2: Overview of halophytes

I. Presentation of halophytes

1. Definition

Halophytes, a term derived from the Greek words (*halos*: "salt" and *phyton* "plant"), are ecologically, physiologically, and biochemically specialized plants which able to survive, grow, and complete their life cycle at salt concentrations of 200 mM NaCl or higher. Although halophytes represent only about 1% of global flora, they encompass a rich taxonomic diversity. The initial database of halophytes included 1,560 species distributed across 550 genera and 117 families. This list was later significantly expanded to around 5,000 to 6,000 species, accounting for about 20% to 30% of the terrestrial halophytic flora, and representing approximately 2% of all angiosperm species worldwide **(Mann *et al.*, 2023)**.

2. Worldwide geographical distribution and habitat

Halophytes thrive in diverse saline habitats, including coastal environments like salt marshes, as well as inland ecosystems such as salt deserts and salt flats. These environments are mainly associated with saline soils, salt marshes, and mangrove ecosystems.

Mediterranean regions of Africa and Europe, the Arabian Peninsula, Southwest Asian countries including Pakistan, India, and Afghanistan, as well as East Asian countries including China and Thailand, represent major areas where halophyte species are widely distributed **(Ferreira et *al.*, 2022)**.

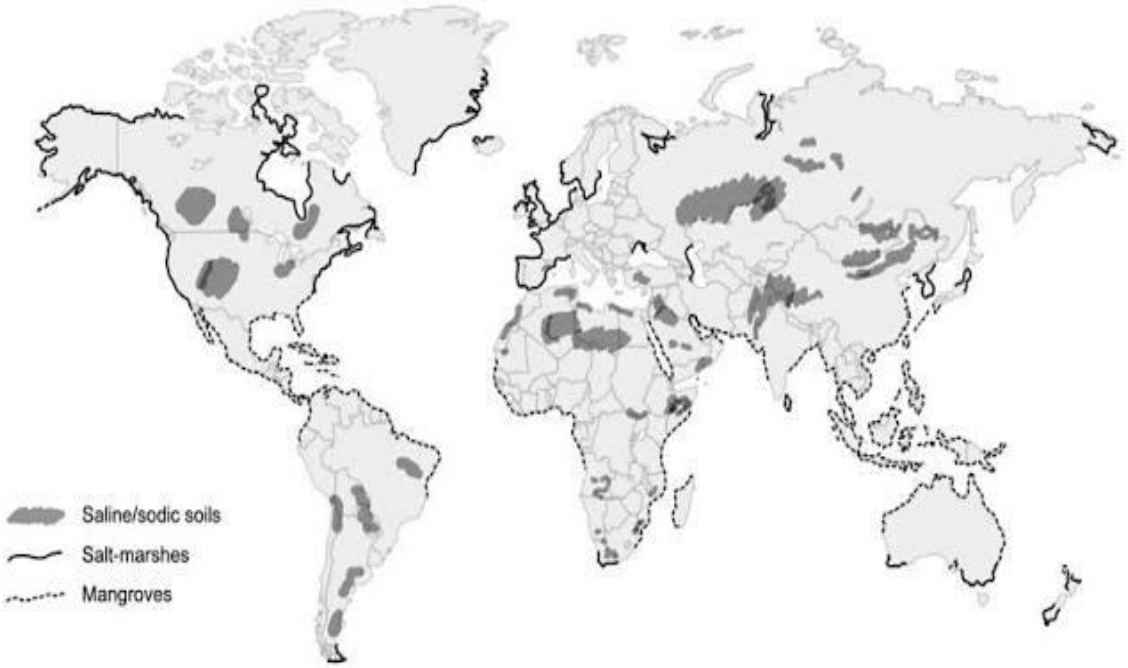


Figure 10. Global distribution of halophyte habitats in relation to soil types **(Ferreira et *al.*, 2022)**.

3. Classification

Halophytes have been classified according to various ecological, physiological, and morphological criteria, reflecting the diversity of their adaptive strategies to saline environments.

Table 04. Classification of halophytes.

Criteria	class of halophytes	Description	Reference
Habitat salinity	Miohalophytes Euhalophytes	Grow in low salinity soil (< 1% NaCl) Grow in high salinity soil (≥ 1% NaCl)	**(Chapman, 1942)**
Response to salinity	Euhalophytes Pseudohalophytes	Salt-tolerant or salt-requiring plants Avoid salt stress	**(Waisel, 1972)**
Ecological behavior	Obligate halophytes Facultative halophytes Habitat-indifferent halophytes	Require saline conditions to grow Tolerate salt but grow better without it Grow in both saline and non-saline habitats	**(Von Sengbusch, 2003)**
Salt regulation	Salt excluders Salt accumulators Salt excreters	Prevent salt entry at roots Store salts in tissues Remove salt through glands or leaves	**(Yensen and Biel, 2006)**
Morpho-anatomical adaptation	Extreme halophytes Mesohalophytes Glycophytes	Strong structural adaptations Intermediate adaptations No salt adaptation structures	**(Grigore and Toma, 2010)**

4. Mechanisms of adaptation to saline environments

Halophytes have evolved a range of adaptive mechanisms that enable them to survive and reproduce under saline conditions. These mechanisms include morphological, anatomical, and physiological adaptations, which collectively maintain water balance, ion homeostasis, and normal metabolic activity.

4.1. Morphological adaptations

Halophytes exhibit several morphological traits that reduce salt stress, including leaf and stem succulence for water storage, salt glands or salt hairs for salt secretion, and leaf shedding to eliminate excess salts. Many species also develop specialized root systems, such as stilt roots for support and pneumatophores for gas exchange in waterlogged soils **(Taia, 2020)**.

4.2. Anatomical adaptations

Anatomically, halophytes possess a thick cuticle, multilayered epidermis, sunken stomata, and wax or trichome coverings, which reduce water loss. They also exhibit specialized internal tissues that enhance water storage and contribute to salt tolerance **(Taia, 2020)**.

4.3. Physiological adaptations

Physiological adaptation involves limiting Na^+ uptake, sequestering excess ions into vacuoles, and secreting salts through specialized structures. Osmotic adjustment, antioxidant defense systems, and, in some species, mycorrhizal associations further enhance tolerance to saline and nutrient-poor environments **(Taia, 2020)**.

5. Phytochemical compositions

The adaptive mechanisms of halophytes involve the biosynthesis of a wide range of bioactive compounds that enhance stress tolerance and exhibit diverse biological activities. The major classes of these compounds include:

- **Phenolic compounds and flavonoids**: extensively studied for their antioxidant, antimicrobial, anti-inflammatory, anticancer, and antimutagenic properties, as well as their beneficial effects on human health.
- **Saponins and alkaloids:** involved in plant defense against herbivores and pathogens while also exhibiting important medicinal properties.
- **Triterpenes and sterols:** responsible for maintaining cell membrane integrity and enhancing tolerance to environmental stresses.
- **Osmoprotectants:** including glycine betaine and proline, which maintain cellular function and osmotic balance under saline conditions **(Lopes et *al.*, 2023)**.

6. Potential applications

6.1. Phytoremediation of saline and polluted soils

Halophytes improve soil and water quality by removing excess salts and, in some cases, accumulating heavy metals. Their use in the rehabilitation of degraded lands and wastewater treatment makes them valuable for sustainable environmental management **(Hameed et *al.*, 2024)**.

6.2. Food security in arid and saline regions

Halophytes provide food and forage resources in areas where conventional crops are constrained by salinity and limited freshwater. Their cultivation offers a sustainable strategy

to enhance agricultural productivity under harsh environmental conditions **(Hameed et *al.*, 2024)**.

6.3. Environmental conservation and ecosystem services

These plants play a key role in coastal protection, soil stabilization, carbon sequestration, and biodiversity conservation. They also contribute to ecosystem restoration and support nature-based tourism initiatives **(Hameed et *al.*, 2024)**.

6.4. Medicinal compounds and essential oil production

Halophytes are a rich source of bioactive compounds with pharmaceutical potential, including antioxidant, antimicrobial, and anti-inflammatory activities. Their essential oils also have applications in the food and cosmetic industries **(Hameed et *al.*, 2024)**.

6.5. Bioenergy and biofuel production

Halophytes can be cultivated on marginal lands as feedstocks for bioethanol, biodiesel, and biogas production. Their use supports renewable energy development while minimizing competition with conventional food crops **(Hameed et *al.*, 2024)**.

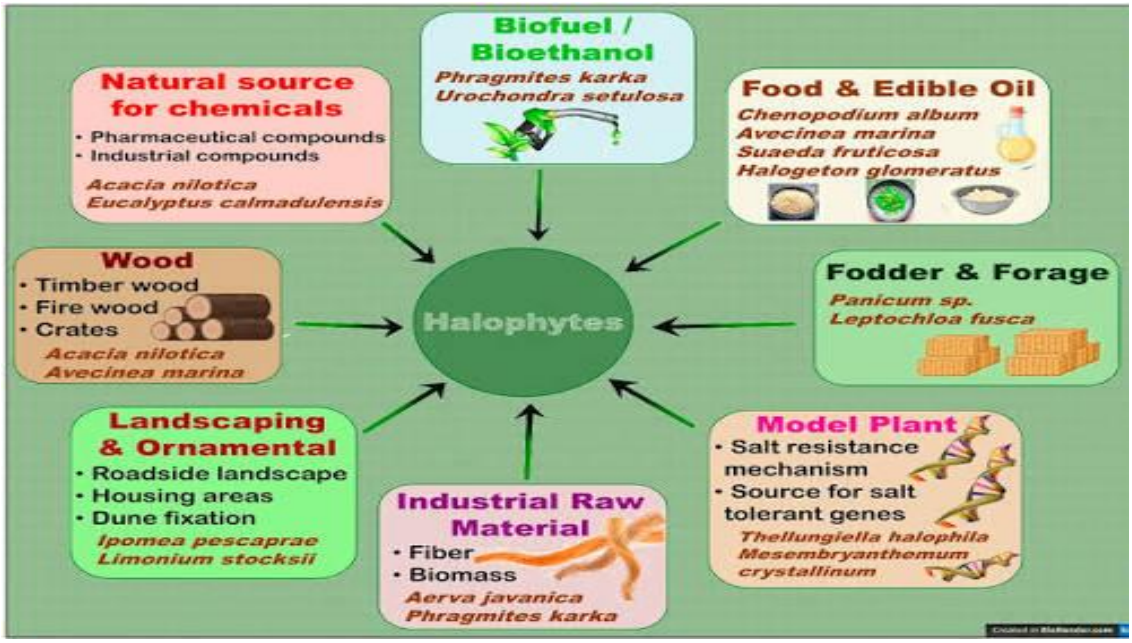


Figure 11. Potential uses of some halophyte species **(Hameed et *al.*, 2024)**.

II. Presentation of the studied halophytes

1. *Atriplex halimus*

1.1. Morphological description

Atriplex halimus, commonly known as «Mediterranean saltbush» or «shrubby» in English, « pourpier de mer » , «arroche marine» or «arroche halume» in French, «salado/a» in Spanish, «alismo» in Italian, and «Gettaf» or «Raghl» in Arabic, is a perennial shrub belonging to the family Amaranthaceae. It is characterized by a highly branched, bushy habit, typically reaching heights of 1.5 to 3 meters and spreading up to 2.4 meters in width. Its deep, horizontally spreading whitish roots allow it to efficiently access soil moisture even under extreme arid conditions.

The plant has small evergreen leaves (10–30 mm long and 5–20 mm wide), which are alternate, entire, and vary in shape from oval to rhomboid. The silvery-grey coloration of the foliage is due to lobed hairs on the surface—an important morphological adaptation that reduces water loss through transpiration. Additionally, fine scales cover both leaves and stems, giving the plant a distinctive velvety appearance **(Walker et *al*., 2014; Tadj et *al*., 2024)**.

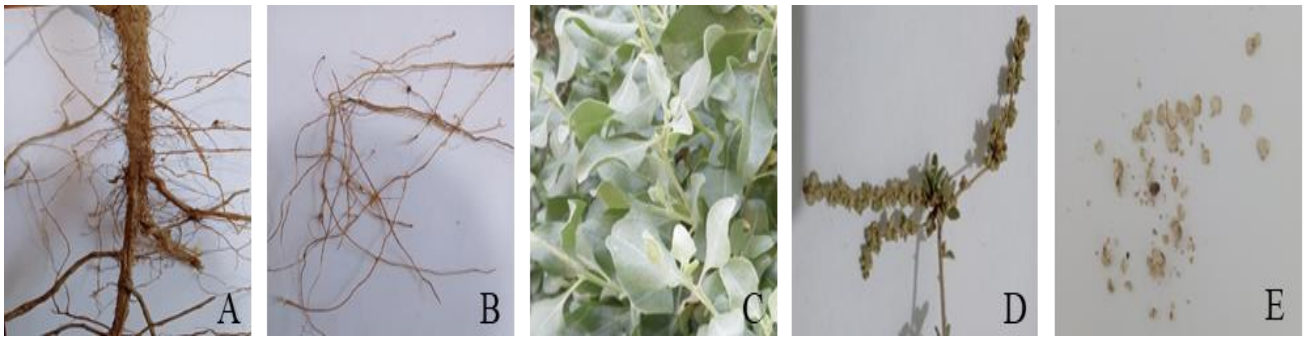


Figure 12. Morphology of *A. halimus*

A: Roots, **B:** Stems, **C:** Leaves, **D:** Flowers, **E:** Seeds **(original, 2024)**.

Taxonomically, *A. halimus* is generally divided into two subspecies, based on distinct morphological characteristics:

Atriplex halimus subsp. *halimus* is characterized by a more upright growth habit and smaller overall size (0.5 to 2.0 meters in height). Its fruiting branches are relatively short (0.2 to 0.5 meters), and the upper branches often exhibit twisted leafy stems arranged in a somewhat scorpioid pattern. The leaves are typically hastate, greenish when young, turning silvery-grey with age. The fruit valves are kidney-shaped with entire (smooth) margins.

Atriplex halimus subsp. *schweinfurthii* grows larger, reaching 1.0 to 3.0 meters in height, with longer fruiting branches (0.5 to 1.0 meters) that are rigid, leafless, and often reddish in color. Leaf morphology is highly variable, with differences in shape, size, and color (ranging from green to greyish). Like the previous subspecies, its fruit valves are also kidney-shaped, but they display weakly toothed margins **(Walker et *al*., 2014).**



Figure 13. Morphological comparison of the two subspecies of *A. halimus*: *A. halimus* subsp. *schweinfurthii* (left) and *A. halimus* subsp. *halimus* (right) in the Region of Murcia (Spain) **(Walker et *al.*, 2014).**

1.2. Taxonomic classification

Table 05. Botanical classification of *Atriplex halimus* **(Quézel and Santa, 1962; Dupont and Guignard, 2007)**

Taxonomic Rank	**Classification**
Kingdom	Plantae
Subkingdom	Tracheobionta
Phylum (Division)	Spermatophyta
Subphylum (Subdivision)	Angiosperms
Class	Dicotyledons
Subclass	Pre-asterids
Order	Caryophyllales
Suborder	Amaranthaceae
Family	Chenopodiaceae
Genus	*Atriplex*
Species	*Atriplex halimus L*
Subspecies	*Atriplex halimus ssp schweinfurthi*

1.3. Geographical distribution

Atriplex halimus is widely distributed in arid and semi-arid regions around the Mediterranean basin. It is found in southern European countries such as Portugal, Spain, Italy, Greece, Malta, and Cyprus. Small populations also exist in France, Brittany and surrounding islands; in North African countries including Tunisia, Algeria, Libya, Egypt, and Morocco; and in Middle Eastern countries such as Jordan, Turkey, Lebanon, Syria and Saudi Arabia.

It has also been introduced to several other regions worldwide, such as sub-Saharan Africa, South America, Oceania, and, in equatorial regions like Kenya and Ethiopia, limited photoperiod variation prevents it from flowering **(Walker et *al*., 2014)**.

1.4. Uses

The nutritional and energetic value of sea orache (*A. halimus*) has contributed to its traditional use as a forage source for livestock, as well as a functional food. It is rich in fiber, protein, mineral salts, vitamins A, C, and D, as well as alkaloids and flavonoids, making it a valuable source of biologically active compounds.

Traditionally, the decoction of *A. halimus* leaves is used as a blood purifier and in the treatment of heart diseases, anemia, diabetes, rheumatism, fever, urinary tract inflammations (such as cystitis), urinary stones, and for the protection of liver tissues against cancer **(Ali et *al*., 2021)**.

Furthermore, *A. halimus* exhibits various biological activities, including antifungal, antimicrobial, antidiabetic, hypoglycemic, and antioxidant properties, reinforcing its potential use in phytotherapy **(Ali et *al*., 2021)**.

2. *Limbarda crithmoides*

2.1. Morphological description

Limbarda crithmoides (L.) Dumort. (syn. *Inula crithmoides*), commonly known as golden samphire, is a perennial halophytic species of the family Asteraceae, widely distributed in Mediterranean and Atlantic coastal regions. It is a robust subshrub, typically reaching 30–100 cm in height, forming dense and rounded stands in saline coastal habitats **(Brzović et al., 2025)**

The stems are erect to ascending, woody at the base, and strongly branched. Young shoots are green, slightly succulent, and become progressively lignified with age. The leaves are alternate, simple, and fleshy, ranging from linear to oblanceolate in shape, usually entire

and occasionally slightly toothed at the apex. They measure approximately 20–60 mm in length, and their succulent tissues and thick cuticle contribute to water storage and salt tolerance under highly saline conditions **(Hoornaert et *al*., 2026)**.

The inflorescences are terminal corymbs composed of numerous capitula. Each capitulum contains yellow ligulate and tubular florets, which bloom from July to October. The involucre consists of several rows of bracts protecting the florets before anthesis. The fruit is a small cypsela (achene-like fruit) crowned with a pappus of fine bristles that facilitates wind dispersal **(Tutin et *al*., 1976)**.



Figure 14. Morphology of *L. crithmoides*
A: Roots, **B:** Stems, **C:** Leaves, **D:** Flowers, **E:** Fruit **(original, 2024)**.

2.2. Taxonomic classification

Table 06. Botanical classification of *L. crithmoides* **(Castroviejo, 2017)**

Taxonomic Rank	**Classification**
Kingdom	Plantae
Phylum	Streptophyta
Class	Equisetopsida
Subclass	Magnoliidae
Order	Asterales
Family	Asteraceae
Subfamily	Asteroideae
Tribe	Inuleae
Genus	*Limbarda*
Species	*Limbarda crithmoides* (L.) Dumort.

2.3. Geographical distribution

L. crithmoides is broadly distributed along the Atlantic and Mediterranean coastlines, where it colonizes salt marshes, estuaries, coastal lagoons, tidal flats, and other saline wetlands. Its Atlantic range includes Portugal, Spain, France, Ireland, and the United Kingdom, whereas its Mediterranean distribution extends across Spain, France, Italy, Slovenia, Croatia, Bosnia and Herzegovina, Montenegro, Albania, Greece, Malta, and Cyprus. In North Africa, the species is native to Morocco, Algeria, Tunisia, Libya, and Egypt, while in western Asia it is found along the eastern Mediterranean coasts of Turkey, Syria, and Lebanon **(Fontana et *al*., 2014; Hoornaert et *al*., 2026)**.

2.4. Uses

L. crithmoides is an edible halophytic plant whose young leaves and shoots are commonly consumed fresh, cooked, or pickled in vinegar. It is traditionally eaten in several Mediterranean countries, particularly Lebanon, Spain, and Italy. Owing to its high nutritional value and desirable sensory attributes, including its pleasant flavor and texture, L. crithmoides has been highly appreciated by culinary experts and is considered a promising species for human consumption and food applications **(Rodrigues et *al*., 2023)**.

Beyond its nutritional importance, the species is also widely used in traditional medicine for the treatment of bronchitis, tuberculosis, anemia, malaria, and urinary tract disorders **(Petropoulos et *al*., 2018)**.

In addition, phytochemical studies have shown that L. crithmoides is rich in iodine, proteins, carotenoids (β-carotene and lutein), water-soluble vitamins (B1 and B6), and essential minerals such as sodium, potassium, and iron **(Rodrigues et *al*., 2023)**.

These bioactive compounds are closely associated with several biological properties, including antioxidant, anti-tyrosinase, antifungal, antibacterial, anticlastogenic, antimutagenic, and herbicidal activities, which further support its potential pharmaceutical and biotechnological applications **(Petropoulos et *al*., 2018)**.

3. *Suaeda fruticosa*

3.1. Morphological description

Suaeda fruticosa ex J.F. Gmel, (synonym: *Suaeda vera*), commonly known as «shrubby seablite» in English, «soude ligneuse» in French, and «السويدا الشجيرية» in Arabic, is an edible and medicinal halophyte belonging to the Amaranthaceae family (formerly Chenopodiaceae) **(Saleem et *al*., 2021)**. This species develops as a dense, dark green succulent shrub that can reach up to 50 cm in height. Its woody stem becomes highly branched with age, while the young branches are initially pubescent before turning glabrous at maturity. The shoots of this halophyte change their colour between seasons, namely from green in spring to red-violet in the summer. The leaves are alternate, fleshy, and generally linear with a rounded cross-section. They measure between 5 and 30 mm in length and 0.5 to 1.5 mm in width, exhibiting a glabrous or slightly glabrescent surface. The small flowers are arranged in axillary spikes containing three to five flowers and are subtended by a leafy bract longer than the flower, together with two shorter membranous bracteoles. The green perianth consists of five nearly equal segments surrounding five stamens with yellow anthers and a superior ovary. The fruit is a membranous achene **(Miller and Morris, 1988)**.



Figure 15. Morphology of *S. fruticosa*
A: Flowering branch, **B:** Male flower, **C:** Stamen, **D:** Fruit, **E:** Seed, **F:** Seed (longitudinal section) **(Quézel and Santa, 1962)**.

3.2. Taxonomic classification

Table 07. Botanical classification of *S. fruticosa* **(Quézel and Santa, 1962)**.

Taxonomic Rank	**Classification**
Kingdom	Plantae
Phylum	Streptophyta
Class	Equisetopsida
Subclass	Magnoliidae
Order	Caryophyllales
Family	Amaranthaceae
Genus	*Suaeda*
Species	*Suaeda fruticosa*

3.3. Geographical distribution

S. fruticosa is widely distributed along the coasts of North Africa and the Mediterranean region, as well as along the Atlantic coasts of Portugal and southern Spain. It is also reported in France, southeastern England, the Arabian Peninsula, Southwest Asia (Afghanistan, Pakistan, and Iran), India and Bangladesh, the Canary Islands, and over the saline regions in southern Africa. This species typically grows in a wide range of halophytic habitats, including sandy salt marshes, coastal alluvial flats subjected to flooding, clayey soils, arid areas, salt plains, and dry foothill regions **(Ahmad et *al*., 2021)**.

3.4. Uses

From an ecological perspective, *S. fruticosa* is used in phytoremediation to reduce soil salinity and contributes to remediate soils contaminated with heavy metals. Due to its high salt content, it is rarely utilized as a sole fodder crop and is instead mainly incorporated into animal feed mixtures **(Saleem et *al*., 2021)**.

Traditionally, leaves, flowers, fruits, and seeds of plant are administered orally in different forms such as powder, decoction, juice, or combined with oil. The species has long been used in folk medicine for the treatment of gastrointestinal disorders, particularly diarrhea, as well as for rheumatism, gout, conjunctivitis, influenza, cough, toothache, and various skin diseases **(Ayaz et *al*., 2022)**. In addition, recent pharmacological studies have reported a range of biological activities, including antioxidant, anti-inflammatory, anticancer, hepatoprotective, hypolipidemic, hypoglycemic, and gastroprotective effects **(Ayaz et *al*., 2022)**.

Chapter 3: Presentation of phenolic compounds

1. Definition

Phenolic compounds, also known as polyphenols, are among the most abundant secondary metabolites synthesized exclusively by Plant Kingdom which are present in fruits, vegetables, green tea, and whole grains. To date, more than 8,000 polyphenolic compounds have been identified and reported in the literature. Structurally, polyphenols are characterized by the presence of one or more aromatic rings bearing one or several hydroxyl (–OH) groups. This structural diversity is responsible involved in important roles in plants, such as pigmentation, growth and reproduction functions, protection against ultraviolet (UV) radiation, resistance to pathogens and herbivores, and many other functions **(González-Sarrías et *al*., 2020; Prabhu et *al*., 2021)**.

2. Classification

Phenolic compounds exhibit considerable structural diversity but are all characterized by the presence of one or more hydroxyl groups attached to one or more aromatic rings. Based on their chemical structure, they are classified into different groups or classes.

2.1. Simple phenolic compounds

Simple phenolic compounds are the simplest class of phenolics, consisting of a single aromatic ring (C6 skeleton) bearing one or more hydroxyl groups and various substituents. These substituents may occupy the ortho (o), meta (m), or para (p) positions relative to the hydroxyl group, giving rise to different structural derivatives and chemical properties **(Al Mamari, 2022)**.

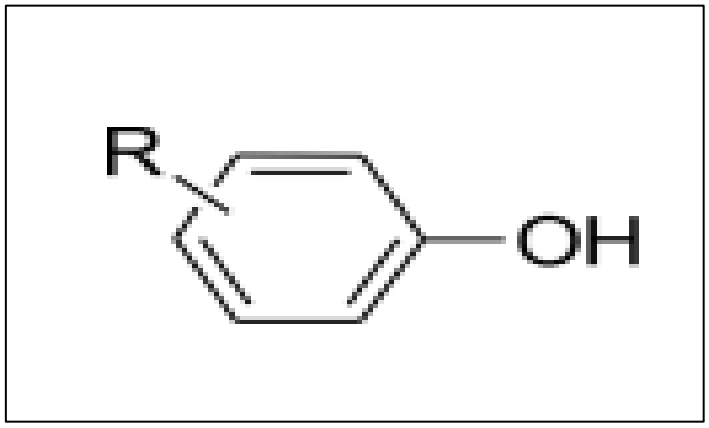


Figure 16. General structure of simple phenolic compounds **(Al Mamari, 2022)**.

2.1.1. Phenolic acid

Phenolic acids constitute one of the largest groups of plant phenolic compounds. They are characterized by the presence of an aromatic ring bearing a carboxylic acid (-COOH) functional group and are generally classified into two main subclasses: hydroxybenzoic acids and hydroxycinnamic acids **(Prabhu et *al.*, 2021; Al Mamari, 2022)**.

2.1.1.1. H ydroxybenzoic acid

Hydroxybenzoic acids are C6–C1 phenolic compounds derived from benzoic acid ($C_7H_6O_2$). They occur predominantly in bound forms within plant tissues and serve as fundamental building blocks for more complex phenolic structures, particularly hydrolyzable tannins **Prabhu et *al.*, 2021)**.

2.1.1.2. Hydroxycinnamic acid

Hydroxycinnamic acids are C6–C3 phenolic acids derived from cinnamic acid ($C_9H_8O_2$).They are distinguished by the presence of a three-carbon side chain containing a carbon–carbon double bond (C=C) that separates the aromatic ring from the carboxylic acid (–COOH) group **(Prabhu et *al.*, 2021)**.

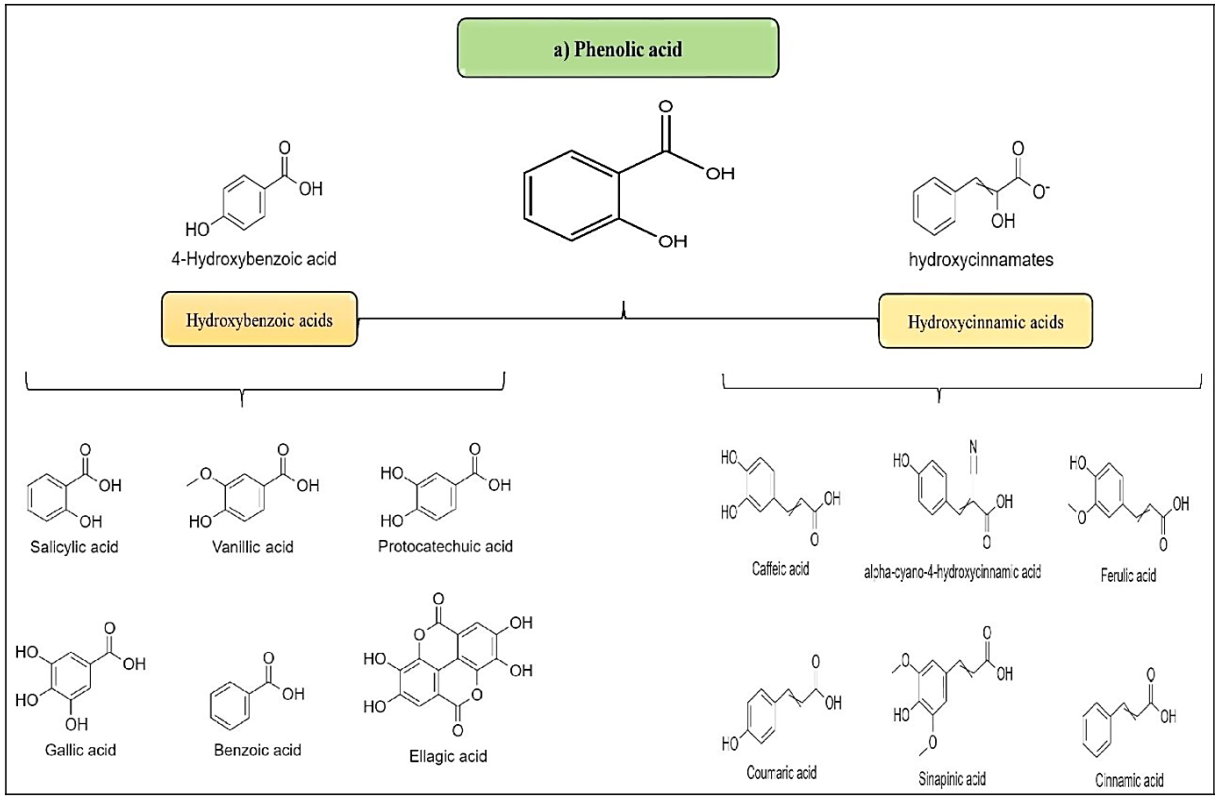


Figure 17. Main subclasses of phenolic acids and their representative compound **(Prabhu et *al.*, 2021)**.

2.2. Polyphenols

Polyphenols are phenolic compounds containing two or more phenolic rings with one or more hydroxyl groups. They constitute a large and diverse group of plant secondary metabolites, including flavonoids, tannins, stilbenes, and lignans **(Al Mamari, 2022)**.

2.2.1. Flavonoids

Flavonoids constitute the largest class of polyphenols, with more than 5,000 compounds identified in dietary plants. They are generally present as glycosides, most commonly conjugated with sugars such as glucose, rhamnose, xylose, or galactose. Structurally, flavonoids possess a C6–C3–C6 carbon skeleton consisting of two aromatic rings (A and B) linked by a three-carbon bridge that forms a heterocyclic oxygen-containing pyran ring (C). Based on variations in this basic structure, flavonoids are classified into seven major subclasses: flavones, flavanones, isoflavones, flavonols, chalcones, flavanols, and anthocyanins **(Al Mamari, 2022; Chen et *al*., 2023)**.

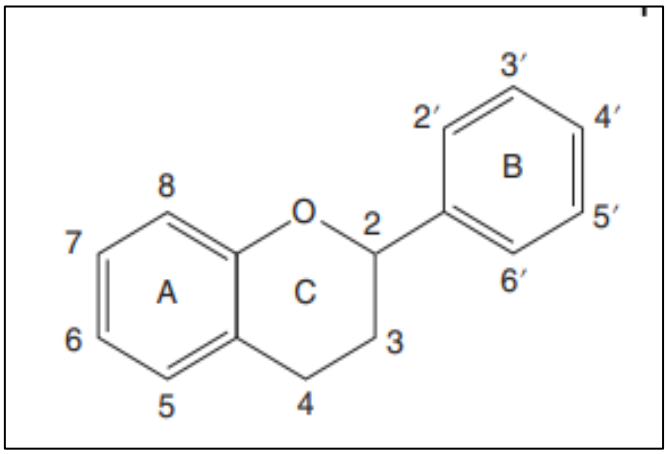


Figure18. General structure of flavonoid **(Al Mamari, 2022)**.

2.2.1.1. Flavones

Flavones are a major subclass of flavonoids characterized by a 2-phenylchromen-4-one backbone, featuring a C2=C3 double bond and a carbonyl group at the C4 position. They are commonly hydroxylated at C5 and C7 of the A-ring and at C3′ and C4′ of the B-ring. Flavones also frequently undergo glycosylation, mainly at C5 and C7, as well as methylation and acylation of their hydroxyl groups. Among flavones, apigenin, luteolin, baicalein, chrysin, and their derivatives are the most abundant **(Zhuang et *al*., 2023)**.

2.2.1.2. Flavonols

Flavonols share the same basic structure as flavones but possess an additional hydroxyl group at the C3 position (3-hydroxyflavones). They are among the most abundant flavonoids in plants, occurring predominantly as glycosides, with kaempferol, quercetin, limocitrin, and isorhamnetin representing the principal flavonols **(González-Sarrías et *al.*, 2020)**.

2.2.1.3. Flavanones

Flavanones and dihydroflavonols differ from flavones and flavonols by the absence of the C2=C3 double bond due to hydrogenation of the heterocyclic C ring. They are commonly present as O-glycosides, most frequently glycosylated at the C7 hydroxyl group with rutinosyl or neohesperidosyl sugar moieties. The principal flavanones are naringenin, hesperetin, and their derivatives **(González-Sarrías et *al.*, 2020)**.

2.2.1.4. Isoflavones

Isoflavones are distinguished from other flavonoids by the attachment of the B ring to the C3 position of the heterocyclic C ring rather than C2. They are found almost exclusively in leguminous plants, mainly as β-glucosides and their acetyl or malonyl derivatives, and exhibit considerable structural diversity depending on the oxidation state of their backbone **(González-Sarrías et *al.*, 2020)**.

2.2.1.5. Neoflavonoids

Neoflavonoids are a rare subclass of flavonoids characterized by a 4-phenylcoumarin backbone and the absence of a hydroxyl group at the C2′ position. They occur infrequently in food plants and are classified into four main structural groups: dalbergiones (dalbergia quinones), dalbergin-type lactones, dalbergia phenols, and benzoylbenzenes **(Zhuang et *al.*, 2023)**.

2.2.1.6. Flavanols

Flavanols (flavan-3-ols) are 3-hydroxylated derivatives of flavanones characterized by the absence of the C2=C3 double bond in the heterocyclic C ring and the presence of a hydroxyl group at the C3 position. They constitute an important subclass of flavonoids and include catechin, epicatechin, gallocatechin, epigallocatechin, and their gallate derivatives (e.g., catechin gallate, epicatechin gallate, and gallocatechin gallate) **(Zhuang et *al.*, 2023)**.

2.2.1.7. Anthocyanidins

Anthocyanidins are naturally occurring plant pigments responsible for the red, blue, purple, and orange coloration of many fruits and vegetables. They occur as the aglycone forms of anthocyanins and are characterized by a 2-phenylbenzopyrylium (flavylium) cation bearing hydroxyl and methoxyl substituents at different positions on the basic skeleton **(Brodowska, 2017)**.

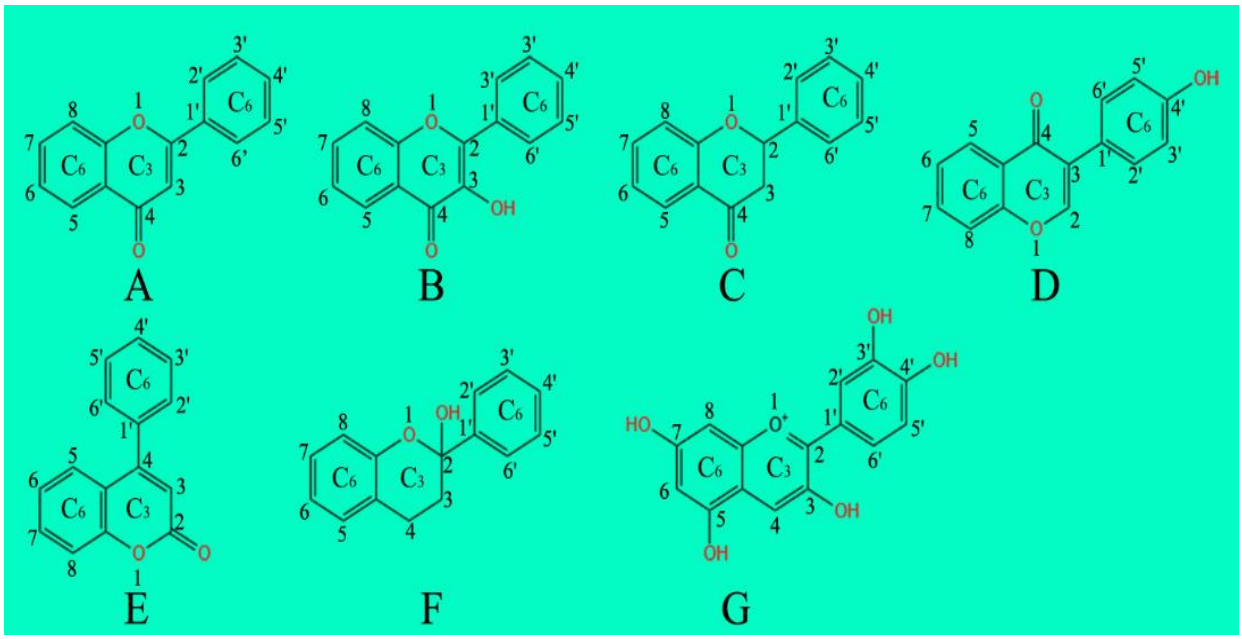


Figure 19. Chemical structures of flavonoid compounds **(A)** Flavones**; (B)** Flavonols**; (C)** Flavanon **(D)** Isoflavonoids**; (E)** Neoflavonoids**; (F)** Flavanols**; (G)** Anthocyanidin **(Zhuang et *al.*, 2023)**.

2.2.2. Tannins

Tannins are a major group of plant secondary metabolites belonging to the polyphenol family. Their chemical structure is characterized by multiple phenolic hydroxyl groups attached to a polyphenolic backbone, enabling strong interactions with proteins, polysaccharides, and metal ions. They are generally classified into four categories: hydrolyzable tannins, condensed tannins, complex tannins, and pseudo-tannins.

Hydrolyzable tannins are composed of a central polyol, typically glucose, esterified with phenolic acids such as gallic acid or ellagic acid. In contrast, condensed tannins, also known as proanthocyanidins, are oligomeric or polymeric flavonoids composed of flavan-3-ol subunits, such as catechin and epicatechin, interconnected by stable carbon–carbon linkages **(Cosme et *al.*, 2025)**.

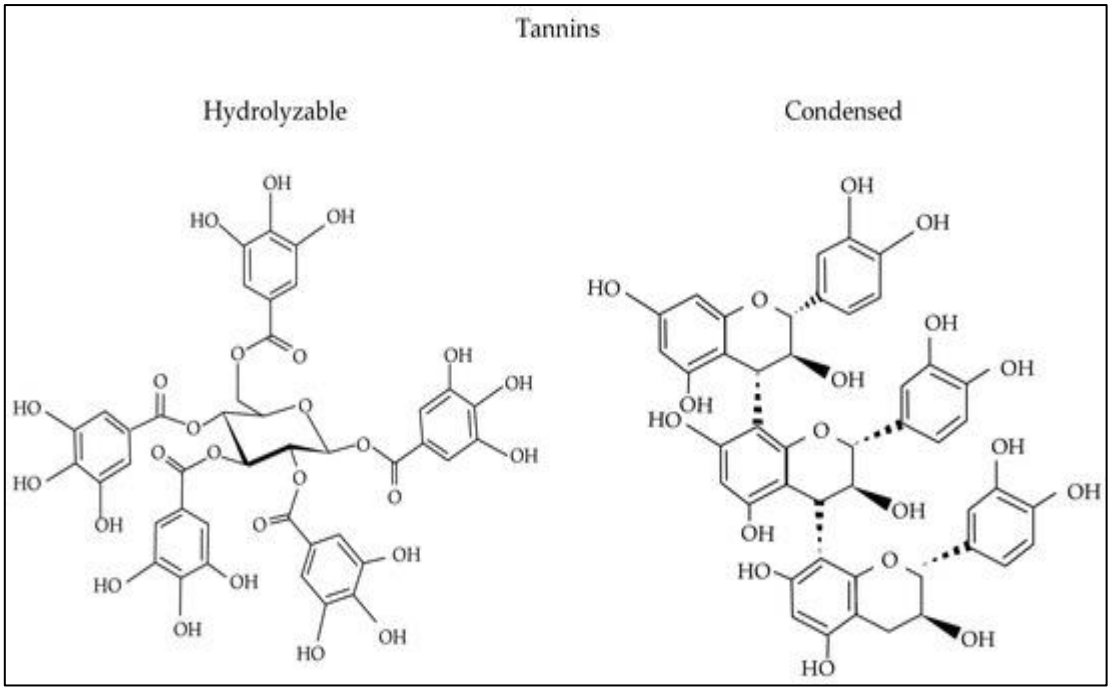


Figure 20. Main chemical structures of tannins **(Cosme et *al*., 2025)**.

2.2.3. Stilbenes

Stilbenes are a minor class of polyphenols characterized by two aromatic rings linked by a two-carbon bridge. In plants, they mainly function as phytoalexins produced in response to pathogen attack or injury. Resveratrol is the most well-known stilbene (**Pandey and Rizvi, 2009)**.

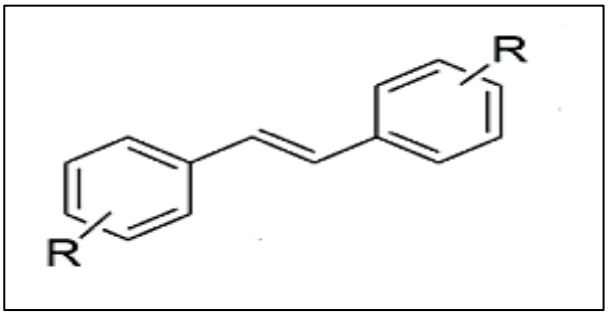


Figure 21. General structure of Stilbenes **(Al Mamari, 2022)**.

2.2.4. Lignans

Lignans are diphenolic compounds formed through the dimerization of two cinnamic acid derivatives, resulting in a characteristic 2,3-dibenzylbutane structure. Some lignans, such as secoisolariciresinol, exhibit phytoestrogenic properties, with flaxseed being their richest dietary source (**Pandey and Rizvi, 2009)**.

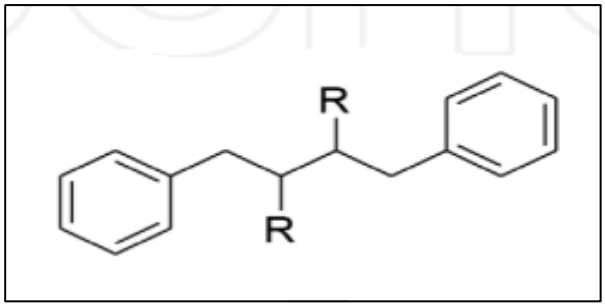


Figure 22. General structure of Lignans **(Al Mamari, 2022)**

3. Biosynthesis

The biosynthesis of phenolic compounds is primarily governed by the shikimate and acetate–malonate pathways, which are closely interconnected.

The shikimate pathway produces the aromatic amino acid L-phenylalanine, the main precursor of most plant phenolics. The conversion of L-phenylalanine into trans-cinnamic acid by phenylalanine ammonia-lyase (PAL), the key regulatory enzyme of the phenylpropanoid pathway, represents the first committed step in phenolic biosynthesis. Trans-cinnamic acid subsequently undergoes a series of hydroxylation, reduction, and oxidation reactions to generate hydroxycinnamic acids and other important phenolic intermediates, including hydroxybenzoic acids, coumarins, lignin precursors, and chlorogenic acid derivatives **(Hu et *al*., 2022; Zagoskina et *al*., 2023)**.

In parallel, the acetate–malonate pathway provides malonyl-CoA, which condenses with p-coumaroyl-CoA through the action of chalcone synthase (CHS) to produce chalcones, the universal precursors of flavonoids. Chalcones are then converted by chalcone isomerase (CHI) into naringenin, which serves as a central intermediate for the biosynthesis of diverse flavonoid subclasses, including flavones, flavonols, flavanones, anthocyanins, flavan-3-ols, and condensed tannins (proanthocyanidins). The biosynthesis and accumulation of these phenolic compounds are tightly regulated by a coordinated network of biosynthetic enzymes and transcription factors, particularly members of the MYB family **(Hu et *al*., 2022; Zagoskina et *al*., 2023)**.

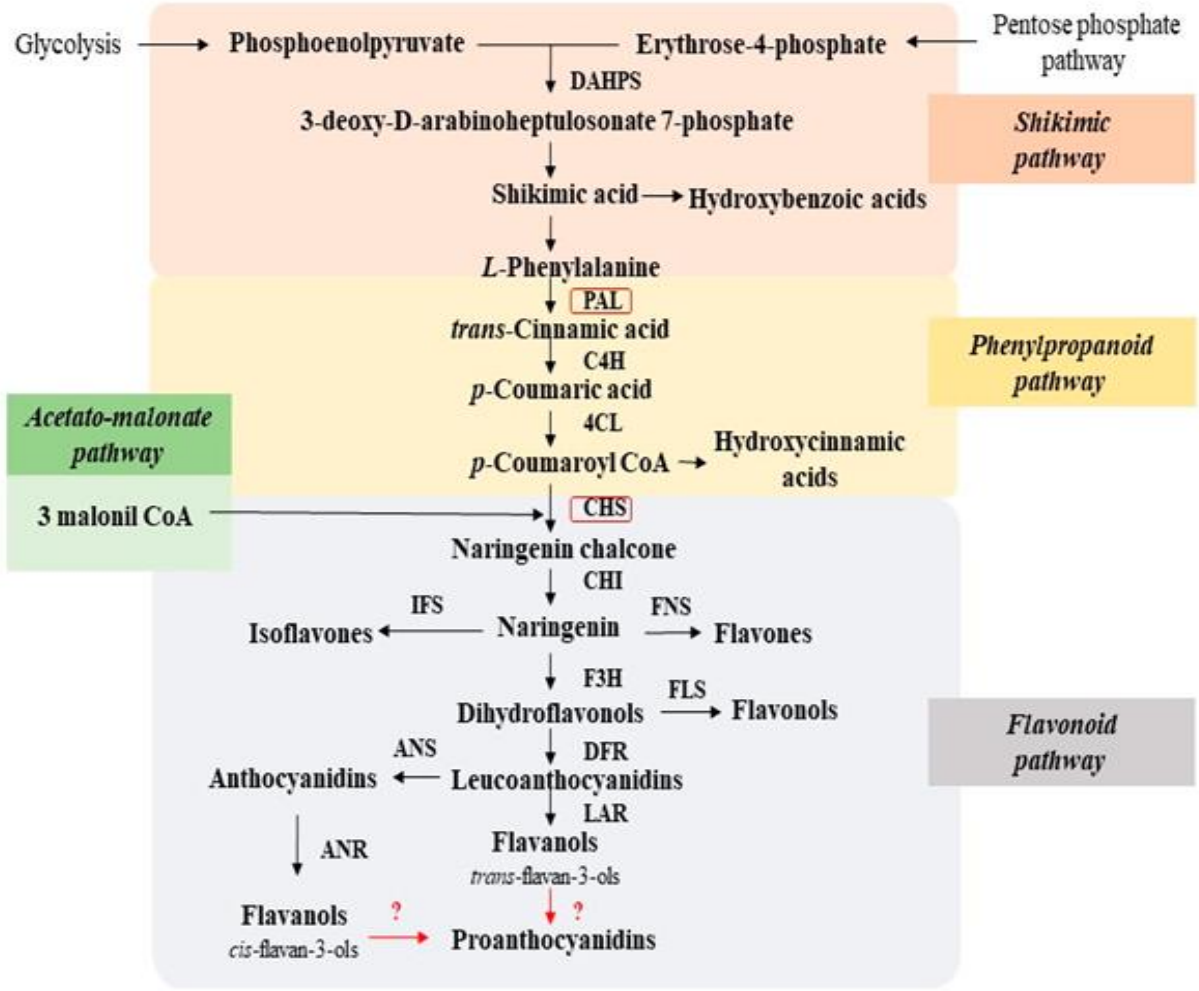


Figure 23. Biosynthesis pathway of phenolic compounds **(Zagoskina et *al*., 2023)**.

4. Extraction methods

Extraction is a crucial step for the isolation of bioactive metabolites, including phenolic compounds, flavonoids, and tannins. It represents the first and essential stage in the recovery of phytochemicals from plant materials for applications in food, pharmaceutical, and cosmetic industries **(Sridhar et *al*., 2021)**.

4.1. Conventional extraction methods

Conventional extraction techniques include maceration, percolation, decoction, heat reflux extraction, and Soxhlet extraction. These methods are widely applied due to their simplicity, low cost, and easy implementation. However, they generally present several limitations, such as long extraction times, high solvent consumption, and relatively lower efficiency in extracting thermolabile or low-abundance compounds **(Sridhar et *al*., 2021)**.

4.2. Non-conventional extraction methods

Non-conventional (or advanced) extraction techniques include ultrasound-assisted extraction, microwave-assisted extraction, supercritical fluid extraction, pulsed electric field extraction, high-voltage electric discharge, enzyme-assisted extraction, membrane-based techniques, and encapsulation-assisted processes. These methods are increasingly adopted due to their higher extraction efficiency, reduced processing time, lower solvent usage, and improved preservation of heat-sensitive compounds. Nevertheless, they also present certain drawbacks, including high capital cost, operational complexity, the requirement for skilled operators, potential scale-up limitations, possible degradation of target compounds under non-optimized conditions, and, in some cases, increased energy demand and limited selectivity **(Sridhar et *al*., 2021)**.

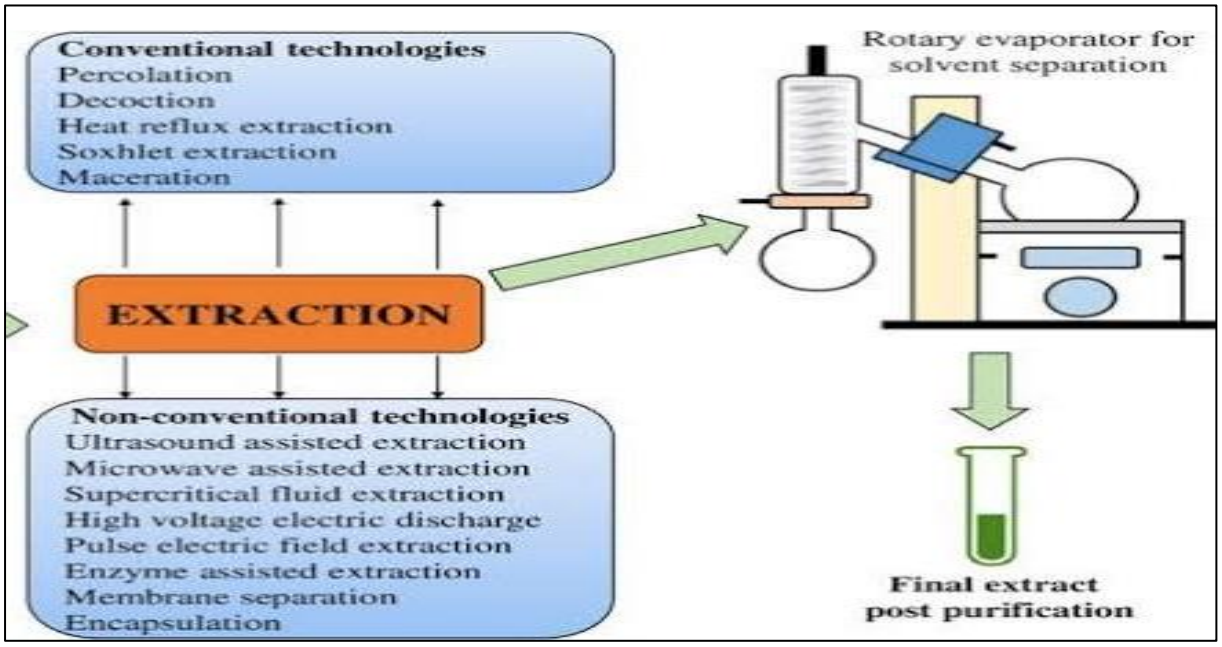


Figure 24. Conventional and non-conventional extraction approaches for phenolic compounds **(Sridhar et *al*., 2021)**.

5. Quantification methods

Several analytical methods have been developed for the quantification of polyphenols, differing in their sensitivity, specificity, and analytical applications. Among them, spectrophotometric assays are the most widely used because they are simple, rapid, and cost-effective. Among these, the Folin–Ciocalteu, aluminum chloride ($AlCl_3$) and vanillin colorimetric assays are the standard methods for determining total phenolic content (TPC), total flavonoid content (TFC), and total condensed tannins, respectively.

Despite their widespread use, these colorimetric methods provide only an estimation of the overall phenolic content and do not allow the identification or accurate quantification of individual compounds.

Therefore, chromatographic techniques, particularly high-performance liquid chromatography (HPLC), are preferred for the separation and quantification of individual polyphenols. Furthermore, liquid chromatography coupled with mass spectrometry (LC–MS) is considered one of the most powerful analytical techniques because of its high sensitivity, selectivity, and ability to identify and characterize phenolic compounds.

Other analytical approaches, including paper chromatography, thin-layer chromatography (TLC), gas chromatography (GC), mass spectrometry (MS), and nuclear magnetic resonance (NMR) spectroscopy, are also employed for the separation, identification, and structural elucidation of polyphenols, especially in advanced phytochemical analyses **(Cutrim and Cortez, 2018)**.

6. Functional properties and health benefits

Phenolic compounds are widely recognized for their numerous beneficial effects on human health. They exhibit strong antioxidant activity mainly through their ability to scavenge free radicals, inhibit oxidative chain reactions, and chelate metal ions involved in oxidative processes.

In addition to these properties, polyphenols also display antimicrobial and anti-inflammatory activities, which help limit the growth of pathogenic microorganisms and modulate inflammatory responses. Furthermore, they are involved in the regulation of various cellular processes, including enzyme activity and signaling pathways associated with cell survival, proliferation, and apoptosis.

Through these mechanisms, polyphenols contribute to the prevention of cellular damage and support overall physiological balance. Their protective effects extend to several pathological conditions, particularly cardiovascular and degenerative diseases, by improving vascular function and reducing oxidative damage in tissues **(Prabhu et *al*., 2021)**.

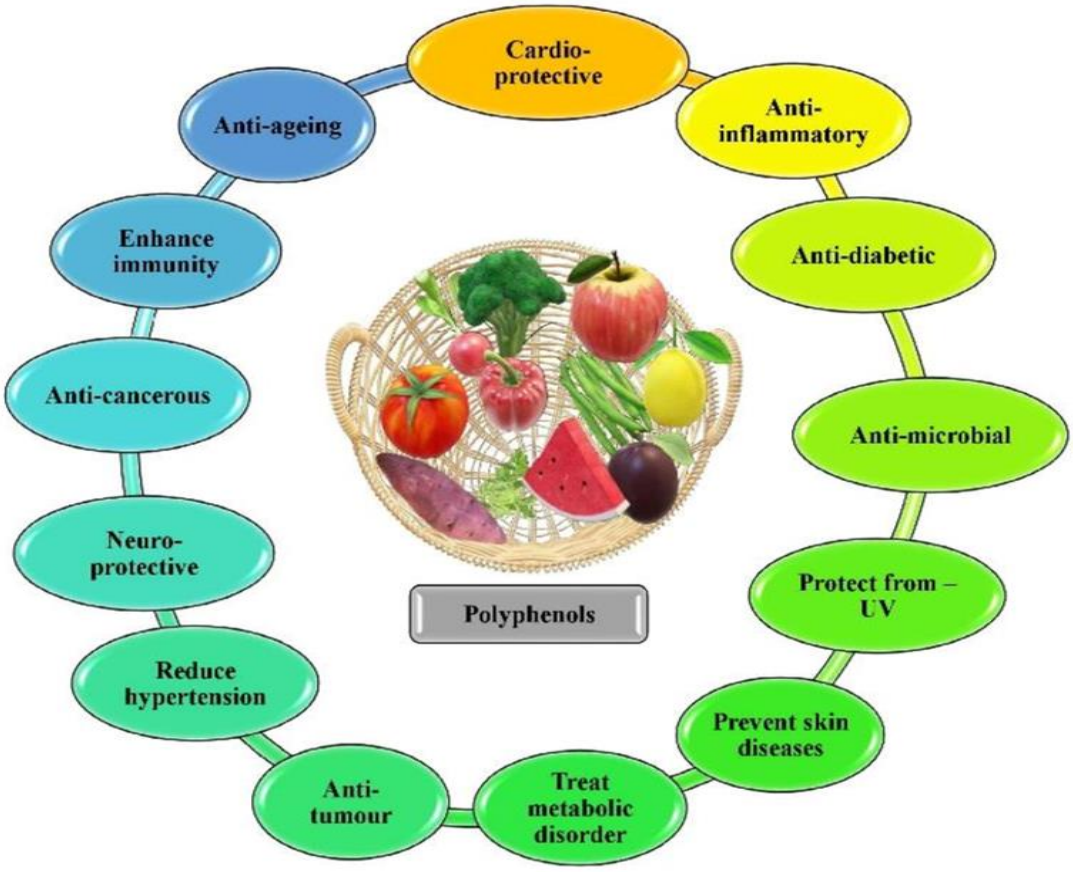


Figure 25. Potential health effects of phenolic compounds on human health and disease **(Prabhu et *al*., 2021)**.

7. Mechanisms underlying antioxidant and insecticidal activities

7.1. Antioxidant mechanisms

The biological activity of phenolic compounds is primarily associated with their antioxidant properties, which are largely determined by their chemical structure, including aromatic rings, conjugated double bonds, and hydroxyl groups.

These compounds protect cells against oxidative stress by scavenging reactive oxygen species (ROS), such as hydroxyl radicals, superoxide anions, hydrogen peroxide, and singlet oxygen, thereby preventing lipid peroxidation, protein oxidation, DNA damage, and other oxidative alterations. Their antioxidant efficiency depends mainly on the number and position of hydroxyl groups, as well as structural modifications such as methylation and esterification. Different classes of phenolic compounds exhibit varying antioxidant capacities; for example, catechin gallates are particularly effective against superoxide radicals, whereas luteolin, kaempferol, and quercetin derivatives show strong radical-scavenging activity **(Zagoskina et *al*., 2023)**.

In addition to directly neutralizing free radicals, phenolic compounds exert antioxidant effects by chelating transition metal ions, inhibiting ROS-generating enzymes, and enhancing endogenous antioxidant defense systems **(Zagoskina et *al*., 2023)**.

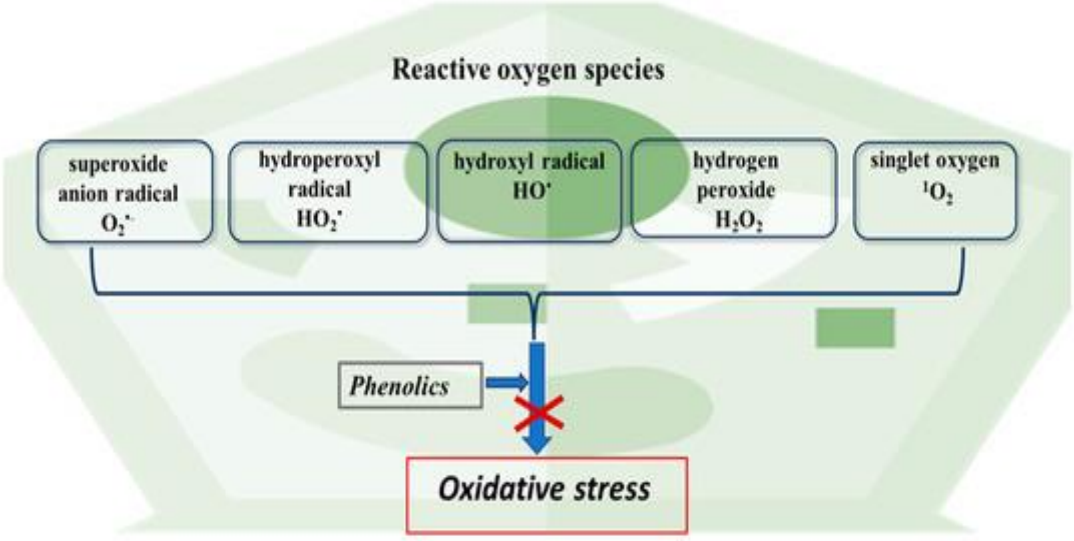


Figure 26. Antioxidant mechanism of phenolic compounds through reactive oxygen species (ROS) scavenging **(Zagoskina et *al*., 2023)**.

7.2. Insecticidal mechanisms

Polyphenols, particularly falvonoids exhibit an important insecticidal activity against insect pests through multiple physiological and biochemical mechanisms.

7.2.1. Oxidative stress and cellular damage

Phenolic acids exert strong insecticidal effects primarily through the induction of oxidative stress within insect cells. They stimulate the overproduction of reactive oxygen species (ROS), This leads to lipid peroxidation, protein oxidation, and membrane damage, causing severe cellular dysfunction and insect mortality. In addition, they may disrupt mitochondrial respiration and energy production, further intensifying cellular collapse **(Pereira et *al*., 2024; Sivakumar et *al*., 2026)**.

7.2.2. Neurotoxicity and disruption of nervous system function

These compounds also affect the insect nervous system by inhibiting acetylcholinesterase (AChE), resulting in continuous nerve impulse transmission. This causes hyperexcitation, loss of coordination, paralysis, and eventually death. They may also disturb ion balance (Na^+/K^+), and interfere with key neuroreceptors such as octopaminergic and

GABA-gated channels, leading to severe neurophysiological disruption **(Pereira et *al*., 2024; Sivakumar et *al*., 2026)**.

7.2.3. Digestive system disruption and antifeedant activity

Phenolic compounds damage the insect digestive system, particularly midgut epithelium and microvilli by reducing nutrient absorption and digestive efficiency. They also inhibit digestive enzymes such as proteases, lipases, and α-amylase, limiting the breakdown of food and leading to starvation and strong antifeedant effects, where insects reduce or completely stop feeding. Moreover, they may impair gut membrane integrity and disrupt normal digestive physiology **(Pereira et *al*., 2024; Sivakumar et *al*., 2026)**.

7.2.4. Growth inhibition and reproductive suppression

These compounds interfere with insect hormonal regulation, causing delayed development, abnormal metamorphosis, and reduced growth. They also act as endocrine disruptors by interfering with molting hormones (ecdysone). In addition, they reduce oviposition, egg viability, and fertility, leading to long-term suppression of insect populations. Phenolic acids can also inhibit detoxification enzymes such as GST and esterases, increasing insect susceptibility to toxic stress **(Pereira et *al*., 2024; Sivakumar et *al*., 2026).**

.

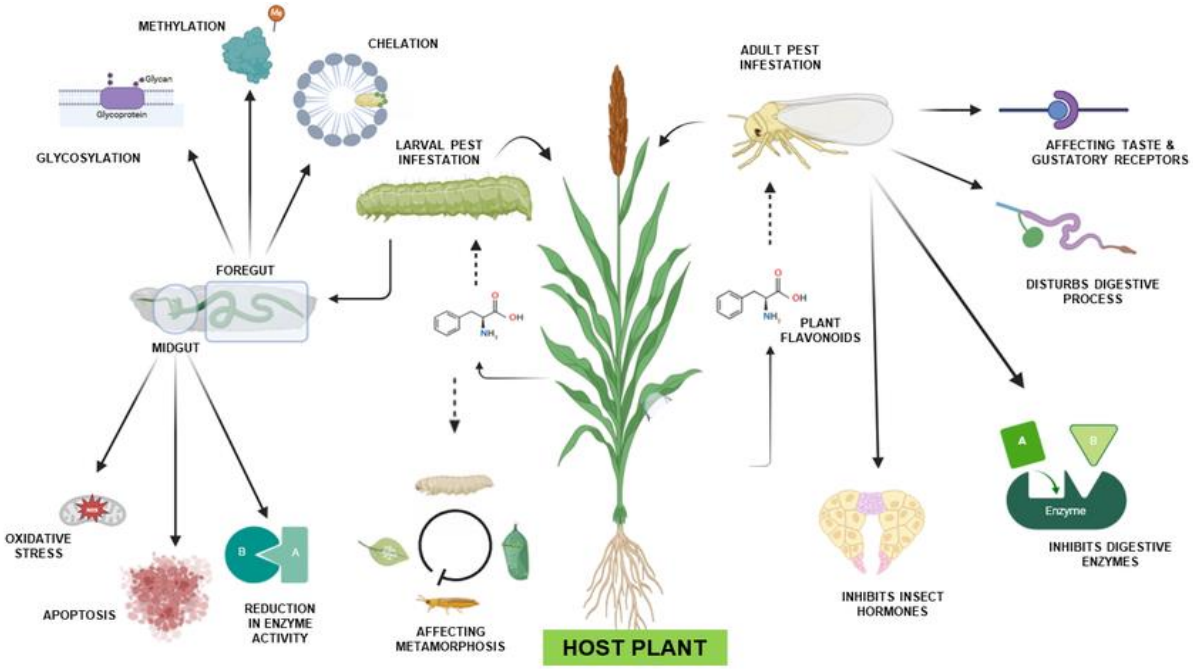


Figure 27. Mode of action of phenolic compounds (flavonoids) in insect larvae and adults **(Sivakumar et *al*., 2026)**.

Part II: Materials and methods

I. Materials

1. Plant material

The aerial parts of *A. halimus*, *L. crithmoides*, and *S. fruticosa* were collected from three different locations of northwestern Algeria; Belassel **(**Relizane), El Mactaa (Mostaganem) and Es Senia (Oran) respectively **(Table 08)**, during February and March 2024. The plant specimens were identified based on their phenotypic characteristics using the botanical reference; "Nouvelle flore de l'Algérie et des régions désertiques méridionales" **(Quézel and Santa, 1962)**, and confirmed with the assistance of Dr. Sekkal (an expert botanist in Mostaganem University, Algeria). The collected leaves were washed several times with tap water, air-dried at room temperature in the absence of direct sunlight. Once completely dried, the plant material was finely ground using a grinder to obtain a very fine powder which was stored in glass jars until its use.

Table 08. Site geography, collection dates and altitude of studied plants.

N°	Plant	Geographic coordinates	Name of region	Collection dates	Altitude
1	*A. halimus*	35°44'12.7"N 0°32'23.9"E	Belassel	28-03-2024	67.91m
2	*L. crithmoides*	35°47'09.0″N 0°07'24.0"W	El Mactaa region	26-02-2024	0.06 m
3	*S. fruticosa*	35°36'11.5"N 0°41'16.2"W	Es Senia (Oran)	12-02-2024	81.75 m



Figure 28. Map showing sample collection locations: **(1)** *A. halimus*; **(2)** *L. crithmoides*; **(3)** *S. fruticosa* **(Google Earth)**.

2. Animal material

The experiment was carried out on *Tribolium confusum* (*T. confusum*), a major pest of stored food products. The choice of this biological material is justified by the extent of the damage caused by this species, which infests various cereal products of economic importance, as well as by its ease of rearing in the laboratory, allowing the production of a large number of individuals required for experimental tests.

The adults of *T. confusum* were collected from an initial stock of infested soft wheat grains collected in the Sidi M'hamed Benali area (Relizane, Algeria).

3. Chemicals and reagents

Methanol, picric acid , Molisch's reagent (alcoholic α-naphthol), Fehling's solutions (A and B), ferric trichloride($FeCl_3$), magnesium ribbon, Baljet's reagent, hydrogen chloride (HCl) , ninhydrin, chloroform, acetic anhydride, sulfuric acid(H_2SO_4), sodium hydroxide (NaOH), glacial acetic acid, formic acid, acetonitrile, trifluoroacetate, phosphazine adduct, Folin-Ciocalteu reagent ,gallic acid, sodium carbonate , aluminum trichloride , quercitine , vanilline ,catechin , DPPH(2,2-diphenyl-1-picrylhydrazyl) , ascorbic acid , ABTS (2,2′-azino-bis(3-ethylbenzothiazoline-6-sulphonate)) , Potassium peroxodisulfate ($K_2O_8S_2$), TPTZ(2,4,6-Tri(2-pyridyl)-s-triazine), ferric chloride hexahydrate ($FeCl_3 \cdot 6H_2O$), sodium acetate , Ammonium Iron(II) Sulfate $(NH_4)_2Fe(SO4)_2$, Tween 80, and sodium hypochlorite.

II. Methods

1. Study Sites

The phytochemical characterization and antioxidant activity of the three halophyte species were carried out at the Laboratory of Biochemistry, Molecular Biology and Environmental Toxicology, University of Mostaganem, Algeria.

The identification of bioactive compounds by HPLC-ESI-QTOF-MS analysis was performed at the Centre for Research and Development of Functional Food (CIDAF), University of Granada, Avda. del Conocimiento 37, 18016 Granada, Spain.

The insecticidal activity assays were conducted at the Laboratory of Environment and Sustainable Development, University of Relizane, Algeria.

2. Extracts preparation

2.5 g of plant powder was subjected to cold maceration in 100 mL of methanol/water (75:25 v/v). The extraction was carried out at room temperature, with continuous stirring and protected from light, for 24h. After maceration, the mixture was filtered through Whatman filter paper (N°:1). After filtration, the methanol is removed from the filtrate by vacuum evaporation in a rotary evaporator (LabTech- EV400) at 40 °C. The resulting residue was then dried in an oven at 40 °C for 48 hours. The extraction yield was calculated with the following equation **(Dirar et *al.*, 2019)**:

$$\text{Yiled (\%)} = \frac{\text{Mass of the evaporated extract (g)}}{\text{Mass of the initial dry plant powder(g)}} \times 10 \quad \textbf{(Equation 01)}$$

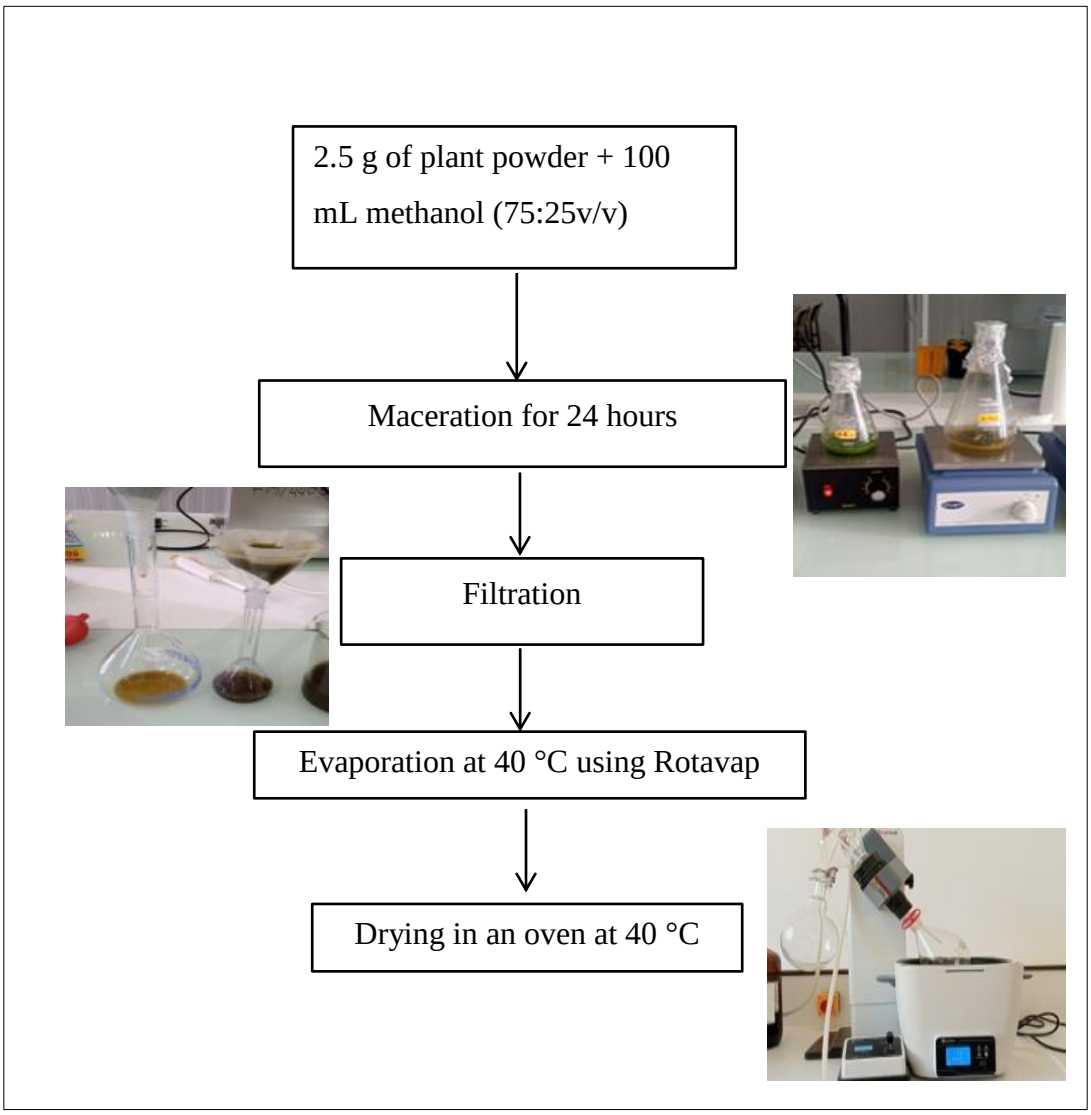


Figure 29. Different stages of methanolic extraction using the maceration method.

3. Phytochemical investigation of plant extracts

3.1. Qualitative phytochemical screening

A preliminary phytochemical screening was performed on the methanolic extracts of *A. halimus*, *L. crithmoides*, and *S. fruticosa* to qualitatively identify the major classes of secondary metabolites, using standard procedures described by **Shaikh and Patil, (2020); Maheshwaran and *al*. (2024)**

Table 09. Preliminary phytochemical screening of the plant extracts.

Compounds	Test	Procedure	Observation
Alkaloids	Picric acid test	1to 2 drops of 2% picric acid solution was mixed with 1mL of extract.	A yellow color
Carbohydrates	Molish's test	1 mL of the extract was mixed with a drop of Molisch's reagent (alcoholic α-naphthol). Then, 0.5 mL of concentrated sulfuric acid (H_2SO_4) was carefully added along the inner wall of the test tube.	A violet ring
Reducing sugars	Fehling's test	Mixture of 1 mL Fehling's A and Fehling's B solutions was added to 1mL of plant extract and heated on water bath for 10 minutes.	A red precipitate
Glycosides	Concentrate H_2SO_4 test	To 1 mL extract, 400 µL glacial acetic acid, one drop of 5% $FeCl_3$ and 1mL conc. H_2SO_4 were added.	Brown ring
Cardiac Glycosides	Baljet test	2 mL of the extract was mixed with one drop of Baljet's reagent, which was prepared by combining 9.5 mL of 1% picric acid with 0.5 mL of 10% sodium hydroxide (NaOH) solutions.	A yellow-orange color
Proteins and Amino acids	Ninhydrin test	One drop of saturated acetonic solution of ninhydrin was added to 1 mL of the extract. The mixture was heated in a water bath.	A purple color
Phenolic compounds	Ferric chloride test	1 to 2 drops of 5% aqueous $FeCl_3$ were added to 1 mL of the extract.	Dark green or bluish black color
Flavonoids	Shinoda's test	To 1 mL of the extract, 0.5 g piece of magnesium ribbon was added, followed by a few drops of HCl.	pink, red, or orange coloration

Tannins	Braymer's test	3mL of distilled water and 3 drops of 10% aqueous $FeCl_3$ solution were added to 1mL of extract.	Blue-green color.
Phlobatannins	HCl test	Mixture of 1mL of extract and 1mL of 1% HCl solution was heated in a water bath.	A red precipitate
Saponins	Foam test	2 mL of plant extract were mixed with 5 mL of distilled water in a test tube and vigorously shaken for 1 minute.	Stable foam more than 10 min.
Cholesterol	Liebermann - Burchard test	1mL of extract was mixed with 2mL of chloroform ,5 drops of acetic anhydride and 2 drops of conc. H_2SO_4	A red-rose color
Terpinoides		1 mL of chloroform was mixed with 2.5 mL of the plant extract and 1 mL of H_2SO_4 was added. The mixture was then heated on a water bath.	Brown rubbish
Steroids	Salkowski's test	1 mL of extract was treated with 2 mL of the chloroform. 1 mL of concentrated sulfuric acid (H_2SO_4) was then added carefully along the sides of test tube.	A red or reddish-brown color in lower layer.
Quinones	Concentrated HCl test	1mL of extract was mixed with 1 mL of concentrated HCl.	A green color
Coumarins	NaOH test	Few drops of 10% sodium hydroxide (NaOh) solution were added to 1ml of each plant extract.	yellow colour
Gums and Mucilages	Alcohol test	0.5 mL of the extract was mixed with 2.5 mL of absolute ethanol.	White or cloudy precipitate
Resins	Acetic anhydride test	To 1mL of plant extrac , 1ml acetic anhydride solution and 1mL of concentrated H_2SO_4 was added .	Orange to yellow color

3.2. Quantitative phytochemical analysis

3.2.1. Total phenolic content (TPC)

The total phenolic content of the crude extracts was determined according to the Folin-Ciocalteu method described by **Al Hawat and Alallan, (2025)**. 20 µL of the extract (1mg/mL) was mixed with 1.58 mL of distilled water and 100 µL of Folin-Ciocalteu reagent. After eight minutes, 300 µL of 20% sodium carbonate solution (Na_2CO_3) was added. The mixture was incubated in the dark for 2 h at room temperature and the absorbance was

measured at 760 nm using Dynamica HALO XB-10 UV-vis spectrophotometer against a blank (the same mixture without extract). The total phenolic content of each plant extract was determined using a gallic acid calibration curve (0.025 to 1 mg/mL) and results were expressed as milligrams of gallic acid equivalent per gram of extract (mg GAE/g dry weight of extract).

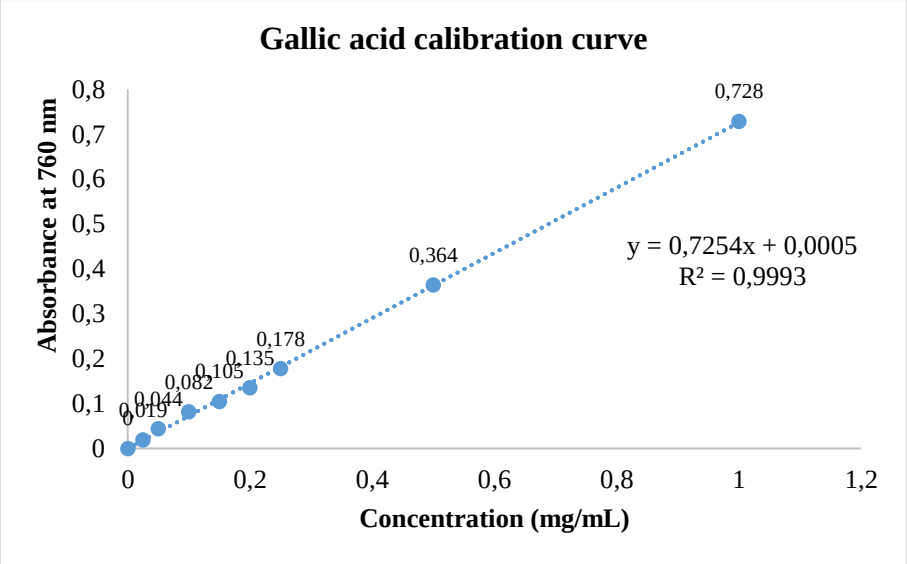


Figure 30. Gallic acid calibration curve for total phenolic content determination.

3.2.2 Total flavonoid content (TFC)

The total flavonoid content was estimated according to the method described by **N'do et *al.* (2024)** using the aluminum trichloride assay. 1 mL of each plant extract (1 mg/mL) was mixed with 1 mL of 2% methanolic aluminium trichloride solution ($AlCl_3$). The mixture was incubated for 30 min at room temperature in the dark. The absorbance was then measured at 415 nm against a blank using methanol. Flavonoid concentrations were expressed as milligrams of quercetin equivalent per gram of dry extract (mg QE/g) using a quercetin standard calibration curve (0 – 0.1 mg/mL).

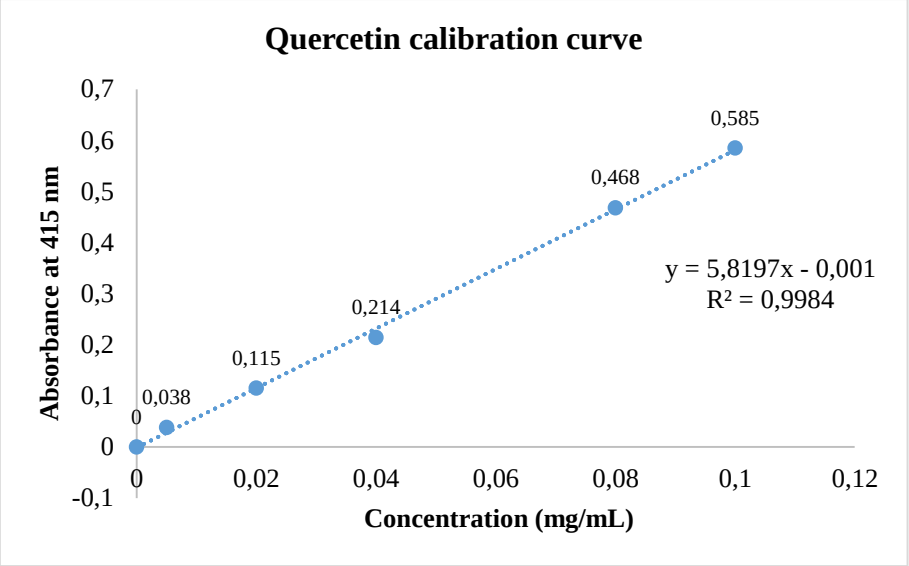


Figure 31. Quercetin standard calibration curve for total flavonoids content determination.

3.2.3. Total tannin content (TTC)

Total tannin content was estimated according to **Elagdi et *al.* (2023)** by the vanillin reagent. 250 µL of each plant extract was mixed with 1.5 mL of 4 % vanillin solution (prepared in methanol) and 750 µL of concentrated hydrochloric acid (HCl). The mixture was incubated for 15 min at room temperature, and the absorbance was measured at 500 nm. Results were expressed as milligrams of catechin equivalents per gram of dry weight (mgCE/g DW) using a catechin standard curve (0 – 0.2 mg/mL).

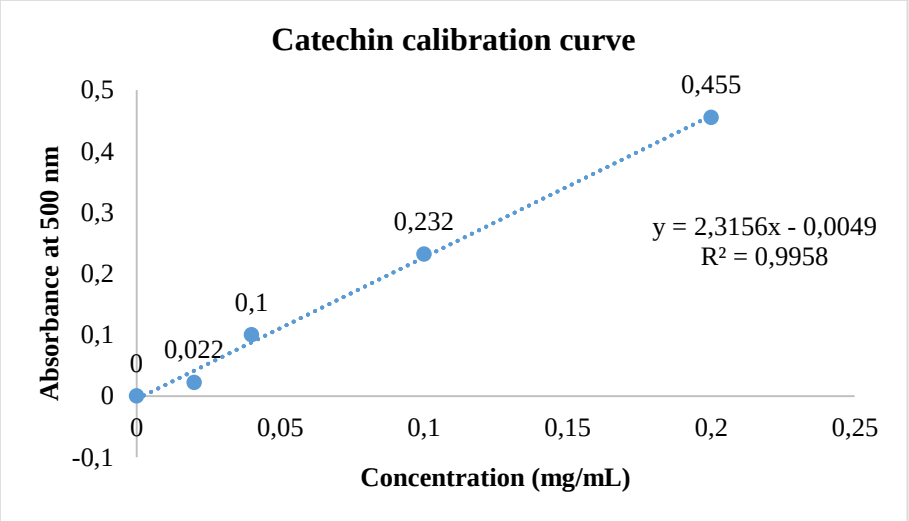


Figure 32. Catechin standard calibration curve for total tannins content determination.

3.3. ATR-FTIR analysis

This spectroscopic technique is used to identify specific chemical functional groups and chemical bonds present in a sample without any prior preparation. Methanolic extract of all species were scanned directly using a Bruker INVENIO FT-IR spectrometer equipped with an ATR accessory at room temperature. Spectra were recorded in the mid-infrared region (4000 – 400 cm^{-1}) with a resolution of 4 cm^{-1} (**Easmin et *al.*, 2017)**.

3.4. Identification of bioactive compounds using HPLC-ESI-QTOF-MS analysis

The bioactive compounds present in the methanolic extracts were identified using HPLC-ESI-QTOF-MS. Samples were prepared at a concentration of 20 mg/mL and then filtered using nylon syringe filters (0.22 µm). Two independent analyses were performed to ensure reproducibility of the results.

Separation and identification of compounds were carried out using an Agilent 1260 HPLC system (Agilent Technologies, Palo Alto, CA, USA) equipped with a Zorbax Eclipse Plus RP-C18 column (150 mm × 4.6 mm, 1.8 µm). The system was coupled to a Q-TOF mass spectrometer (model 6540, Agilent Technologies) equipped with an electrospray ionization source (ESI Jet Stream), operating in negative ionization mode over a mass range of 50 to 1700 m/z. The used mobile phases consisted of acidified water with 0.1% formic acid (A) and acetonitrile (B), according to the following gradient: 0 min, 5% B; 5 min, 35% B; 22 min, 85% B; 24 min, 95% B; 25 min, 5% B, maintained for 5 min for column equilibration (total analysis time: 30 min). The flow rate was set at 0.5 mL/min, the injection volume at 10 µL, and the column temperature at 25 °C. The samples were maintained at 4°C during analysis.

The mass spectrometer parameters were as follows: capillary voltage 4000 V, nebulizer pressure 320 psig, fragmentor 130 V, nozzle voltage 500 V, skimmer 45 V, and octupole 750 V. The instrument was calibrated and adjusted according to the manufacturer's instructions, with continuous internal calibration using m/z 112.985587 (trifluoroacetate) and m/z 1033.988109 (phosphazine adduct) ions **(Kumar et *al.*, 2017)**. The main compounds were detected by Molecular Feature Extraction (MFE), with a relative volume cutoff of 0.2%, after subtracting solvent blanks. Their identification was achieved by comparing the obtained data with databases of phenolic compounds such as Phenol Explorer and SciFinder, as well as with relevant scientific literature **(Quirantes-piné et *al.*, 2013; Dorta et *al.*, 2014)**.



Figure 33. HPLC-ESI-QTOF-MS system **(Original, 2025)**.

4. Evaluation of biological activities *in vitro*

4.1. Antioxidant Activity assessment

4.1.1. DPPH radical scavenging assay

The free radical scavenging activity of extracts was determined using DPPH assay, as described by **Chekroun et *al*. (2019)**. The reaction mixture contained 1950 µL of methanolic DPPH solution (100 µM) and 50 µL of plant extract at various concentrations (0.25, 0.5, 1, 2, 4, 8, 16, 32, and 64 mg/mL). After incubation in the dark at room temperature (25°C) for 30 min, the absorbance was measured at 517 nm using methanol as the blank. Ascorbic acid was used as the positive control, while a mixture of 50 µL of methanol and 1950 µL of DPPH solution was used as the negative control. The percentage inhibition was calculated according to the formula:

$$\text{DPPH scavenging activity (\%)} = \frac{\text{A control} - \text{A sample}}{\text{A control}} \times 100 \quad \textbf{(Equation 02)}$$

Where $A_{control}$ is the absorbance of negative control and A_{sample} is the absorbance of the test sample.

The IC_{50} values (concentration of the sample required to scavenge 50% of the DPPH free radicals) were calculated using radical inhibition percentage curves against sample concentration **(Annex 01)**.

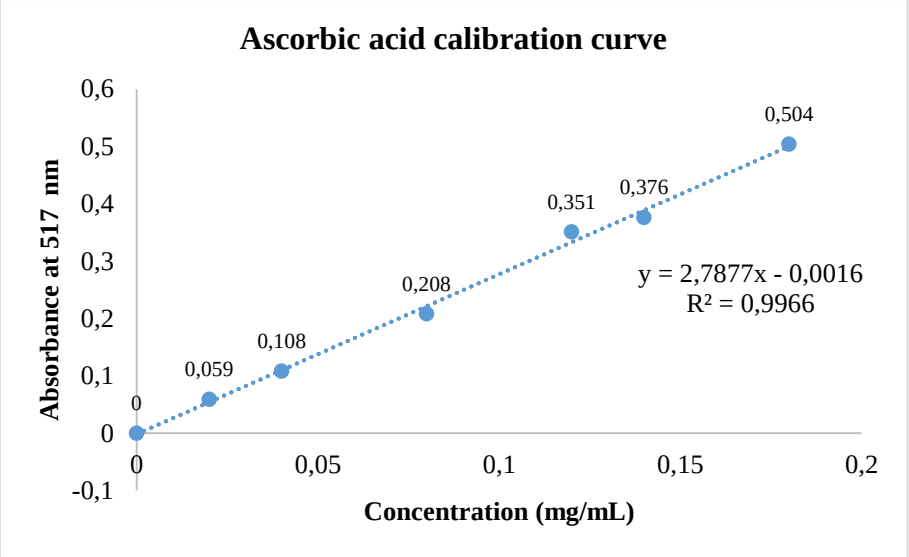


Figure 34. Ascorbic acid calibration curve for the DPPH radical scavenging assay.

4.1.2. ABTS radical scavenging activity

The antioxidant activity based on ABTS (2,2 -Azino-bis (3-ethylbenzthiazoline-6-sulphonic) radical scavenging was determined according to **Nassrallah and Abdel-Mobdy, (2021)** with minor modifications. Equal volumes of ABTS (7 mM) and potassium persulfate (2.45 mM) were mixed and then left to react in the dark at room temperature for 16 hours to generate the ABTS radical cation. The resulting solution was diluted with distilled water to obtain an absorbance of 0.7 ± 0.02 at 734 nm, serving as the working solution. For the assay, 980 µL of the ABTS working solution was added to 20 µL of plant extract at different concentrations. After incubation for 10 min at 30 °C, absorbance was measured at 734 nm against distilled water as a blank. Ascorbic acid was used as the positive control.

The percentage inhibition was calculated using the equation:

$$\% \text{ Inhibition } = [(Ac - As)/Ac] \times 100 \quad \textbf{(Equation 03)}$$

Where A_c is the absorbance of the control and A_s is the absorbance of the sample.

The IC_{50} values were calculated using radical inhibition percentage curves against sample concentration **(Annex 02)**.

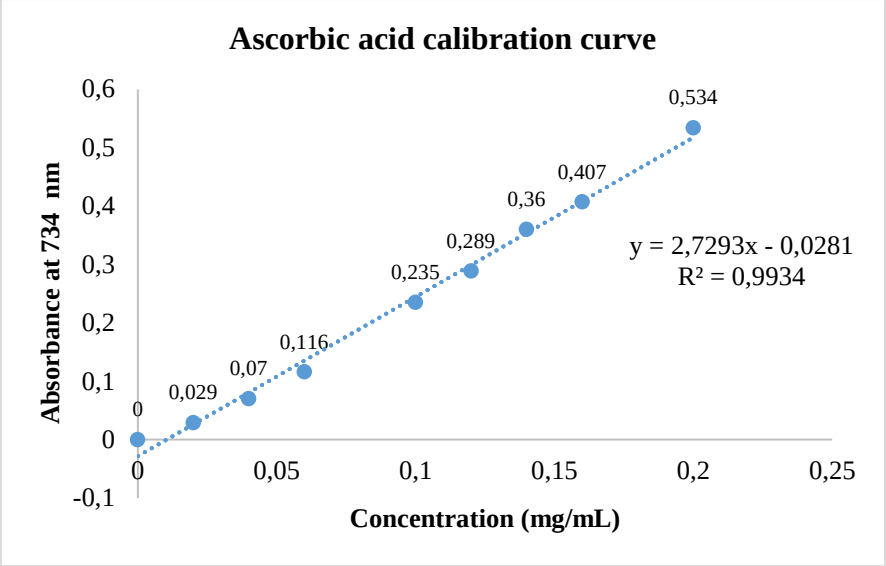


Figure 35. Ascorbic acid calibration curve for the ABTS radical scavenging assay.

4.1.3. Ferric reducing antioxidant power (FRAP) method

The FRAP assay was performed according to **Mavric-Scholze and *al.* (2025)** with slight modifications. In brief, 30 µL mL of each plant extract was mixed with 90 µL of distilled water and 900 µL of FRAP reagent, consisting of 300 mM acetate buffer (pH 3.6), 10 mM 2,4,6-Tri(2-pyridyl)-s-triazine (TPTZ) in 40 mM HCl, and 20 mM $FeCl_3.6H_2O$ in a ratio of 10:1:1 (v/v/v) respectively. The mixture was incubated in the dark at 37 °C for 30 min, and absorbance was recorded at 593 nm. A calibration curve was prepared using ferrous ammonium sulfate solutions (200 - 2000 µM) under the same conditions. Results were expressed as µM Fe^{+2} equivalents per gram of sample (µM Fe^{+2}/g).

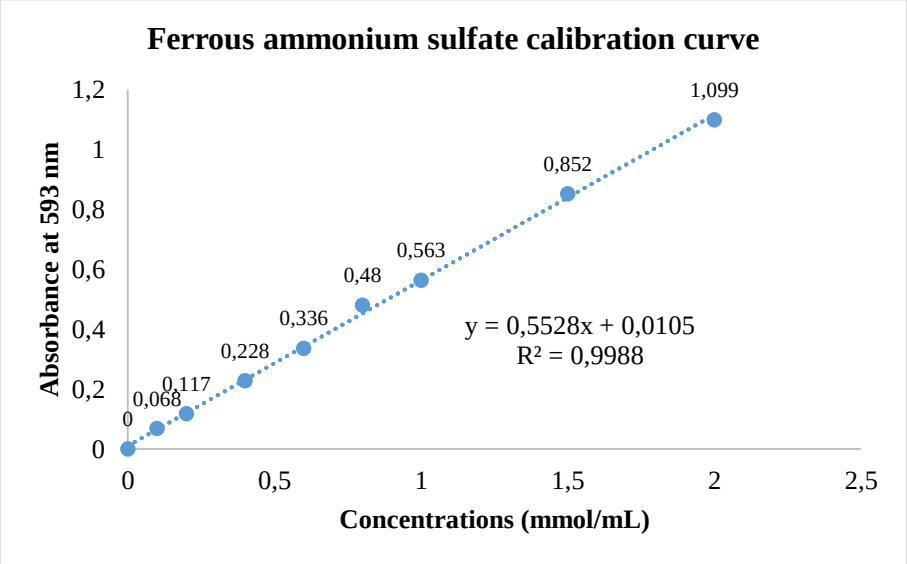


Figure 36. Calibration curve of ferrous ammonium sulfate for the FRAP reducing power assay.

4.2. Insecticidal activity

4.2.1. Insect breeding

Mass rearing was conducted at the Laboratory of Environment and Sustainable Development, Department of Biological Sciences, Ahmed Zabana University, in glass jars containing soft wheat flour as a food substrate. Each jar was covered with a fine mesh screen to ensure proper ventilation while preventing the escape of insects. All jars were kept in darkness at a temperature of 28 ± 2 °C and a relative humidity of 70 ± 5 % **(Figure 37) (Djidel et *al.*, 2018)**.



Figure 37. Mass rearing of *T. confusum* **(Original, 2024)**.

4.2.2. Repellency test

The repellent effect of methanolic extracts derived from halophytic plants against *Tribolium confusum* adults was assessed using the filter paper preference zone assay as described by **McDonald et *al.* (1970)**. Circular filter paper discs (9 cm in diameter) were bisected to create two equal halves. Four concentrations of extracts were prepared in a 2% (v/v) Tween 80 solution at 25, 50, 100, and 200 mg/mL. Each concentration was evenly applied to one half of a disc, while the opposite half received 0.5 mL of 2% Tween 80 solution alone, serving as the control. Ten adult beetles were released at the center of each disc. Three independent replicates were conducted for each plant extract and concentration.

After a two-hour exposure period, the percentage repellency (PR) was calculated using the following equation:

$$PR\ (\%) = ((Nc - Nt) / Nc + Nt) \times 100$$ **(Equation 04)**

Where

$\mathbf{N_t}$ = number of insects on the treated half of the filter paper

$\mathbf{N_c}$ = number of insects on the control (untreated) half of the filter paper

The mean percentage repellency for each extract was determined and subsequently classified according to the **McDonald et *al.* (1970)** repellency scale, ranging from Class 0 to Class V:

- **Class 0:** PR < 0.1%
- **Class I:** PR = 0.1–20%
- **Class II:** PR = 20.1–40%
- **Class III:** PR = 40.1–60%
- **Class IV:** PR = 60.1–80%
- **Class V:** PR = 80.1–100%

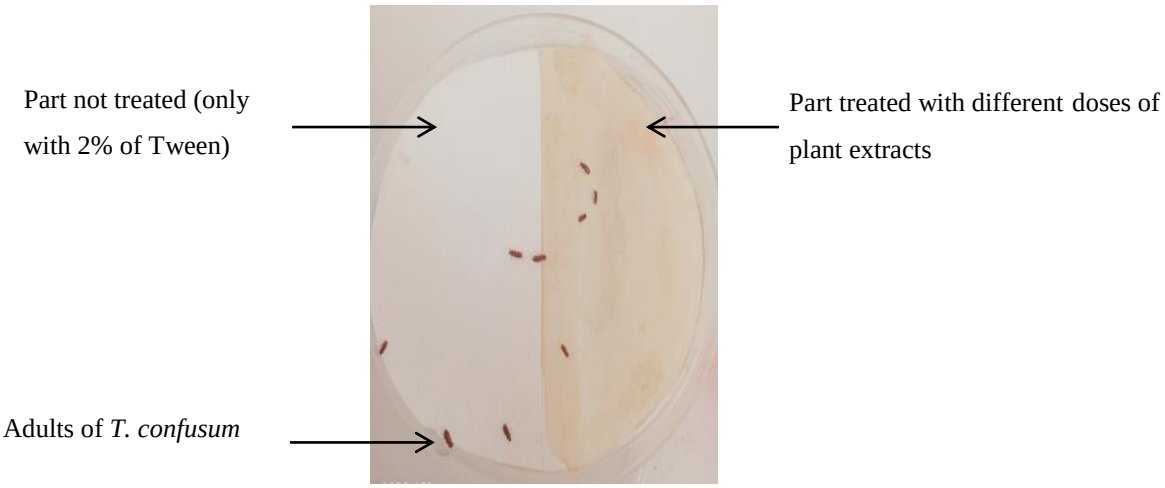


Figure 38. Repellency test for different doses of plant extracts compared with the control **(Original, 2025)**.

4.2.3. Contact toxicity test

The contact toxicity of methanolic extracts obtained from the three halophytes against adults of *Tribolium confusum* was assessed following the method described by **Djidel et *al.* (2019)**, with slight modifications. Four concentrations of each extract (25, 50, 100, and 200 mg/mL) were prepared using a 2% Tween solution as an emulsifying agent. For each treatment, 0.5 mL of the test solution was uniformly sprayed onto a group of ten adult insects using a hand-held sprayer. Following treatment, the insects were transferred to Petri dishes

lined with filter paper cut to fit the dimensions of the dishes. A negative control consisting solely of 2% Tween solution was included in all experiments. To ensure adequate ventilation, small perforations were made in the lids of the Petri dishes. Each concentration was tested in triplicate, along with the corresponding control treatment.

Insect mortality was assessed after 24, 48, 72, and 96 h of exposure. Mortality data were corrected for control mortality using **Abbott's** formula **(1925)**

$$\text{Corrected mortality (\%)} = \frac{(\text{mortality in treatment} - \text{\% mortality in control})}{100 - \text{\% mortality in control}} \times 100$$

(Equation 05)

Bioassays were repeated whenever mortality in the control group exceeded 20%.

The median lethal concentration (LC_{50}) values of the tested extracts were estimated by Probit analysis of the concentration–mortality response data according to the procedure described by **Finney, (1971)**

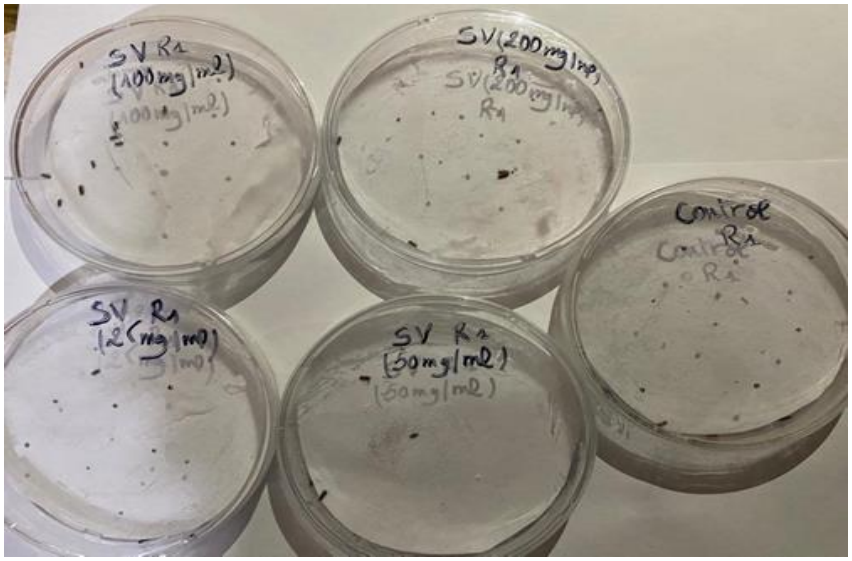


Figure 39. Contact bioassays of extract against *T. confusum* **(Original, 2025)**.

4.2.4. Oral toxicity bioassay using plant powders

The oral toxicity of plant powders against adult *T. confusum* was evaluated according to the method of **Sekrane et *al*. (2022)**. Different concentrations of plant powder (0.2, 0.4, 0.6, and 0.8 g) were mixed with flour to obtain a total weight of 1 g. Flour without plant powder served as the untreated control. Ten adult *T. confusum* were introduced into each Petri dish containing the treated substrate. Each treatment was replicated three times. The Petri dishes were maintained under laboratory conditions throughout the experimental period.

Insect mortality was recorded after 4, 8, 12, and 16 days of exposure. Mortality percentages were corrected using Abbott's formula as previously described.

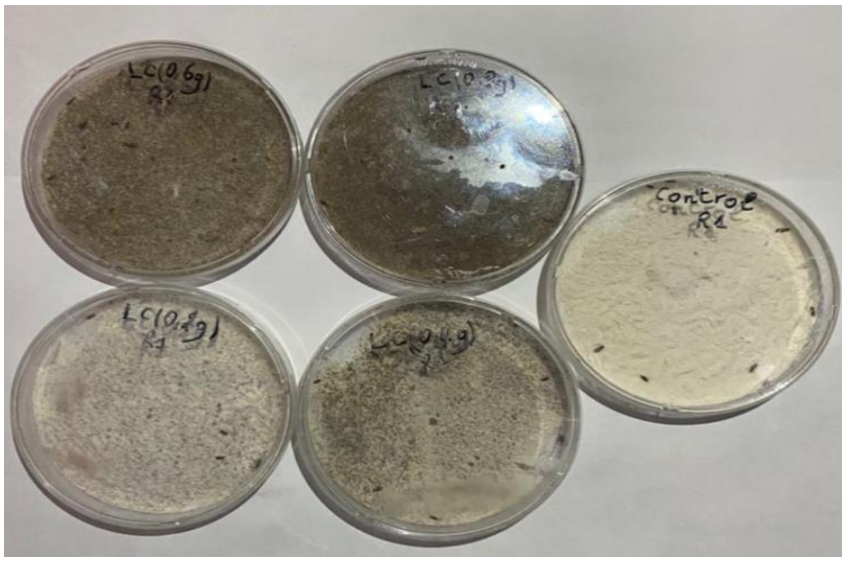


Figure 40. Toxic potentials of plant powders on survival of *T. confusum* **(Original, 2025)**.

5. Validation of extract safety on wheat seed germination

To evaluate the effect of methanolic extract treatments on seed germination capacity, 100 healthy wheat seeds were selected and surface-sterilized using a sodium hypochlorite solution. Following sterilization, the seeds were placed in Petri dishes lined with cotton moistened with distilled water to maintain adequate humidity for germination. The seeds were then treated with the highest concentration of extract (200 mg/mL). A control group consisting of 100 untreated wheat seeds was maintained under the same experimental conditions **(Salah et *al*., 2023)**.

After 8 days of incubation, the number of germinated seeds was recorded, and the germination rate was calculated according to the following equation:

$$\text{Germination rate (\%)} = \frac{\text{Number of germinated seeds}}{\text{Total number of seeds}} \times 100 \quad \textbf{(Equation 06)}$$



Figure 41. Wheat seed germination test **(Original, 2025)**.

6. Insecticidal activity *in silico*

6.1. Protein preparation

Acetylcholinesterase is an important enzyme involved in nerve signal transmission by breaking down acetylcholine. Inhibition of this enzyme causes disruption of the nervous system, leading to insect paralysis and death **(Sha et *al.*, 2025)**. Therefore, it is widely used as a target in insecticidal and molecular docking studies. The three-dimensional (3D) structure of Acetylcholinesterase (PDB ID: 6XYS) from the fruit fly *Drosophila melanogaster* **(Rawat et *al.*, 2024)** was retrieved from the RCSB Protein Data Bank and saved in PDB file format. Water molecules, heteroatoms, and co-crystallized ligands were removed using Discovery Studio 2025 Client. The protein structure was then prepared by adding polar hydrogen atoms and assigning appropriate charges prior to docking using UCSF Chimera software 1.19 to optimize the protein for further analysis.

6.2. Ligand preparation

The three-dimensional structures of the phenolic compounds identified in *A. halimus*, *L. crithmoides*, and *S. fruticosa* by HPLC-ESI-QTOF-MS analysis were obtained from the PubChem database (https://pubchem.ncbi.nlm.nih.gov/) in Structure Data File (SDF) format. The retrieved structures were then converted into Protein Data Bank (PDB) format using the Open Babel graphical user interface (GUI) for subsequent molecular docking studies.

6.3. Molecular docking procedure

Molecular docking was carried out using PyRx. The prepared protein structure and the optimized ligands were imported into the PyRx platform and converted into PDBQT format. Docking simulations were performed using the Vina Wizard tool integrated within PyRx. The grid box was centered at coordinates x = 25.88, y = 62.50, and z = 12.34, with dimensions of 22 × 22 × 22 Å to ensure adequate coverage of the binding pocket. The binding affinities of ligand–receptor complexes were assessed with the Vina Wizard tool in PyRx, The docking parameters were set as follows: exhaustiveness = 8, number of modes = 9, and energy range = 3 kcal/mol.

For each ligand, multiple binding conformations were generated. The best docking pose was selected based on the lowest binding affinity value (kcal/mol), with more negative binding energies indicating stronger predicted interactions and greater binding stability within the active site **(Verma et *al*., 2023)**.

The docked complexes obtained from PyRx were exported in CSV format and subsequently analyzed using Discovery Studio 2025 Client. Ligand–protein interactions within the active site were thoroughly examined and visualized in both two-dimensional (2D) and three-dimensional (3D) representations. Various interaction types, including hydrogen bonds, hydrophobic interactions, π–π stacking interactions, π–alkyl interactions, and electrostatic contacts, were identified to characterize the binding modes of the investigated compounds

6.4. Validation of docking results

To validate the docking protocol, the co-crystallized ligand was extracted from the protein structure and re-docked into the binding site using the same docking parameters. The predicted pose was then compared with the original crystallographic conformation by calculating the Root Mean Square Deviation (RMSD). An RMSD value below 2.0 Å was considered acceptable, confirming the reliability and accuracy of the docking methodology.

7. Statistical analysis

All experiments were conducted in triplicate (n = 3), and the results were expressed as mean ± standard deviation (mean ± SD). Statistical analyses were performed using the Statistical Package for the Social Sciences (SPSS) software, version 26.0 (IBM, 2019). The normality of the data distribution was evaluated using the Shapiro–Wilk test. Differences in extraction yield, total phenolic, flavonoid, and tannin contents among the tested samples were assessed by one-way analysis of variance (ANOVA), followed by Tukey's post hoc test for multiple comparisons. The half-maximal inhibitory concentration (IC_{50}) and median lethal concentration (LC_{50}) values for the antioxidant and insecticidal activities, respectively, were estimated by log-probit regression analysis. Statistical significance was considered at $P \leq 0.05$.

Part III: Results and discussion

Results and discussion

1. Extraction yield

Significant differences for extraction yields were obtained by cold methanolic maceration for the halophytic species used in this study with values ranging from 15.08 ± 0.29% to 25.12 ± 0.01% and highest extraction yield for *L. crithmoides* **(Table 10)**.

Table 10. Yields extract results expressed as percentage.

	A. halimus	***L. crithmoides***	***S. fruticosa***
extract mass (g)	0.52 ± 0.007	0.6281 ± 0.00	0.377 ± 0.007
Yield (%)	20.81 ± 0.3 ^{b}	25.12 ± 0.01^{c}	15.08 ± 0.29 ^{a}

Data are presented as the mean of three replicates ± standard deviation. Means followed by different letters (a, b, and c) are significantly different with ($p \leq 0.05$).

After solvent evaporation, the extract appeared as a dark brown, pasty, and resinous residue containing small whitish crystalline particles, likely related to the mineral content characteristic of this halophytic species. This result is in agreement with the findings of **Adorisio et *al*. (2020)**, who reported a MeOH extraction yield of 26% for the same species collected in Italy.

A yield of 20.81 ± 0.30% was obtained for methanolic extract from *A. halimus* with a dark green, pasty appearance. Similarly a yield of 24.00 ± 1.41% was reported for *A. halimus* methanolic leaf extract collected from Bechar, Algeria **(Benhamou et *al*., 2009).** However, lower yields ranging from 4.91 to 17.47% reported from samples collected in Mazagran, Biskra, and Sig with leaf extracts consistently yielding more than stem **(Ould Kaddour et *al*., 2019)**. These variations highlight the influence of both the geographical origin and the plant organ on extraction efficiency.

The lowest extraction yield (15.08 ± 0.29%) was noted for *S. fruticosa* which exhibited a dark brown color and a semi-liquid to pasty texture. Nevertheless, this yield remained higher than the 9.88% previously reported by **Ayaz et *al*. (2022)**.

As indicated above, these variations observed in extraction values may be attributed to differences in botanical composition, environmental and geographical conditions, harvesting period, as well as extraction parameters **(Ould Kaddour et *al*., 2019)**.

2. Phytochemical characterization of plant extracts

2.1. Phytochemical screening

The preliminary qualitative phytochemical screening provides an initial insight into the distribution of primary and secondary metabolites within plant extracts. Accordingly, colorimetric and precipitation assays carried out in the present study revealed distinct variations in the phytoconstituents of the three investigated halophyte species **(Table 11)**.

In general, all extracts contained major groups of bioactive constituents, including proteins, amino acids, glycosides, reducing sugars, phenolic compounds, flavonoids, tannins, gums and mucilages, although their occurrence varied among species.

Alkaloids, cardiac glycosides, cholesterol, and coumarins were detected in *L. crithmoides* and *S. fruticosa* but were absent in *A. halimus*. Saponins were present in both *A. halimus* and *S. fruticosa*, with a greater abundance in the latest species. Quinones were found exclusively in *A. halimus*, whereas terpenoids and resins were detected only in *S. fruticosa*, but carbohydrates, steroids, and phlobatannins were not observed in any of the examined extracts.

Among the investigated species, *S. fruticosa* exhibited the most diverse phytochemical composition, followed by *A. halimus* and *L. crithmoides*.

Table 11. Phytochemical screening of the three different solvent extracts from the studied halophyte species.

Phytoconstituents	*A. halimus*	*L. crithmoides*	*S. fruticosa*
Alkaloids	-	+++	+
Carbohydrates	-	-	-
Reducing sugars	+	+	++
Glycosides	+	++	+
Cardiac glycosides	-	+++	++
Proteins and Aa	++++	++	++++
Phenolic compounds	++	+	+++
Flavonoids	+++	+	++
Tannins	++	+	+++
Phlobatinis	-	-	-
Saponins	++	-	+++
Cholesterol	-	+	++

Terpinoides	-	-	+
Steroides	-	-	-
Quinones	+++	-	-
Coumarins	-	+++	+
Gums and mucilages	+ (White)	+ (White)	+ (Brown)
Resins	-	-	++

-: Absence, **+:** Low presence, **++:** Moderate presence, **+++:** Strong presence, **++++:** Very strong presence.

These findings are in agreement with previous reports on *A. halimus*, *S. fruticosa*, and *L. crithmoides* **(Bounouar et *al*., 2022; Suthar and Solanki, 2022; Bokri et *al*., 2023)**, with some differences.

The absence of certain phytochemicals in one plant sample and their presence in another may be attributed to differences in the physiological and biosynthetic processes occurring within each plant. However, environmental factors should also be considered, as they play a crucial role in influencing the synthesis and accumulation of secondary metabolites. Preliminary phytochemical screening is therefore an important and useful approach for detecting the major classes of chemical constituents present in plant materials. It provides a basis for subsequent quantitative analyses and facilitates the identification of pharmacologically active compounds **(Shrestha et *al*., 2015)**.

2.2. Total phenolic, flavonoid and tannin contents

The quantitative phytochemical analysis of the methanolic extracts showed noticeable variation between the studied species **(Table 12)**. The highest contents of total phenols (119.33 ± 7.24 mg GAE/g DW) and tannins (4.51 ± 0.09 mg CE/g DW) were observed in *S. fruticosa* compared to *A. halimus* (22.23 ± 0.89 mg GAE/g DW and 3.53 ± 0.15 mg CE/g DW, respectively for phenols and tannins) and *L. crithmoides* (30.18 ± 1.45 mg GAE/g DW and 1.83 ± 0.09 mg CE/g DW, respectively for phenols and tannins). However, *A. halimus* showed the highest flavonoid content (73.07 ± 0.19 mg QE/g DW), followed by *S. fruticosa* (63.92 ± 0.01 mg QE/g DW), whereas *L. crithmoides* recorded the lowest value (11.22 ± 0.79 mg QE/g DW).

Table 12. Total phenolic, flavonoids and tannins content in the studied plant extracts.

	Phenolic content (mg GAE/g DW)	**Flavonoid content (mg QE/g DW)**	**Tannins content (mg CE/g DW)**
A. halimus	22,23 ± 0,89 [a]	73,07 ± 0,19 [c]	3,53 ± 0,15 [b]
L. crithmoides	30,18 ± 1,45 [a]	11,22 ± 0,79 [a]	1,83 ± 0,09 [a]
S. fruticosa	119,33 ± 7,24 [b]	63,92 ± 0,01 [b]	4,51 ± 0,09 [c]

Data are presented as the mean of three replicates (n=3) ± standard deviation. Means followed by different letters (a, b, and c) are significantly different ($p \leq 0.05$).

In the present study, the methanolic extract of *A. halimus* collected from Relizane exhibited a higher total phenolic content (TPC) than that previously reported for the same species from Bechar **(Benhammou et *al.*, 2009; Bounouar et *al.*, 2022)**, but lower than the ethanolic leaf extracts collected from Sig, Mazagran, and Biskra **(Ould Kaddour et *al.*, 2019)**. The total flavonoid content (TFC) was relatively comparable to the values reported by **Roubi et *al.* (2023) and Tadj et *al.* (2024)**, whereas the total tannin content (TTC) remained lower than those described by these authors **(Roubi et *al.*, 2023; Tadj et *al.*, 2024)**.

Regarding *L. crithmoides*, **Brzović et *al.* (2025)** demonstrated significant seasonal variations in TPC, TFC, and TTC. The highest levels were recorded in leaf samples collected in August, but these higher values remained considerably lower than those obtained in the present study. In contrast, **Abdelaal et *al.* (2024)** reported significant higher TPC, TFC, and TTC values in *L. crithmoides* methanolic extract collected from the Egyptian Mediterranean coast (127.82 mg GAE g^{-1}, 7.28 mg CE g^{-1}, and 4.45 mg TAE g^{-1} dry extract, respectively for TPC, TFC and TTC).

For *S. fruticosa*, both TPC and TFC were higher than those reported in samples collected from Oran and El-Oued, Algeria **(Chekroun et *al.*, 2019; Gheraissa et *al.*, 2023)**. Likewise, the TTC reported by **Chekroun et *al.* (2019)** was lower than that obtained in the present study.

Several factors can affect the synthesis and accumulation of secondary metabolites in halophytes. These include the phenological stage of the plant, harvesting period, the analyzed plant organ, plant origin, geographical characteristics of the collection area, climatic conditions, drought stress, soil characteristics, and salinity levels **(Brzović et *al.*, 2025)**. In addition, methodological factors, particularly the extraction procedure, solvent type, and solvent polarity, may also influence the recovery and quantification of these phytoconstituents **(Arya et *al.*, 2025)**.

2.3. ATR-FTIR analysis

ATR-FTIR spectroscopy is an analytical technique used for the identification of functional groups in liquids such as oils and plant extracts through characteristic infrared absorption bands. It is a fast and sensitive method, requiring only a small amount of sample with no prior preparation, and allowing repeated measurements for result verification **(Nikalje et *al*., 2019)**.

ATR-FTIR analysis of the three studied halophyte extracts (*A. halimus*, *L. crithmoides*, and *S. fruticosa*) was performed in the mid-infrared region (4000–400 cm^{-1}). The identified peaks, their assigned bonds, and functional group interpretations, in comparison with reference wave numbers reported by **Thummajitsakul et *al*. (2020)** are summarized in **Table 13.** The FTIR spectrum **(Figure 42 A, B and C)** revealed differences in the number of absorption bands among the studied halophytes. *S. fruticosa* exhibited the highest number of peaks (18), followed by *A. halimus* (16), and *L. crithmoides* which showed the lowest number of peaks (9).

Within the 3600–3000 cm^{-1} spectral region, *S. fruticosa* exhibited three distinct absorption bands at 3404.35, 3201.85, and 3050.34 cm^{-1}, whereas only single bands were observed in *A. halimus*, and *L. crithmoides* extracts at 3375.25 cm^{-1} and 3331.85 cm^{-1} respectively. These bands are characteristic of O–H stretching vibrations, indicating the presence of alcohol and phenolic functional groups in all extracts, with a higher abundance and structural diversity of hydroxyl-containing compounds in *S. fruticosa*.

The absorption bands observed at 2930.11 cm^{-1} in *S. fruticosa* and at 2930.96 cm^{-1} in *A. halimus* are assigned to C–H stretching vibrations, indicating the presence of alkane functional groups **(Table 13)**.

The presence of characteristic C=O stretching bands in the 1700–1799 cm^{-1} region suggests the occurrence of lipid-related constituents in *A. halimus* and *S. fruticosa*, whereas no corresponding absorption bands were observed in *L. crithmoides*.

In the amide I region (1600–1706 cm^{-1}), a single absorption band was observed in all extracts at 1618.68, 1623.77, and 1615.03 cm^{-1} for *A. halimus*, *L. crithmoides*, and *S. fruticosa*, respectively. These bands correspond to amide I vibrations (C=O, C–N, and C=N), indicating the presence of proteins.

In the amide II region (1460–1590 cm^{-1}), *S. fruticosa* exhibited three absorption bands at 1530.59, 1490.97, and 1472.93 cm^{-1}, whereas *A. halimus* and *L. crithmoides* showed two bands at 1492.03 and 1474.41 cm^{-1}, and 1489.59 and 1474.25 cm^{-1}, respectively. These

bands are attributed to N–H bending and C–N stretching vibrations, confirming the presence of proteinaceous compounds in the studied extracts.

In the 1450–1300 cm^{-1} region, *A. halimus* showed bands at 1450.67, 1436.81, 1395.46, and 1335.47 cm^{-1}; *L. crithmoides* at 1428.09, 1407.28, and 1344.50 cm^{-1}; and *S. fruticosa* at 1449.84, 1392.64, and 1330.97 cm^{-1}. These bands are attributed to O–H bending vibrations associated with phenolic or tertiary alcohol groups, suggesting the presence of aromatic compounds.

In the 1270–1150 cm^{-1} region, *A. halimus* showed peaks at 1238.10, 1201.27, and 1168.89 cm^{-1}; *L. crithmoides* at 1236.86 cm^{-1}; and *S. fruticosa* at 1238.10 and 1203.06 cm^{-1}, corresponding to C–O stretching of acids and esters.

In the 1140–997 cm^{-1} region, *A. halimus* exhibited peaks at 1122.72 and 1045.28 cm^{-1}; *L. crithmoides* at 1070.87 cm^{-1}; and *S. fruticosa* at 1124.68, 1067.03, and 1044.60 cm^{-1}, indicating C–O vibrations associated with carbohydrates like mono-, oligosaccharides and glycoproteins.

The fingerprint region below 1000 cm^{-1} is characterized by multiple overlapping peaks **(figure 42)**, which complicates spectral interpretation and makes it difficult to analyze **(Petit and Puskar, 2018)**.

Taken together, these findings revealed a strong concordance between the qualitative and quantitative analyses and the FTIR results, with *S. fruticosa* consistently displaying the most pronounced phytochemical richness and spectral features among the three studied species.

FTIR analysis of *A. halimus*-based biosorbent obtained via Soxhlet extraction by **Douara et *al*. (2022)** showed comparable spectral profiles, with minor variations. Their study revealed characteristic bands corresponding to hydroxyl (O–H), amine (N–H), carbonyl (C=O), and aliphatic C–H functional groups.

FTIR analysis reported by **Joshi et *al*. (2023)** on methanolic extracts of both leaves and stems of *S. fruticosa* revealed the presence of major functional groups including O–H, C–H, C=O, Amide I and II, C–O, and N–H vibrations, corresponding to alcohols, phenols, lipids, proteins, and carbohydrates. These results are in strong agreement with the results obtained for *S. fruticosa*, indicating the presence of comparable functional groups in this species, despite differences in the number of peaks, their positions, and intensities.

Table 13. Wavenumber ranges and corresponding functional groups identified by ATR-FTIR in methanolic plant extracts.

peak	Wavenumbers (cm^{-1}) of studied plant extracts			Bond	Functional groups	Reference Wavenumbers (cm^{-1})
	A.h	*L.c*	*S. f*			
01	3375.25	3331.85	3404.35	O-H Stretching	Alcohols,	3000–3600
02	-	-	3201.85		Phenols	
03	-	-	3050.34			
04	2930.96	-	2930.11	C-H stretching	Alkanes,	2850–2970
05	1773.80	-	1774.57	C=O stretching	Lipids	1700–1799
06	1727.34	-	1727.38			
07	1618.68	1623.77	1615.03	Amide I, C=O, C–N, C=N	Proteins	1600–1706
08	-	-	1530.59	Amide II of	proteins	1460–1590
09	1492.03	1489.59	1490.97	proteins, N–H,		
10	1474.41	1474.25	1472.93	C–N		
11	1450.67	-	1449.84	O–H bending,	Primary or	1300–1450
12	1436.81	1428.09	-	phenol or	secondary	
13	1395.46	1407.28	1392.64	tertiary alcohol	phenyl groups	
14	1335.47	1344.50	1330.97	(O–H bend)		
15	1238.10	1236.86	1238.10	C–O stretching	acid or ester	1150–1270
16	1201.27	-	1203.06	vibrations		
17	1168.89	-	-			
18	1122.72	-	1124.68	C–O stretching	mono–, oligo–	997–1140
19	-	-	1067.03	vibrations	saccharides,	
20	1045.28	1070.87	1044.60		glycoprotein	

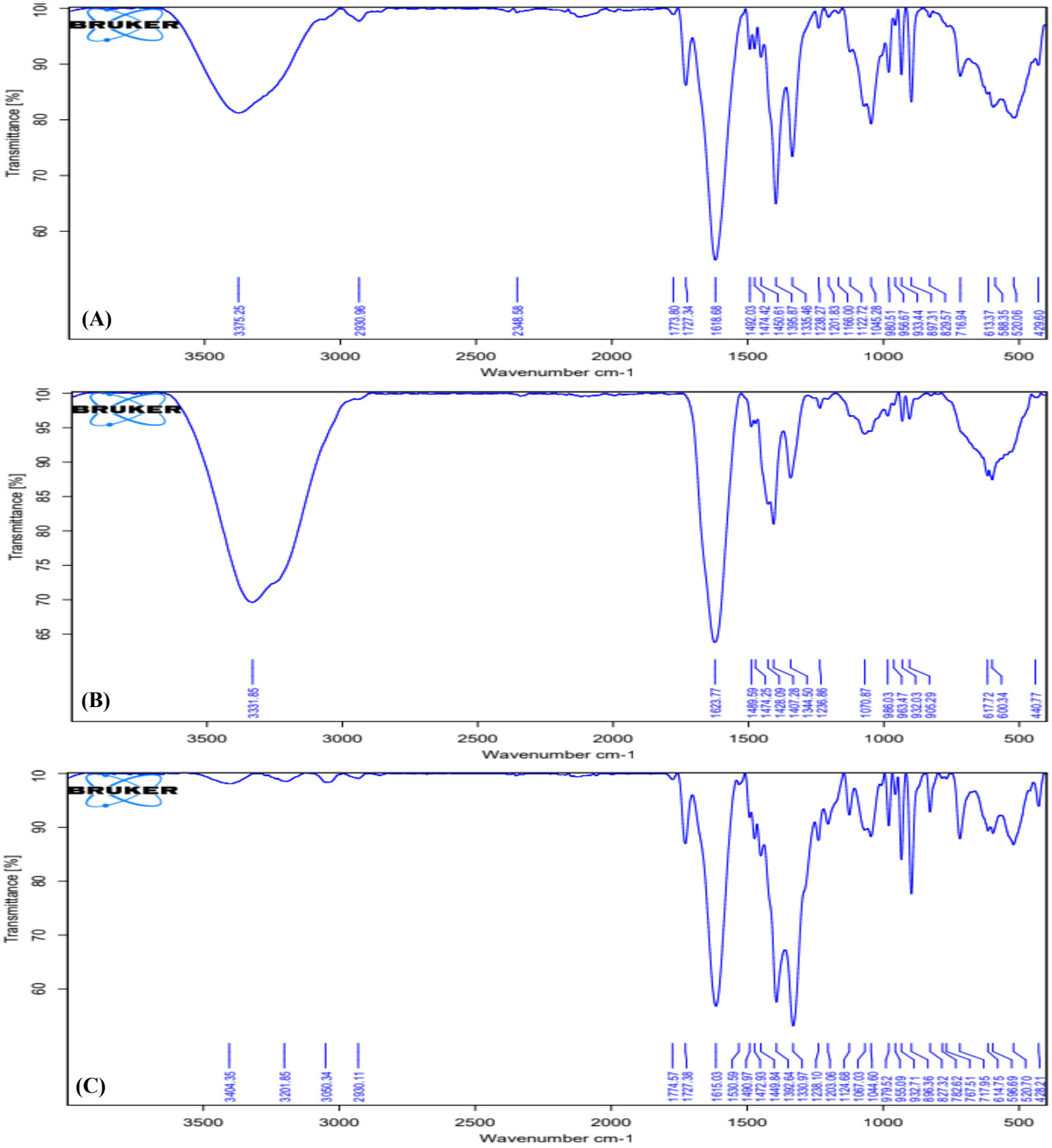


Figure 42. ATR-FTIR Spectrum of different extracts **(A):** *A. halimus*, **(B):** *L. crithmoides*, **(C):** *S. fruticosa.*

2.4. HPLC-ESI-QTOF-MS results

Figure 43 (A, B, and C), **Tables 14, 15, and 16** summarize the base peak chromatograms and the characteristics of the compounds identified in plant extracts, including molecular formulae, retention times, molecular ions (m/z), and molecular masses obtained by HPLC-ESI-QTOF-MS analysis in negative ionization mode.

Metabolic profiling revealed a high level of chemical diversity, a total of 24, 27 and 29 compounds were identified in *A. halimus*, *L. crithmoides*, and in *S. fruticosa* respectively. In addition to secondary metabolites, several primary metabolites were detected, such as sugars (glucose and D-sedoheptulose), amino acid derivatives (N-acetyl-L-phenylalanine) and lipids (palmitoleic, azelaic, malyngic, coronaric acids, and cratenacin), reflecting essential physiological and metabolic functions.

Regarding the phenolic fraction, *A. halimus* exhibited a limited but structurally diverse profile. The identified phenolic compounds included protocatechuic acid 4-*O*-glucoside, caffeic acid 3-sulfate, dihydroxybenzoic acids, salicylic acid, and feruloyltyramine, representing both hydroxybenzoic and hydroxycinnamic acid derivatives. Quercetin dihydrate was the only flavonoid detected in this species, while phenol and related aromatic derivatives also contributed to the phenolic composition. These findings are consistent with those reported by **Clauser et *al*. (2013)** who identified quercetin derivatives and caffeic acid sulfate in the methanolic extract of the aerial part of *A. halimus*.

Table 14. Compounds **i**dentified in the methanolic extract of *A. halimus* by HPLC-ESI-QTOF-MS analysis.

N	Formula	R_t (min)	$[M-H]^-$ (m/z)	Molecular mass	Compounds
1	$C_6H_{12}O_7$	3.122	195.0512	196.0585	Gluconic acid
2	$C_6H_{12}O_6$	3.265	179.0565	180.0637	Glucose
3	$C_7H_{14}O_7$	3.444	209.0671	210.0744	D-Sedoheptulose
4	$C_4H_6O_5$	3.663	133.0144	134.0217	Malic acid
5	$C_5H_7NO_3$	4.368	128.0355	129.0428	Pyroglutamic acid
6	$C_4H_6O_5$	4.519	133.0146	134.0219	Malic acid
7	$C_6H_8O_7$	5.035	191.019	192.0269	Citric acid
8	$C_5H_7NO_3$	5.077	128.0356	129.0428	Pyrrolidinemonocarboxylic acid
9	$C_5H_8O_5$	5.994	147.0303	148.0375	Citramalic acid

10	$C_4H_6O_4$	6.229	117.0195	118.0268	Succinic acid
11	$C_{13}H_{16}O_9$	7.821	315.0726	316.0799	Protocatechuic acid 4- glucoside
12	$C_{13}H_{24}O_7S$	8.812	323.1173	324.1246	2-Octyl-2-sulfopentanedioic acid
13	$C_9H_8O_7S$	9.197	258.9921	259.9995	Caffeic acid 3-sulfate
14	$C_9H_8O_7S$	9.387	258.9923	259.9996	Caffeic acid 3-sulfate
15	$C_7H_6O_4$	10.063	153.0198	154.0271	Dihydroxybenzoic acids
16	$C_6H_6O_6$	10.2	173.0094	174.0166	Trans-Aconitic acid
17	$C_{15}H_{14}O_9$	10.342	337.0569	338.0641	Quercetin dihydrate
18	$C_{13}H_{24}O_6S$	11.048	307.1227	308.13	Oxo-tridecanoic acid sulphate
19	$C_8H_8O_5S$	11.354	215.0022	216.0095	Alpha-sulfophenylacetic acid
20	$C_{18}H_{19}NO_4$	12.469	312.1246	313.1318	Feruloyltyramine
21	$C_7H_6O_3$	13.474	137.0246	138.0318	Salicylic acid
22	C_6H_6O	13.476	93.0348	94.0421	Phenol
23	$C_{18}H_{34}O_5$	14.35	329.2336	330.2409	Pinellic acid
24	$C_{18}H_{28}O_4$	17.116	307.1921	308.1993	Monomethyl ambelin
25	$C_{18}H_{30}O_3$	22.979	293.2127	294.22	17-Hydroxylinolenic acid
26	$C_{18}H_{30}O_3$		293.2127	294.22	17-Hydroxylinolenic acid
27	$C_{18}H_{32}O_3$	24.94	295.228	296.2353	Coronaric acid
28	$C_{16}H_{30}O_2$	27.556	253.2173	254.2246	Palmitoleic acid

L. crithmoides was characterized by a predominance of phenolic compounds, mainly represented by hydroxycinnamic acid derivatives, along with a single flavonoid. Among the identified phenolic acids and their derivatives were caffeic acid 4-*O*-glucuronide, chlorogenic acid, feruloylglucaric acid, glucocaffeic acid, 5-*O*-caffeoylshikimate, 3-*O*-feruloylquinic acid, cynarin, coumarinic acid, veratric acid, and caffeoylglucaric acid. Quercetin 3-*O*-glucoside was the only flavonoid detected in this species**.** In addition, other phenolic conjugates, such as 1-*O*-vanilloyl-β-D-glucose, were also identified.

The presence of chlorogenic acid, caffeic acid, quercetin, and their derivatives was previously reported by **Jallali et *al.* (2018)** in the floral fraction extract of golden samphire obtained by Centrifugal Partition Chromatography (CPC). Similarly, **Castañeda-Loaiza et *al.* (2024)** identified several of these bioactive compounds in the methanolic extract of *L. crithmoides* seeds. However, slight differences were observed, particularly the absence of rutin and other flavonoids in the present analysis.

Table 15. Identified compounds in the methanolic extract of *L. crithmoides* by HPLC-ESI-QTOF-MS analysis.

N	Molecular Formula	R_t (min)	$[M-H]^-$ (m/z)	Molecular mass	Compounds
1	$C_7H_{12}O_6$	3.298	191.0562	192.0635	Quinic acid
2	$C_4H_4O_4$	3.639	115.0039	116.0112	Fumaric acid
3	$C_4H_6O_5$	3.641	133.0143	134.0216	Malic acid
4	$C_6H_8O_7$	5.021	191.0197	192.027	Citric acid
5	$C_5H_7NO_3$	5.067	128.0354	129.0427	Pyroglutamic acid.
6	$C_4H_6O_4$	6.228	117.0196	118.0269	succinic acid
7	$C_9H_{11}NO_2$	7.629	164.0717	165.079	Phenylalanine
8	$C_{15}H_{16}O_{11}$	7.926	371.0624	372.0698	Caffeoylglucaric acid
9	$C_{15}H_{16}O_{10}$	8.596	355.0677	356.075	Caffeic acid 4-O-glucuronide
10	$C_7H_6O_4$	8.719	153.0195	154.0268	Protocatechuic acid
11	$C_{21}H_{20}O_{12}$	8.785	465.1442	466.1514	Quercetin 3-O-glucoside
12	$C_{16}H_{18}O_9$	8.823	353.0881	354.0953	Chlorogenic acid
13	$C_{16}H_{18}O_{11}$	8.837	385.078	386.0852	Feruloylglucaric acid
14	$C_{14}H_{18}O_9$	9.024	329.0916	330.0986	1-O-Vanilloyl-beta-D-glucose
15	$C_{16}H24O_7$	9.498	373.1511	328.1519	Rhododendrin
16	$C_{15}H_{18}O_9$	9.504	341.0916	342.0988	Glucocaffeic acid
17	$C_{16}H_{16}O_8$	9.509	335.0777	336.085	5-O-caffeoylshikimate
18	$C_{17}H_{20}O_9$	9.65	367.104	368.1112	3-O-Feruloylquinic acid
19	$C_{10}H_{18}O_4$	10.123	201.1135	202.1207	Sebacic acid
20	$C_{25}H_{24}O_{12}$	10.547	515.1209	516.1279	Cynarine
21	$C_9H_8O_3$	10.834	163.0404	164.0476	Coumarinic acid
22	$C_{33}H_{28}O_{17}$	10.949	695.1263	696.1336	Maclurin
23	$C_{16}H_{26}O_7$	11.182	329.161	330.1682	Picrocrocin
24	$C_9H1_6O_4$	11.497	187.0976	188.1049	Azelaic acid
25	$C_{18}H_{32}O_5$	13.503	327.218	328.2252	Malyngic acid
26	$C_{18}H_{34}O_5$	14.302	329.2338	330.241	Pinellic acid
27	$C_9H_{10}O_4$	15.977	181.0507	182.058	3.4-dimethoxybenzoic acid

Finally, *S. fruticosa* exhibited a pronounced enrichment in phenolics, accounting for more than 50% of the identified metabolites. A total of 17 phenolic compounds were detected, including phenolic acids such as sinapic, *p*-coumaric, protocatechuic, and salicylic acids, together with several caffeic acid derivatives, notably diacetyl caffeic acid and fertaric acid. Flavonoids were mainly represented by rutin, quercetin 3-*O*-sambubioside, kaempferol 3-*O*-rutinoside-7-*O*-glucoside, isorhamnetin, isorhamnetin-3-*O*-glucoside, and the flavanone glycoside naringin, highlighting the marked flavonoid diversity of the extract. Other phenolic constituents, including vanilloloside, fraxin, eugenitin, cratenacin, and monomethyl embelin, further contributed to the overall phenolic profile of the species.

These findings differ from those reported by **Gheraissa et *al*. (2023)**, who identified gallic acid, vanillic acid, caffeic acid, p-coumaric acid, vanillin, rutin, and quercetin in extracts of the same species.

Table 16. Identified compounds in methanolic extract of *S. fruticosa* by HPLC-ESI-QTOF-MS analysis.

N	Molecular Formula	R_t (min)	$[M-H]^-$ (m/z)	Molecular mass	Compounds
1	$C_6H_{12}O_7$	3.113	195.0516	196.0589	Gluconic acid
2	$C_{11}H_{12}O_5$	3.458	223.046	224.0534	Sinapic acid
3	$C_4H_6O_5$	3.657	133.0148	134.0221	Malic acid
4	$C_6H_8O_7$	4.177	191.02	192.0273	Citric acid
5	$C_5H_7NO_3$	4.355	128.0357	129.043	L-Pyroglutamic acid
6	$C_4H_4O_4$	4.523	115.0042	116.0115	Fumaric acid
7	$C_6H_8O_7$	5.025	191.0201	192.0273	Citric acid
8	$C_5H_7NO_3$	5.072	128.0356	129.0424	L-Pyroglutamic Acid
9	$C_4H_6O_4$	6.224	117.0194	118.0266	Succinic acid
10	$C_{14}H_{20}O_8$	7.802	315.1086	316.1159	Vanilloloside
11	$C_{14}H_{14}O_9$	8.426	325.0566	326.064	Fertaric acid
12	$C_{33}H_{40}O_{20}$	9.091	755.206	756.2133	Kaempferol 3-O-rutinoside 7-O-glucoside
13	$C_{16}H_{18}O_{10}$	9.288	369.0834	370.0907	Fraxin
14	$C_{26}H_{28}O_{16}$	9.346	595.1308	596.1382	Quercetin 3-O sambubioside

15	$C_{12}H_{12}O_4$	9.392	219.0668	220.074	Eugenitin
16	$C_{13}H_{12}O_6$	9.395	263.0563	264.0636	Diacetyl caffeic acid
17	$C_{27}H_{30}O_{16}$	9.741	609.1472	610.1545	Rutin
18	$C_{13}H_{12}O_6$	9.89	263.0566	264.0637	Diacetyl caffeic acid
19	$C_7H_6O_4$	10.103	153.0198	154.027	Protocatechuic Acid
20	$C_{22}H_{22}O_{12}$	10.361	477.1045	478.1118	isorhamnetin-3-O-glucoside
21	$C_{11}H_{13}NO_3$	10.414	206.0825	207.0899	N-Acetyl-L-phenylalanine
22	$C_{27}H_{32}O_{14}$	10.748	579.1742	580.1816	Naringin
23	$C_9H_8O_3$	10.867	163.0401	164.0474	Coumaric acid
24	$C_{13}H_{12}O_6$	11.141	263.0566	264.0639	Diacetyl caffeic acid
25	$C_{13}H_{24}O_6S$	11.251	307.122	308.13	Oxo-tridecanoic acid sulphate
26	$C_9H_{16}O_4$	11.534	187.0977	188.105	Azelaic acid
27	$C_{29}H_{32}O_{15}$	11.628	619.1677	620.175	Cratenacin
28	$C_7H_6O_3$	13.476	137.0245	138.0318	Salicylic acid
29	$C_{18}H_{32}O_5$	13.548	327.218	328.2253	Malyngic acid
30	$C_{18}H_{34}O_5$	14.34	329.2336	330.241	Pinellic acid
31	$C_{16}H_{12}O_7$	15.27	315.0513	316.0586	Isorhamnetin
32	$C_{18}H_{28}O_4$	17.081	307.1919	308.1993	Monomethyl embelin
33	$C_{18}H_{30}O_3$	22.986	293.2124	294.2197	17-Hydroxylinolenic acid
34	$C_{18}H_{30}O_3$	23.332	293.2124	294.2197	17-Hydroxylinolenic acid
35	$C_{18}H_{32}O_3$	24.948	295.2279	296.2352	13-Hydroxyoctadecadienoic acid

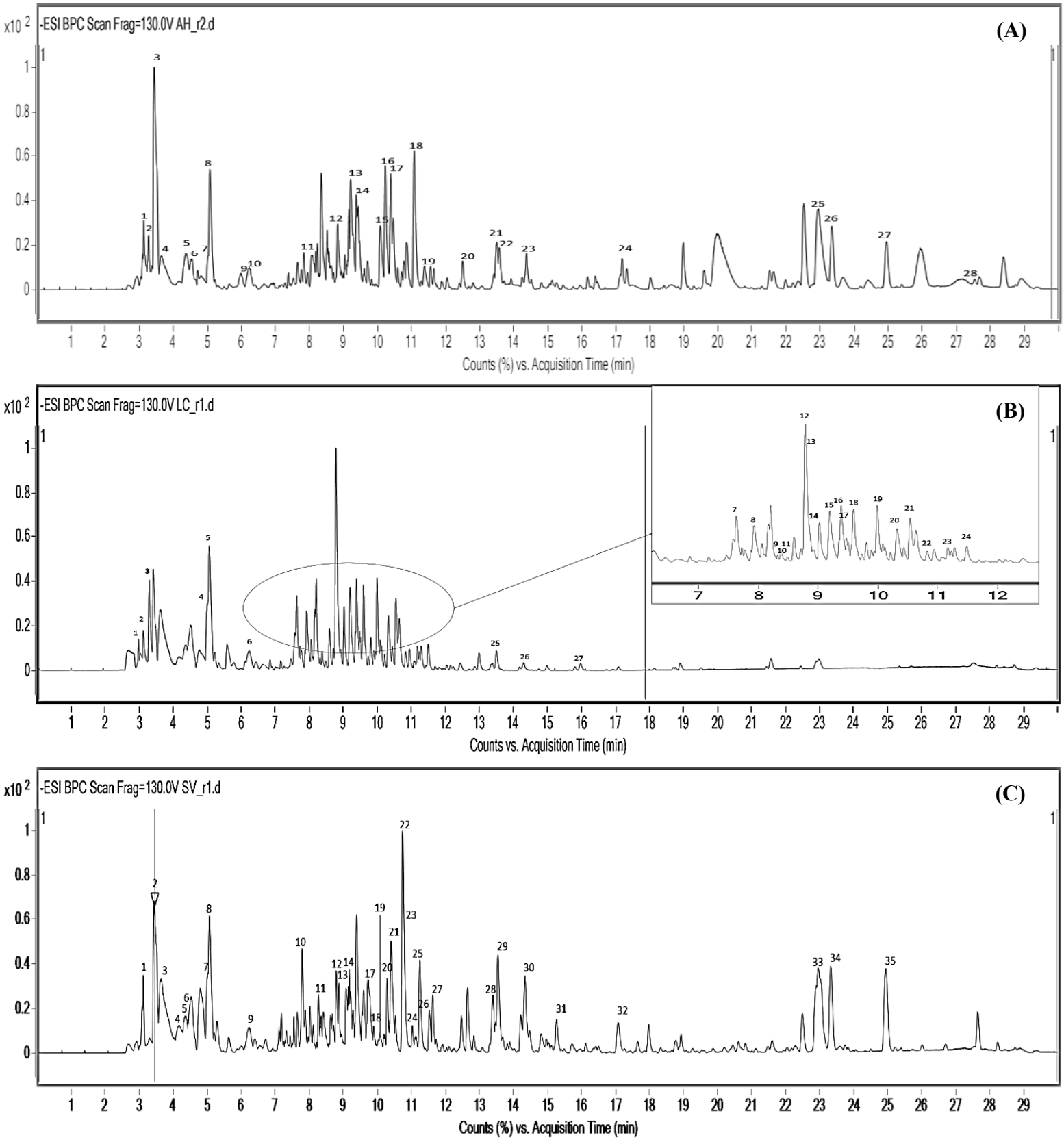


Figure 43. Base peak chromatogram of different extracts **(A):** *A. halimus*, **(B):** *L. chritmoides*, **(C):** *S. fruticosa* obtained by HPLC-ESI-QTOF-MS.

3. Biological activities *in vitro*

3.1. Antioxidant activity

The antioxidant activity of the halophyte extracts, evaluated *in vitro* by DPPH and ABTS radical scavenging assays as well as the FRAP reducing power method, is presented in **Table 17**.

In both DPPH and ABTS assays, the hydromethanolic extract of the aerial parts of *S. fruticosa* exhibited the strongest radical-scavenging activity, with the lowest IC_{50} values (DPPH IC_{50} = 0.48 ± 0.001 mg/mL; ABTS IC_{50} = 1.03 ± 0.006 mg/mL), compared with *A. halimus* (DPPH IC_{50} = 25.19 ± 0.02 mg/mL; ABTS IC_{50} = 3.19 ± 0.07 mg/mL) and *L. crithmoides* (DPPH IC_{50} = 33.59 ± 0.24 mg/mL; ABTS IC_{50} = 5.43 ± 0.14 mg/mL).

The FRAP assay further confirmed the superior antioxidant potential of *S. fruticosa*, which exhibited the highest ferric reducing capacity (2130.96 ± 2.55 µmol Fe^{2+} equivalents/g extract), followed by *A. halimus* (260.49 ± 1.27 µmol EFe^{2+}/g extract) and *L. crithmoides* (133.86 ± 1.27 µmol EFe^{2+}/g extract).

Ascorbic acid showed a significant greater antioxidant activity than the three species as indicated by its lower IC_{50} values (DPPH IC_{50} = 0.139 mg/mL; ABTS IC_{50} = 0.130 mg/mL).

Table 17. DPPH, ABTS radical scavenging activity, and ferric reducing antioxidant power of plant extracts.

	Radical scavenging		**Reducing power capacity**
Plant extract	**DPPH IC_{50} (mg/mL)**	**ABTS IC_{50} (mg/mL)**	**FRAP (µmol EFe^{+}/g DW)**
A. halimus	25.19 ± 0.02^{b}	3.19 ± 0.07^{b}	260.49 ± 1.27 ^{b}
L. chritmoides	33.59 ± 0.24^{a}	5.43 ± 0.14^{a}	133.86 ± 1.27 ^{a}
S. fruticosa	0.48 ± 0.001^{c}	1.03 ± 0.006^{c}	2130.96 ± 2.55 ^{c}
Ascorbic acid	0.139	0.130	/

Data are presented as the mean of three replicates ± standard deviation. Means followed by different letters (a, b, and c) are significantly different ($p \leq 0.05$).

Several studies have reported the antioxidant activity of *A. halimus* **(Ould Kaddour et *al.*, 2019; Roubi et *al.*, 2023; Tadj et *al.*, 2024)**, with DPPH IC_{50} values ranging from a few micrograms per milliliter to several hundred milligrams per milliliter. For example, **Benhammou et *al.* (2009)** reported a DPPH IC_{50} value of 31.83 mg/mL for the methanolic

extract of the same species, which was higher than the value obtained in the present study (25.19 ± 0.02 mg/mL). Furthermore, the ethanolic leaf extracts of *A. halimus* collected from the Biskra and Mazagran regions exhibited DPPH radical-scavenging activities of 85.77% and 74.76% inhibition, respectively, at a concentration of 100 mg/mL **(Ould Kaddour et *al.*, 2019)**.

Notably, the hydromethanolic extract analyzed in the present study achieved 78.25% inhibition at only 32 mg/mL **(Annex 01)**, highlighting its strong antioxidant potential despite being tested at a substantially lower concentration.

Djillali et *al.* (2026) showed an IC_{50} value of 1.024 mg/mL for the ABTS radical scavenging activity of the ethanolic extract of the aerial parts of *A. halimus* from the Algerian Sahara, lower than that obtained in the present study (3.19 mg/mL), indicating stronger antioxidant activity in their samples. This difference suggests that environmental conditions may influence the biosynthesis and accumulation of antioxidant compounds in plants.

In addition, the antioxidant activity of *L. crithmoides* extracts in different seasons using DPPH and FRAP assays has been investigated **(Brzović et *al.*, 2025)**. The IC_{50} values for DPPH were about 24.74, 24.21, and 22.91 mg/mL in June, July, and August, respectively, accompanied by increasing FRAP values from 811 to 1086 and 1149 µmol Fe^{2+}/g of extract, indicating enhanced antioxidant capacity during the summer period. In our study, the February sample extract showed a lower antioxidant potential (DPPH IC_{50} value of 33.59 ± 0.24 and a FRAP value of 133.86 ± 1.27 µmol Fe^{2+}/g) compared to those of **Brzović et *al.* (2025)**. Overall, our results confirm that this variation is mainly due to differences in phenolic content and composition depending on the harvest period, particularly during plant development stages.

The antioxidant potential observed in the present study for *S. fruticosa* is consistent with the findings of **Zaier et *al.* (2022)**, who reported comparable DPPH (IC_{50} = 0.32 ± 0.001 mg/mL) and ABTS (IC_{50} = 1.47 ± 0.07 mg/mL) values for samples collected in Sousse, Tunisia. Similarly, the strong reducing power revealed by the FRAP assay agrees with the values reported for the methanolic (5.32 ± 0.56 mM Fe^{2+}/g) and acetone (3.76 ± 0.15 mM Fe^{2+}/g) extracts **(Qasim et *al.*, 2016)**.

In general, the antioxidant activity of plant extracts is influenced by several factors, including the concentration, chemical structure, and overall abundance of phenolic constituents **(Chaouche et *al.*, 2014)**. Phenolic compounds, particularly flavonoids and tannins, are recognized as major contributors to antioxidant potential due to their redox properties, which enable them to donate hydrogen atoms or electrons and neutralize free

radicals **(Tadj et *al*., 2024)**. In the present study, a positive relationship was observed between the phytochemical profile of the three halophyte extracts, as characterized by phytochemical screening, TPC, TFC, TTC, ATR-FTIR, and HPLC-ESI-QTOF-MS analyses, and their antioxidant capacities assessed by DPPH, ABTS, and FRAP assays. Among the investigated species, *S. fruticosa* exhibited the richest phytochemical profile and the strongest antioxidant potential, as evidenced by its superior reducing power and radical-scavenging activity, reflected by the lowest IC_{50} values obtained in the DPPH and ABTS assays.

3.2. Insecticidal activity

3.2.1. Repellent effect

The repellency results were expressed as percentage repellency according to the McDonald method **Table 18.** After two hours of exposure, all tested plant extracts at concentrations of 25, 50, 100, and 200 mg/mL exhibited repellent activity against adults of *T. confusum*. It was observed that the repellency rate was found to increase in a dose-dependent manner, with the highest concentrations generally exhibiting the strongest repellent effects against *T. confusum* adults. *S. fruticosa* showed the highest overall repellent effect (RP = 89.81%), achieving complete repellency (100%) at concentrations of 100 and 200 mg/mL, followed by *A. halimus* (RP = 83.23%), which reached 100% repellency at 200 mg/mL. *L. crithmoides* displayed comparatively lower repellency (RP = 72.05%), although its repellent effect also increased progressively with increasing extract concentration, reaching 96.29% at 200 mg/mL.

Table 18. Repellency effect of methanolic extracts against *T. confusum* adults.

	25 mg/mL	**50 mg/mL**	**100 mg/mL**	**200 mg/mL**	**RP%**
A. halimus	69,04 %	79,62 %	84,25 %	100 %	83,23 %
L. crithmoides	49,20 %	63,09 %	79,62 %	96,29 %	72,05 %
S. fruticosa	75 %	84,25 %	100 %	100 %	89,81 %

The present findings are in agreement with previous studies of **(Elhawary et *al*., 2026)**, who demonstrated that *A. halimus* fractions exhibited significant repellent activity against the malaria vector *Anopheles pharoensis* starved females, with the dichloromethane fraction showing the highest effect (81.92% at 6.67 mg/cm²), followed by butanol (74.49%), ethyl acetate (66.48%), and methanol (57.76%).

The repellent activity of four plant extracts evaluated by **Atta et *al.* (2020)** against *T. castaneum* at concentrations ranging from 20 to 80 mg/mL showed repellency values varying from 10% to 86.66%, indicating a clear concentration-dependent increase in repellency.

Similarly, **Salim et *al.* (2019)** reported that five medicinal plant extracts exhibited repellent activity against *T. confusum*, with *Moringa oleifera* showing the highest effect (73.3%) at 30% concentration after 30 minutes of exposure.

Several plant species produce a wide range of chemical compounds that may act as repellents, deterrents, or even toxic agents against insect pests. Some of these secondary metabolites can also be toxic to the plant itself and are therefore stored in specialized organs such as flowers and seeds. These bioactive compounds constitute a chemical defense system directly targeting phytophagous insect pests **(Atta et *al.*, 2020)**.

In this context, the strong repellent activity observed in *S. fruticosa* compared to *A. halimus* and *L. crithmoides* may be attributed to its high content of phenolic compounds, as well as to the variability and diversity of these chemical classes revealed by HPLC-ESI-QTOF-MS analysis.

3.2.2. Contact effect

Figure 44 (A, B, and C) illustrates the mortality rate of adult populations of *T. confusum* exposed to different concentrations (25, 50, 100, and 200 mg/mL) and exposure times (24, 48, 72, and 96 h) of hydromethanolic plant extracts, compared to the control group. The results showed that mortality increased in a dose- and time-dependent manner. After 24 h, minimal mortality (6.66 ± 5.77%) was recorded for both *A. halimus* and *S. fruticosa*, while 10% of mortality was observed for *L. crithmoides* at the lowest concentration (25 mg/mL). In contrast, the highest mortality rates were recorded after 96 h at 200 mg/mL, reaching 76.67 ± 5.77%, 80.00 ± 0.00%, and 86.66 ± 5.77% for *L. crithmoides*, *A. halimus*, and *S. fruticosa*, respectively. No mortality was observed in the control group.

At 48 and 72 h, mortality rates were higher than those recorded at 24 h and lower than those observed at 96 h for all the tested plant extracts. Mortality values also increased with increasing concentrations, with the highest rates recorded at 100 and 200 mg/mL compared to 25 and 50 mg/mL.

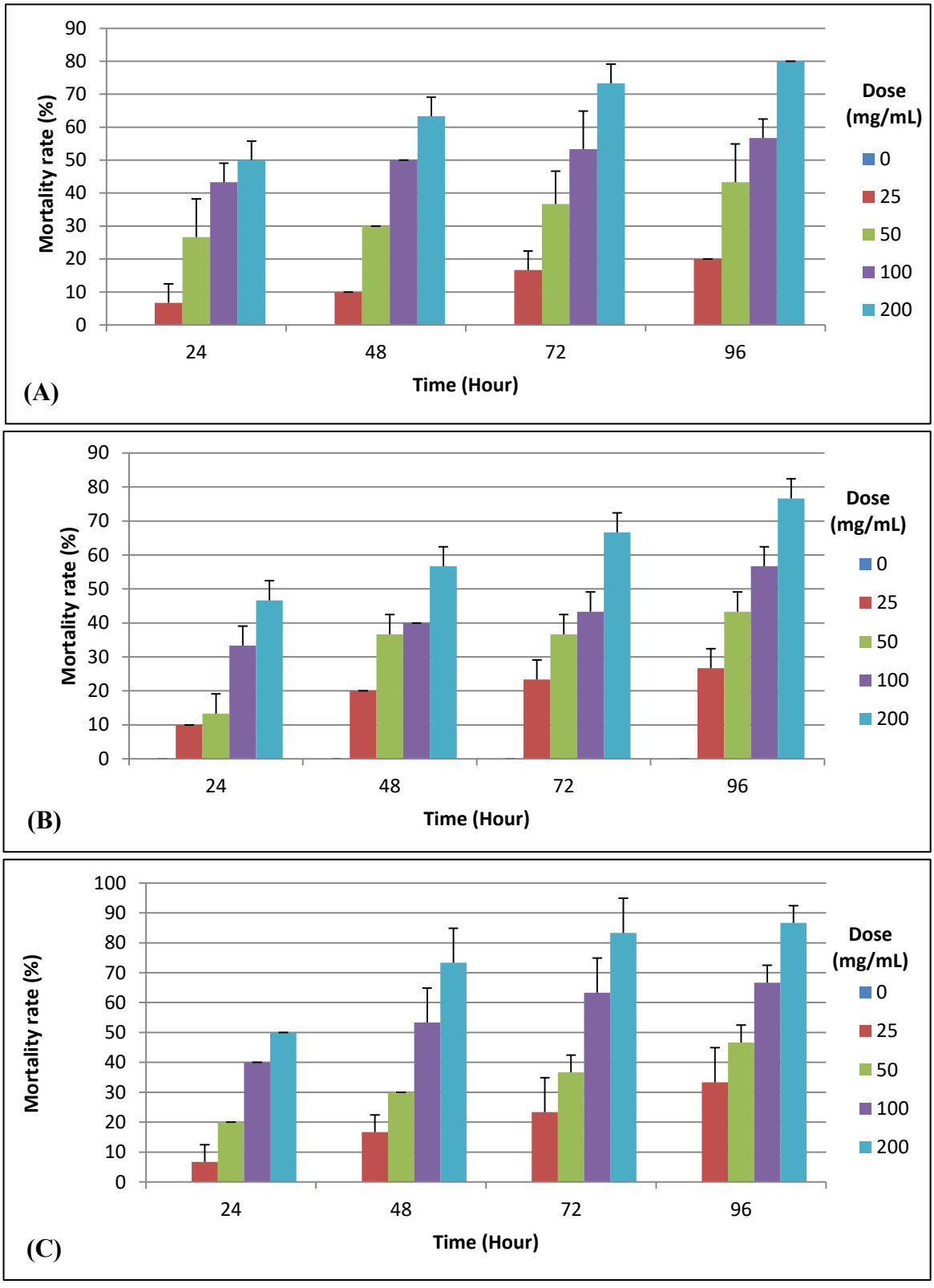


Figure 44. Mortality of *T. confusum* exposed by direct contact to different concentrations of methanolic extracts: **(A):** *A. halimus*, **(B):** *L. crithmoides*, **(C):** *S. fruticosa.*
Columns show the mean of three replicates and bars show the standard deviation of means.

On the other hand, the probit analysis used to estimate LC_{50} values at 24, 48, 72 and 96 h is presented in **Table 19**. The LC50 values for *A. halimus*, *L. crithmoides*, and *S. fruticosa* decreased from 164.75 ± 26.22, 220.75 ± 23.83, and 169.66 ± 8.85 mg/mL at 24 h, respectively, to 84.73 ± 0.00, 88.86 ± 17.52, and 50.03 ± 12.65 mg/mL at 96 h.

Table 19. LC_{50} values of plant extracts against *T. confusum* adults at 4 times intervals.

Time	**LC_{50} (mg/mL)**		
	A. halimus	*L. crithmoides*	*S. fruticosa*
24h	164.75 ± 26.22	220.75 ± 23.83	169.66 ± 8.85
48h	116.49 ± 18.77	148.325 ±28.83	108.12 ± 16.004
72h	89.63 ± 21.91	106.14± 22.98	82.72 ± 2.36
96h	84.73 ± 00	88.86 ± 17.52	50.03 ± 12.65

Data are presented as the mean of three replicates ± standard deviation with ($p \leq 0.05$).

The insecticidal activity observed in the present study is consistent with previous reports, highlighting the potential of these species as natural bioinsecticides.

For instance, **Naboulsi et *al.* (2022)** demonstrated the insecticidal efficacy of a hydromethanolic extract of *A. halimus* using direct contact assays against both developmental stages of *Dactylopius opuntiae*. Mortality of adult females reached 90.00 ± 10.00% after 8 days of exposure to a 5% extract, whereas nymph mortality attained 80.20 ± 8.43% at 5 mg/mL. Furthermore, the 20% methanolic extract showed an LC_{50} value of 3.06 mg/mL. The authors attributed this activity mainly to the high saponin content and the diversity of secondary metabolites identified by LC-MS analysis.

The work of **Saidana et *al.* (2007)** evaluated the bio-insecticidal activity of different extracts of *Suaeda fruticosa* on larval and adult stages of *Tribolium confusum* (Coleoptera: Tenebrionidae). The obtained results revealed a lower efficacy compared to our study, particularly in terms of mortality rates, especially for the methanolic extract. These findings confirm that the effectiveness of plant extracts is strongly dependent on the plant species, the extraction solvent, the insect developmental stage, as well as the exposure time.

The insecticidal activity evaluated by contact bioassays for the three halophytic species investigated in our study was previously reported by **Solimane et *al.* (2005)**, who tested the same species along with 22 other plants using five different solvents against the cotton aphid (*Aphis gossypii*). Their findings showed that contact toxicity was generally higher than that observed in our work, as indicated by lower LC_{50} values. Moreover, significant variations in LC_{50} were recorded according to both plant species and extraction

solvent. For instance, LC_{50} values ranged from 2.49 mg/cm^2 (diethyl ether extract) to 7.48 mg/cm^2 (hexane extract) for *A. halimus*, from 4.675 mg/cm^2 (ethanolic extract) to 17.71 mg/cm^2 (ethyl acetate extract) for *L. crithmoides*, and from 1.506 mg/cm^2 (diethyl ether extract) to 14.104 mg/cm^2 for *S. fruticosa*. Overall, *S. fruticosa* exhibited the highest insecticidal efficacy, followed by *A. halimus*, whereas *L. crithmoides* showed the lowest activity

The variability of insecticidal activity among these plants can be explained by differences in the polyphenolic composition identified by HPLC-ESI-QTOF-MS among the studied species. Flavonoids such as quercetin derivatives, rutin, kaempferol derivatives, isorhamnetin derivatives, and naringin are known to contribute significantly to insecticidal activity. These compounds can interfere with insect growth, development, reproduction, and feeding behavior. They may also affect the nervous system by inhibiting key enzymes such as acetylcholinesterase and modulating neuronal channels. In addition, flavonoids have been reported to induce developmental delays, morphological abnormalities, and reproductive disorders in insects. Their exposure may also disrupt detoxification enzymes, leading to oxidative stress. Moreover, they can inhibit digestive enzymes (amylase, protease, and lipase) in the insect midgut, reducing nutrient assimilation **(Pereira et *al.*, 2024)**.

3.2.3. Powder plant effect

The effects of different plant powder doses (0.2, 0.4, 0.6, and 0.8 g/g diet) on the mortality of adult *T. confusum* after 4, 8, 12, and 16 days of exposure are presented in **Figure 45 (A, B, and C)**. The results showed that the insecticidal activity of all three halophyte powders increased progressively with both increasing dose and exposure time.

At 4 days of exposure, mortality was relatively low at the lowest dose (0.2 g/g diet) but increased considerably with higher doses. This dose- and time-dependent trend persisted throughout the experiment, with the highest mortality recorded after 16 days of exposure.

A. halimus exhibited a marked insecticidal effect, with mortality increasing from 13.33% at the lowest dose after 4 days to complete mortality (100%) at 0.6 and 0.8 g of plant powder/g diet after 16 days. *L. crithmoides* showed the lowest efficacy among the tested species, reaching a maximum mortality of 100% only at the highest dose (0.8 g/g diet) after 16 days, whereas lower doses produced comparatively lower mortality rates. However, *S. fruticosa* displayed the greatest insecticidal activity, achieving complete mortality at doses of 0.4, 0.6, and 0.8 g/g diet after 16 days of exposure, while the lowest dose resulted in 83.33% mortality.

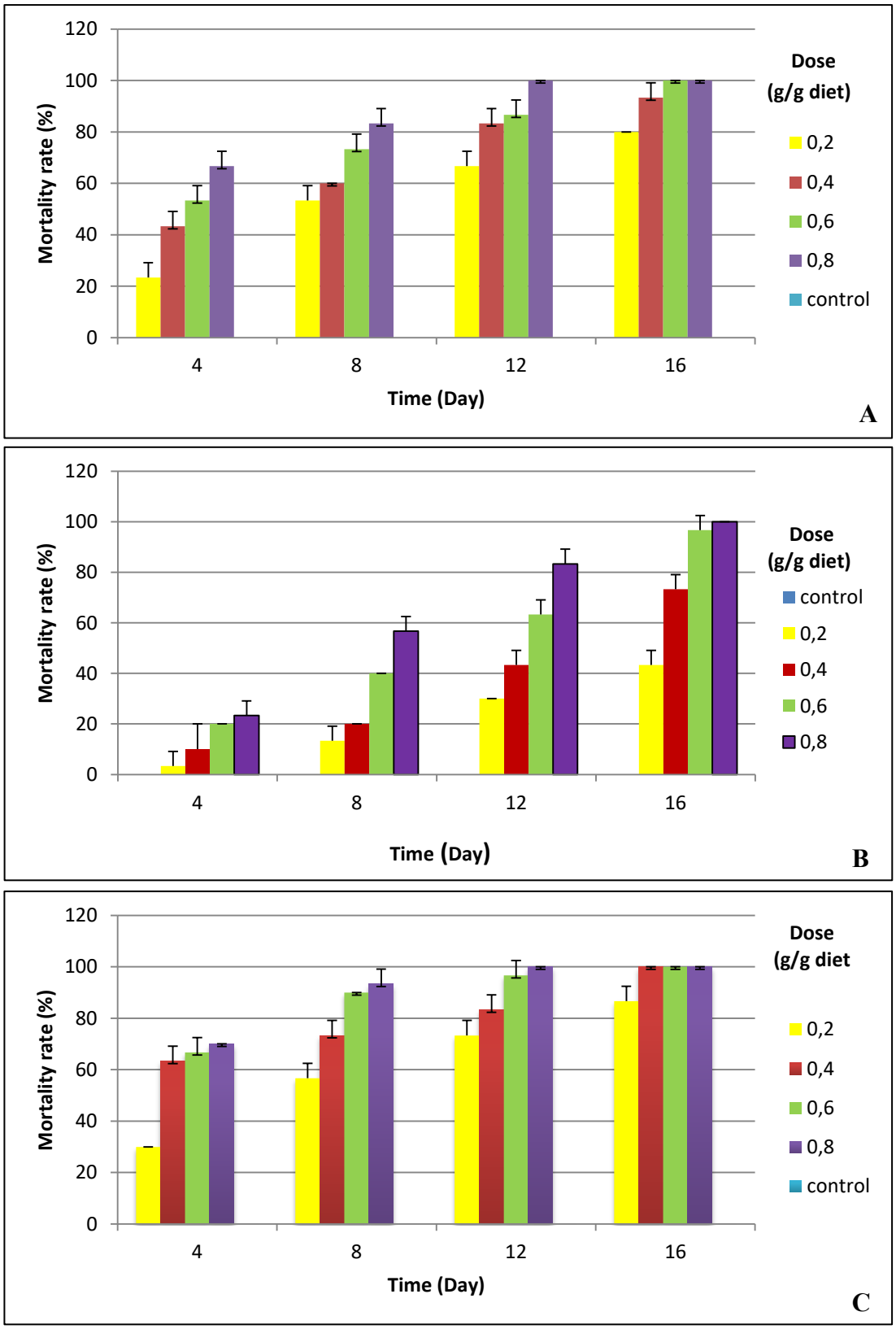


Figure 45. Mortality of *T. confusum* fed diets supplemented with different concentrations of plant powder **(A):** *A. halimus*, **(B):** *L.crithmoides*, **(C):** *S. fruticosa.*

Columns show the mean of three replicates and bars show the standard deviation of means.

Soummane et *al*. (2011) investigated the insecticidal activity of *S. fruticosa* against the Mediterranean fruit fly (*Ceratitis capitata*). The plant extract was incorporated into an artificial diet to assess its toxicity through ingestion under laboratory conditions over a 24-hour exposure period. Their findings demonstrated a clear dose-dependent insecticidal effect, with LC_{50} values of 0.5 mg/g of diet for larvae and 0.03 mg/g of diet for adults, indicating a particularly high susceptibility of the adult stage to the treatment.

To the best of our knowledge, very few studies have investigated the insecticidal activity of *A. halimus* and *L. crithmoides* powders. Therefore, comparisons were extended to other medicinal and aromatic plant powders exhibiting similar insecticidal properties.

For example, **Ahmad et *al*. (2019)** reported the insecticidal potential of six medicinal plant powders against different developmental stages of *Tribolium castaneum* (larvae, pupae, and adults) when incorporated into corn, rice, and wheat flours at a dose of 5% (w/w; 1 g of plant powder per 19 g of substrate), resulting in significant mortality. The treated diets also disrupted insect development by reducing larval growth, pupation success, and adult emergence.

In addition, the study conducted by **Ziaee and Moharramipour, (2013)** showed the insecticidal activity of *Cuminum cyminum* powder against *Sitophilus granarius* and *Tribolium confusum*. Their results showed mortality rates exceeding 50% after 7 days of exposure for both species, while complete mortality (100%) was recorded in adult *T. confusum* after 14 days of treatment.

Righi et *al*. (2017) demonstrated the insecticidal activity of three Algerian plant powders against the stored-product pest *Rhyzopertha dominica*. At a dose of 1.2 g, the plant powders exhibited pronounced biocidal effects, resulting in mortality rates of 96%, 90%, and 75% after 96 h of exposure for *Satureja calamintha*, *Mentha rotundifolia*, and *Schinus molle*, respectively.

Ileke and Ogungbite, (2014) found that the powders of *Azadirachta indica*, *Zanthoxylum zanthoxyloides*, *Anacardium occidentale*, and *Moringa oleifera* exhibited remarkable insecticidal activity against *Sitophilus oryzae*, *Oryzaephilus mercator*, and *Rhyzopertha dominica*. At a dose of 1.0 g, 100% mortality was achieved with some of the tested plant powders, particularly *A. indica* and *Z. zanthoxyloides*, after 72 h of exposure.

The insecticidal activity of these plant powders may be attributed to the combined action of a wide range of bioactive constituents, including secondary metabolites and insecticidal proteins such as lectins, protease inhibitors, chitinases, and ureases. When incorporated into the diet, these compounds are ingested by insects, where they interfere with feeding behavior,

digestive processes, growth, and development, ultimately leading to increased mortality **(Spochacz et *al*., 2018)**. Furthermore, the efficacy of plant powders generally increases with both the applied dose and the duration of exposure, which is consistent with the dose- and time-dependent mortality patterns observed in the present study **(Spochacz et *al*., 2018)**.

4. Effect of plant extracts on wheat germination

The germination test was conducted to evaluate whether the application of the plant extracts as bioinsecticides could adversely affect the germination of stored wheat grains. The results obtained at the highest tested concentration (200 mg/mL) after one week of treatment are presented in **Figure 46**. No significant differences were observed between the treated and control groups, as all treatments achieved a 100% germination rate. These findings demonstrate that the extracts did not compromise seed viability or early germination performance.

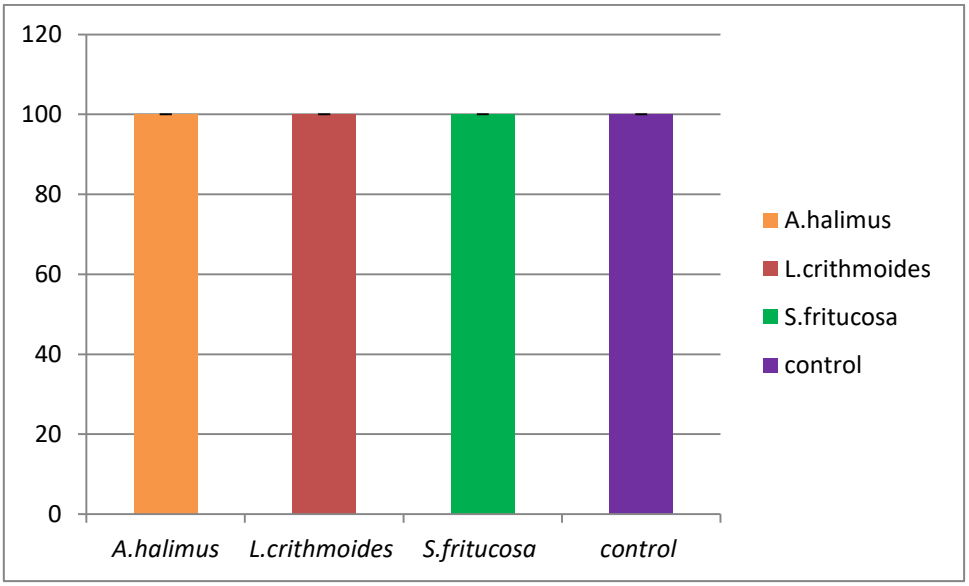


Figure 46. Effect of plant extracts at the highest tested concentration (200 mg/mL) on the germination of stored wheat grains.

Columns show the mean of three replicates and bars show the standard deviation of means.

Similar observations were reported by **Salah et *al*. (2023**), who demonstrated that aqueous extracts of *Artemisia annua* and *Nigella sativa* at concentrations of 5, 10, 15, and 20% (v/v) had no detrimental effects on wheat seed germination or seedling growth. Comparable results were obtained by **Adesina and Aderibigbe, (2021)**, showing that *Secamone afzelii* extracts, evaluated against several stored-product insect pests, did not

significantly affect the germination of stored wheat grains compared with the untreated control, confirming that seed viability was maintained during storage.

The absence of phytotoxic effects suggests that the bioactive compounds present in the extracts did not interfere with the physiological processes involved in seed germination, including water uptake, enzyme activation, and embryo development. This selective biological activity highlights their potential as environmentally friendly bioinsecticides capable of protecting stored wheat while preserving grain quality and viability, making them suitable for human consumption, animal feed, and subsequent cultivation.

5. Insecticidal activity *in silico* (molecular docking)

Acetylcholinesterase (AChE) is an essential enzyme in the insect nervous system, where it catalyzes the hydrolysis of acetylcholine (ACh) into choline and acetic acid, thereby terminating nerve impulse transmission and ensuring normal neuronal function. Inhibition of AChE causes the accumulation of acetylcholine at synaptic junctions, leading to continuous nerve stimulation, paralysis, and eventually insect death. Therefore, AChE is considered one of the most important molecular targets for the development of insecticidal agents **(Sha et *al*., 2025)**.

To correlate the phytochemical profiling results with the observed *in vitro* inhibitory activity against *T confusum*, molecular docking studies were performed on compounds previously identified by HPLC-ESI-QTOF in the studied extracts.

As presented in **Tables 20, 21, and 22**, molecular docking studies of polyphenolic compounds identified in the extracts of *A. halimus*, *L. crithmoides*, and *S. fruticosa* revealed variable binding affinities toward the target protein, with binding energies ranging from −10.2 to − 5.0 kcal/mol. The negative binding energy values indicate favorable interactions between the selected phenolic and flavonoid compounds and the active site of the enzyme. Furthermore, all RMSD values were below 2.0 Å, confirming the reliability of the docking protocol and a good agreement between the predicted binding poses and the reference crystallographic conformations.

The molecular docking analysis of *A. halimus* phytochemicals revealed binding energies ranging from − 9.5 to − 5.0 kcal/mol, indicating different affinities toward the target enzyme. Feruloyltyramine exhibited the strongest binding affinity (− 9.5 kcal/mol), forming a conventional hydrogen bond with TYR71 at the shortest interaction distance (2.39 Å), followed by quercetin dihydrate (− 8.3 kcal/mol), which established two π-donor hydrogen bonds with ASP375 and TYR324 **(Figure 47, Table 20)**. Caffeic acid 3-sulfate,

protocatechuic acid 4-glucoside, dihydroxybenzoic acid, salicylic acid, and phenol showed progressively weaker binding affinities (− 7.2 to − 5.0 kcal/mol), mainly through π-donor hydrogen, π-alkyl, π–π T-shaped, π–π stacked, and π-sigma interactions. A general trend was observed in which compounds forming shorter and stronger interactions, particularly hydrogen bonds, exhibited more negative binding energies, whereas longer-distance π interactions were associated with lower binding affinities.

Table 20. Molecular docking results of the major polyphenols identified in *A. halimus* extract with insect acetylcholinesterase (AChE) protein.

Compounds	Binding energies (kcat/mol)	Amino acids and interaction types	Distance (Å)
Feruloyltyramine	− 9.5	TYR A: 71: Conventional Hydrogen bond	2.39
Quercetin dihydrate	− 8.3	ASP A: 375: Pi-Doner Hydrogen Bond	2.50
		TYR A: 324: Pi-Doner Hydrogen Bond	2.90
Caffeic acid 3-sulfate	− 7.2	TYR A: 324: Pi-Doner Hydrogen Bond	2.92
Protocatechuic acid 4-glucoside	− 6.6	ARG A: 259: Pi-Alkyl	5.08
Dihydroxybenzoic acid	− 6.3	PHE A: 371: Pi-Pi T-shaped	5.08
Salicylic acid	− 6.0	TRP: 83 A : Pi-Pi T-shaped	5.36
		TRP: 83 A : Pi-Pi T-shaped	5.49
		GLY: 150 A: Pi sigma	3.75
		TYR: 370 A: Pi-Pi T-shaped	5.31
Phenol	− 5.0	TYR: 374 A: PiPi Stacked	4.91

The docking results were validated by re-docking, with an RMSD value of 1.52 Å.

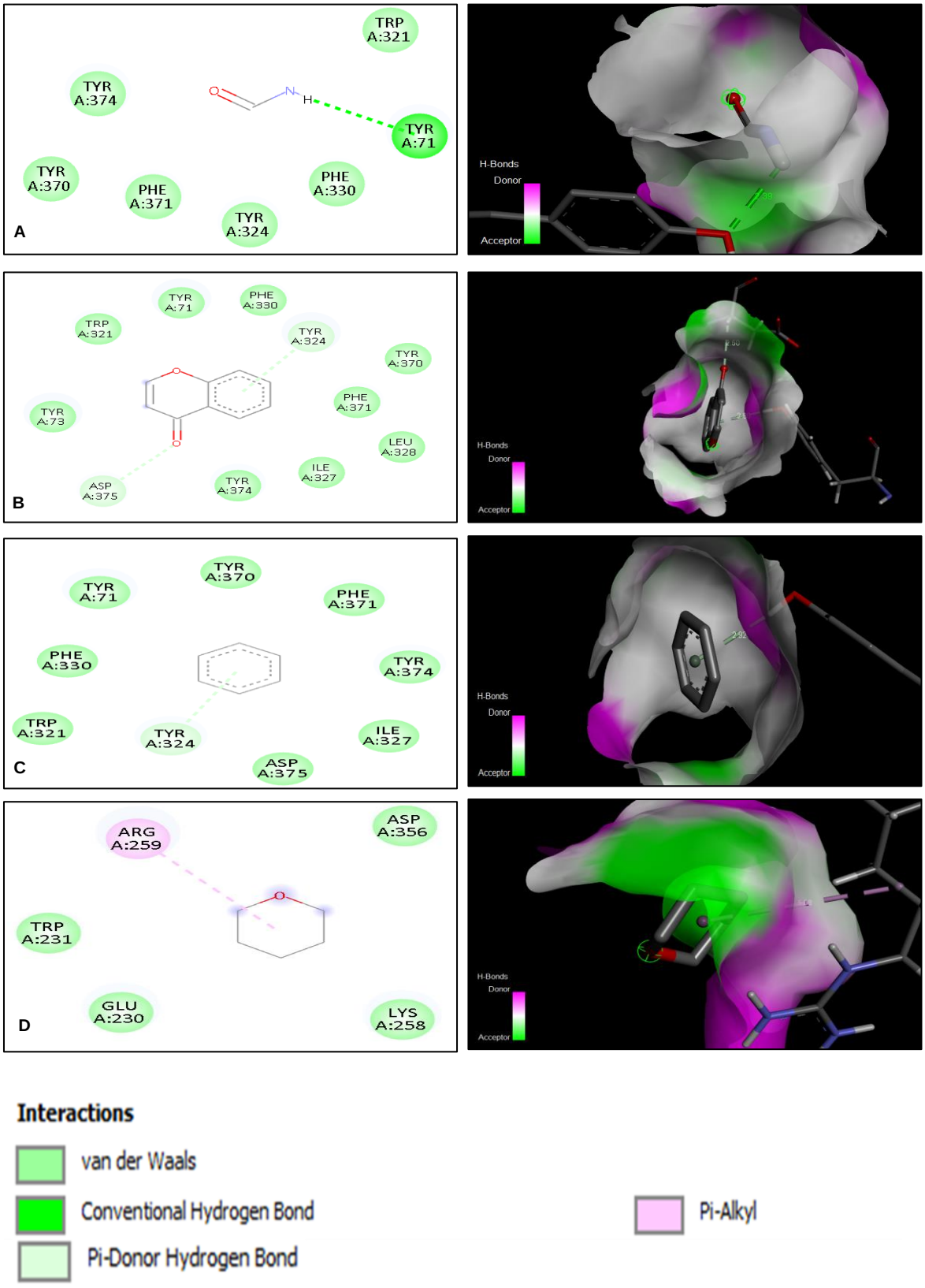


Figure 47. 2D (left) and 3D (right) intermolecular interactions of the four top-scoring compounds from the *A. halimus* extract within the active site of acetylcholinesterase (AChE): **(A)** Feruloyltyramine, **(B)** Quercetin dihydrate, **(C)** Caffeic acid 3-sulfate, and **(D)** Protocatechuic acid 4-glucoside.

The major polyphenols identified in *L. crithmoides* exhibited higher binding energies (−8.8 to − 5.7 kcal/mol), indicating weaker binding affinity toward AChE, which is consistent with its lower insecticidal activity observed *in vitro*. Cynarine (dicaffeoylquinic acid) exhibited the strongest binding affinity (− 8.8 kcal/mol), stabilized by multiple interactions including π-donor hydrogen bonding, π-alkyl, π–π T-shaped, and carbon hydrogen bonds, despite the presence of one unfavorable acceptor–acceptor interaction. Quercetin 3-*O*-glucoside (− 8.6 kcal/mol), chlorogenic acid (− 8.1 kcal/mol), and 3-*O*-feruloylquinic acid (− 8.0 kcal/mol) also showed strong binding affinities through a combination of hydrogen bonding, π–π stacking, π-alkyl, and π-anion interactions, contributing to stable ligand–protein complexes **(Figure 48, Table 21)**. The remaining compounds displayed moderate binding energies (− 7.3 to − 5.7 kcal/mol), mainly involving conventional hydrogen bonds and hydrophobic interactions, suggesting comparatively lower binding stability.

Table 21. Molecular docking results of the major polyphenols identified in *L. crithmoides* extract with insect acetylcholinesterase (AChE) protein.

Compounds	**Binding energies (kcat/mol)**	**Amino acids and interaction types**	**Distance (Å)**
Cynarine (dicaffeylquinic acid)	− 8.8	TYR A: 324: Pi-Doner Hydrogen Bond	2.46
		ILE A: 327: Pi-Alkyl	5.49
		TYR A: 374: Pi-Pi T-shaped	5.88
		ASP A: 375: Carbon Hydrogen Bond	3.46
		TYR A: 71: Unfavorable Acceptor-Acceptor	2.77
Quercetin 3-O-glucoside	− 8.6	TRP A: 321: Pi-Pi Stacked	4.90
		TYR A: 71: Conventional Hydrogen Bond	3.88
		TYR A: 324: Pi-Doner Hydrogen Bond	2.58
Chlorogenic acid	− 8.1	ILE A:82: Pi-Alkyl	3.88
		ASP A: 160: Conventional Hydrogen Bond	2.66
3-O-Feruloylquinic acid	−8.0	ILE A:82: Pi-Alkyl	3.88
		ILE A:82: Alkyl	4.96
		ILE A:160: Pi-Alkyl	5.45
		ASP A: 160: Pi-Anion	3.92

Caffeic acid 4-O-glucuronide	− 7.3	ILE A:161: Pi-Alkyl	5.48
		GLU A: 485: Pi-Anion	3.40
		TYR A: 498: Conventional Hydrogen Bond	2.93
Caffeoylglucaric acid	−7.3	GLY A: 79: Conventional Hydrogen Bond	2.55
Glucocaffeic acid	− 7.0	ARG A: 259: Conventional Hydrogen Bond	1.96
		ARG A: 259: Conventional Hydrogen Bond	2.71
		LYS A: 518: Conventional Hydrogen Bond	2.52
Feruloylglucaric acid	− 6.8	ASP A: 482: Conventional Hydrogen Bond	2.37
Maclurin	− 6.8	TRP A: 83: Conventional Hydrogen Bond	2.09
		LEU A: 471: Conventional Hydrogen Bond	2.40
		SER A: 470: Carbon Hydrogen Bond	3.66
		ASP A: 482: Pi-Anion	3.80
		ILE A: 82: Pi-Sigma	3.97
		TRP A: 472: Unfavorable Acceptor-Acceptor	1.10
1-O-Vanilloyl-beta-D-glucose	− 6.6	ILE A:82: Alkyl	3.85
		ILE A:161: Alkyl	4.31
		LEU A: 496: Pi-Alkyl	5.22
Coumarinic acid	− 6.0	TYR A: 73: Conventional Hydrogen Bond	2.04
Veratric acid	− 5.7	TYR A: 73: Conventional Hydrogen Bond	2.71
		ASP A: 375: Carbon Hydrogen Bond	3.35

The docking results were validated by re-docking, with an RMSD value of 1.52 Å.

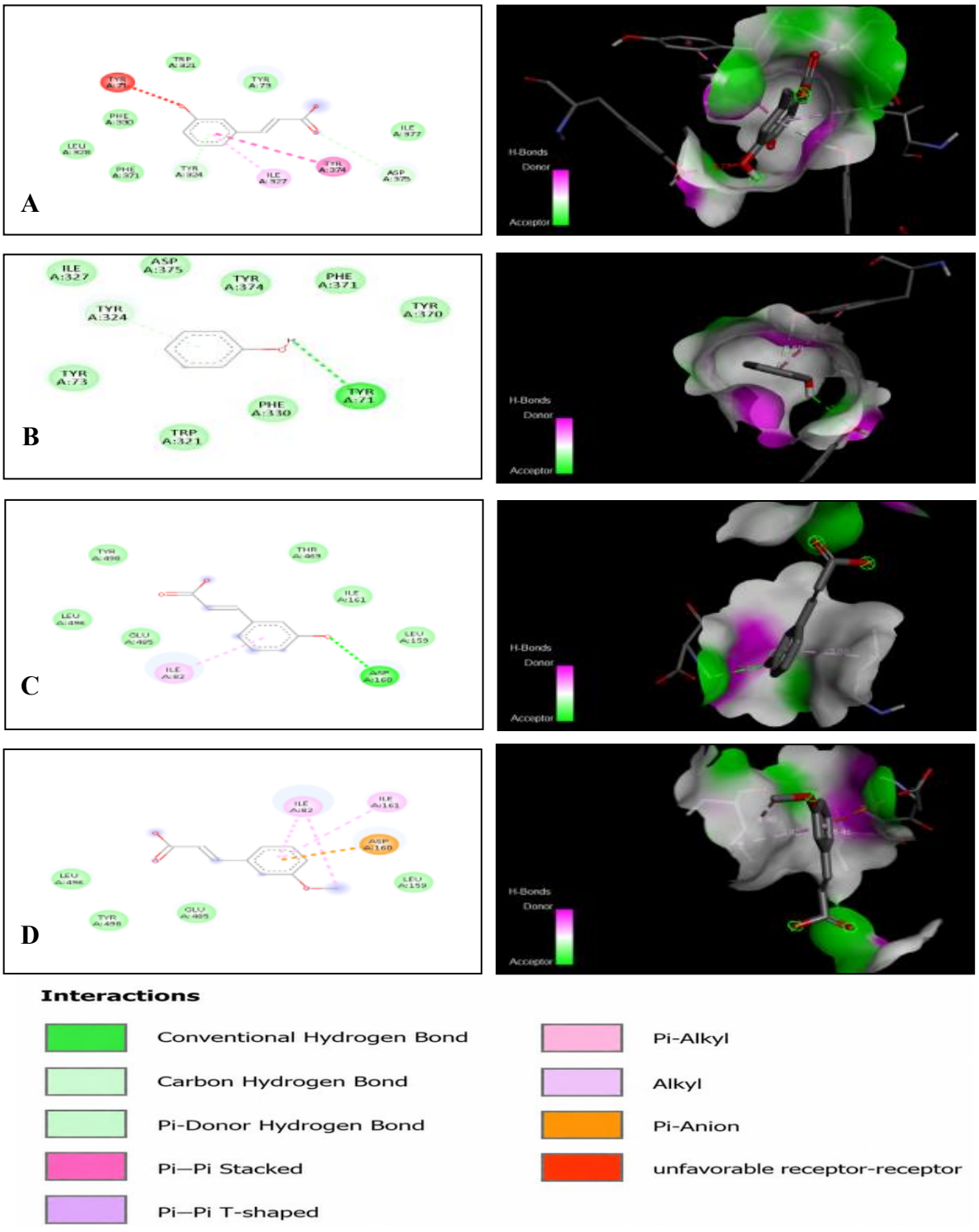


Figure 48. 2D (left) and 3D (right) intermolecular interactions of the four top-scoring compounds from the *L. crithmoides* extract within the active site of acetylcholinesterase (AChE)**: (A)** Cynarine**, (B)** Quercetin 3-O-glucoside**, (C)** Chlorogenic acid, and (**D)** 3-O-Feruloylquinic acid.

The molecular docking analysis of the major polyphenols identified in *S. fruticosa* revealed binding energies ranging from − 10.2 to − 6.0 kcal/mol, indicating strong interactions with the AChE active site. Kaempferol 3-*O*-rutinoside 7-*O*-glucoside exhibited the highest binding affinity (− 10.2 kcal/mol), stabilized by multiple π–π stacked interactions with TRP321, followed by naringin (− 9.5 kcal/mol), rutin (− 8.7 kcal/mol), and isorhamnetin (−8.5 kcal/mol), which formed π-alkyl, carbon hydrogen, π-sigma, and π-donor hydrogen bond interactions **(Figure 49, Table 22)**. The remaining compounds showed moderate binding affinities (− 8.3 to − 6.0 kcal/mol) through a combination of hydrogen bonding and hydrophobic interactions, contributing to stable ligand–protein complexes. Overall, *S. fruticosa* exhibited the most favorable binding energies among the three halophytic species, suggesting the highest potential against insect AChE, consistent with its superior insecticidal activity *in vitro*.

Table 22. Molecular docking results of the major polyphenols identified in.*S. fruticosa* extract with insect acetylcholinesterase (AChE) protein.

Compounds	Binding energies (kcat/mol)	Amino acids and interaction types	Distance (Å)
Kaempferol	− 10.2	TRP A:321: PiPi Stacked	4.67
3−O−rutinoside		TRP A:321: PiPi Stacked	4.72
7−O−glucoside		TRP A:321: PiPi Stacked	5.1
		TRP A:321: PiPi Stacked	5.28
Naringin	− 9.5	VAL A: 318: Pi-Alkyl	4.08
Rutin	− 8.7	ASP A: 375: Carbon Hydrogen Bond	3.32
		TYR A: 73: Pi-Sigma	3.61
		TYR A: 73: Pi-Alkyl	5.49
Isorhamnetin	− 8.5	TYR A: 324: Pi-Doner Hydrogen Bond	2.87
Isorhamnetin−3−O	− 8.3	TRP A: 321: PiPi Stacked	4.19
−glucoside		TRP A: 321: PiPi Stacked	4.52
		TRP A: 321: PiPi Stacked	4.33
		TRP A: 321: PiPi Stacked	4.89
		TYR A: 73: PiPi Stacked	5.99
Quercetin	− 8.2	TYR A: 71: PiPi Stacked	5.67
3−O−sambubioside		TYR A: 324: PiPi Stacked	4.92
		TRP A: 321: Pi-Pi T-shaped	4.31

		TRP A: 321: Pi-Pi T-shaped	4.43
		TRP A: 321: Pi-Pi T-shaped	4.69
		TRP A: 321: Pi-Pi T-shaped	4.94
Cratenacin	− 8.1	TYR A: 71: Pi-Doner Hydrogen Bond	2.60
		TRP A: 321: Pi-Pi T-shaped	5.11
		TRP A: 321: PiPi Stacked	3.86
		TRP A: 321: PiPi Stacked	4.33
		TRP A: 321: Pi-Pi T-shaped	4.63
		TYR A: 324: Pi-Pi T-shaped	4.67
Fraxin	− 6.9	ASP A: 356: Conventional Hydrogen Bond	1.97
		ARG A: 259: Conventional Hydrogen Bond	3.08
		ASP A: 358: Carbon Hydrogen Bond	3.46
Fertaric acid	− 6.4	THR A: 469: Conventional Hydrogen Bond	2.71
		GLU A: 485: Carbon Hydrogen Bond	3.54
Eugenitin	− 6.3	TRP A: 83: Pi-Sigma	3.92
		TRP A: 83: PiPi-shaped	5.92
		GLY A: 150: Pi-Sigma	3.51
		SER A: 238: Conventional Hydrogen Bond	1.94
		TRP A: 271: Pi-Alkyl	4.01
		TRP A: 271: Pi-Alkyl	4.39
		PHE A: 330: Pi-Alkyl	4.79
		PHE A: 371: PiPi-shaped	4.74
		PHE A: 440: Pi-Alkyl	5.29
		TYR A: 37 : PiPi-shaped	5.54
		TYR A: 370: Pi-Alkyl	5.23
Sinapic acid	− 6.1	TRP A: 321: PiPi Stacked	4.02
		TRP A: 321: PiPi Stacked	4.32
Diacetyl caffeic acid	− 6.0	ILE A: 82: Pi-Sigma	3.50
		LEU A: 471: Pi-Alkyl	5.23
Salicylic acid	− 6.0	TRP A: 83: Pi-Pi T-shaped	5.36
		TRP A: 83: Pi-Pi T-shaped	5.49
		GLY A: 150: Pi-Sigma	3.75
		TYR A: 370: Pi-Pi T-shaped	5.31

The docking results were validated by re-docking, with an RMSD value of 1.52 Å.

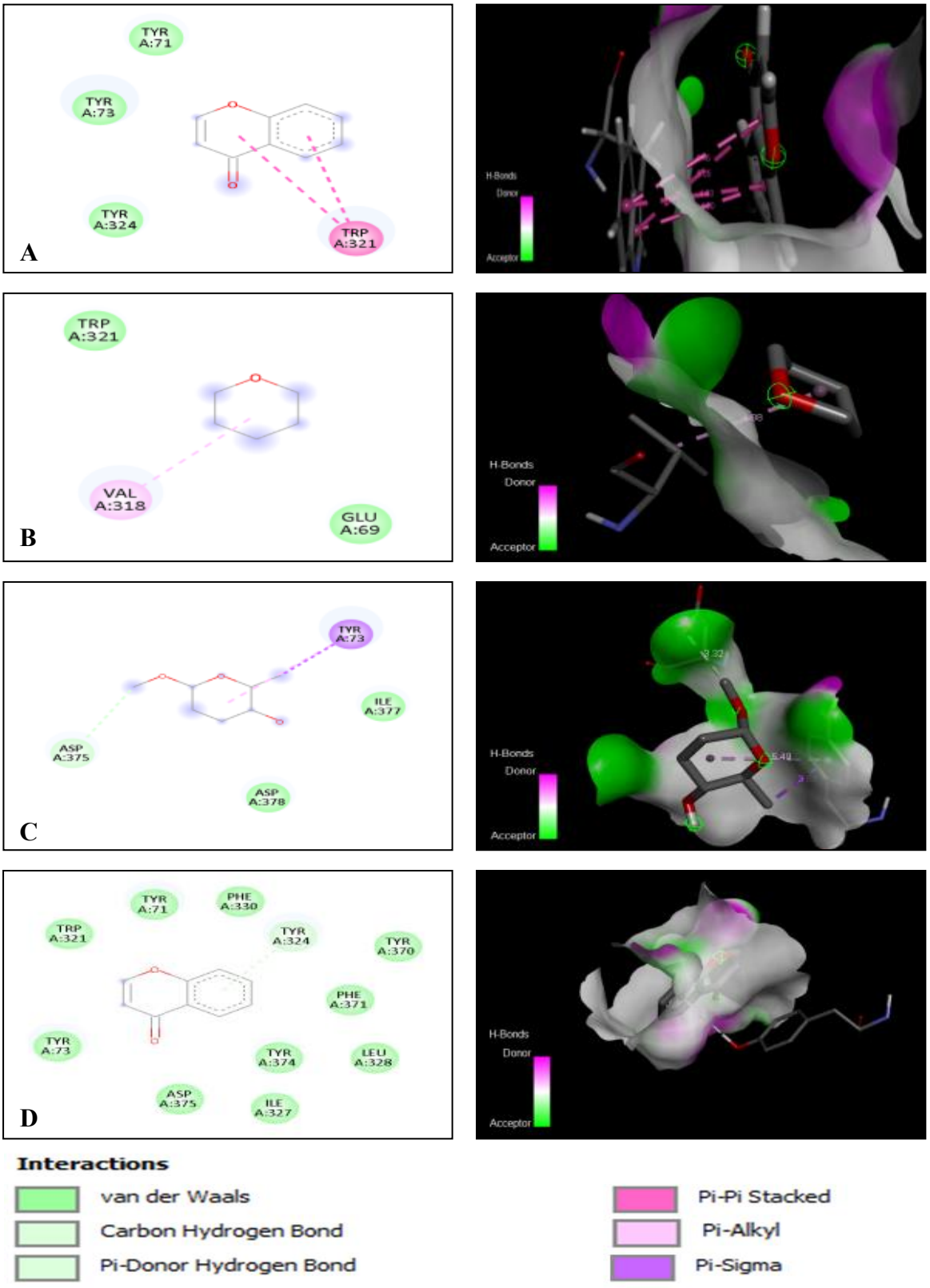


Figure 49. 2D (left) and 3D (right) intermolecular interactions of the four top-scoring compounds from the *S. fruticosa* extract within the active site of acetylcholinesterase (AChE): **(A)** Kaempferol 3-*O*-rutinoside 7-*O*-glucoside, **(B)** Naringin, **(C)** Rutin, **(D)** Isorhamnetin.

Overall, the molecular docking analysis demonstrated that the major polyphenols identified in the three halophytic species exhibited favorable binding affinities toward insect AChE, supporting their potential role as natural insecticidal agents. Among them, *S. fruticosa* showed the strongest inhibitory potential, with kaempferol 3-*O*-rutinoside 7-*O*-glucoside displaying the lowest binding energy (−10.2 kcal/mol), followed by *A. halimus* with feruloyltyramine (−9.5 kcal/mol), whereas *Limbarda crithmoides* exhibited comparatively higher binding energies, indicating a weaker overall affinity for the target enzyme. These *in silico* findings are consistent with the *in vitro* insecticidal activity observed for the three plant extracts.

Conclusion

The increasing demand for sustainable and environmentally friendly alternatives to synthetic products has encouraged the application of green chemistry principles for the exploration and valorization of plant-derived secondary metabolites, particularly those from halophytes.

In this context, the present study aimed to investigate three medicinal halophyte species, *A. halimus*, *L. crithmoides*, and *S. fruticosa*, and to evaluate the antioxidant and insecticidal activities of their methanolic extracts. To achieve this objective, their phytochemical composition was characterized through qualitative and quantitative phytochemical analyses, ATR-FTIR spectroscopy, and HPLC-ESI-QTOF-MS analysis.

Phytochemical screening and ATR-FTIR analysis confirmed the presence of the major classes of secondary metabolites in the methanolic extracts of the investigated halophytes. Quantitative analyses indicated variations in the total phenolic, flavonoid, and tannin contents, confirming the richness of these species in bioactive constituents. Among them, *S. fruticosa* exhibited the highest levels of these compounds.

Further analysis by HPLC-ESI-QTOF-MS was used to characterize the individual phenolic profiles, leading to the identification of 24, 27, and 29 phenolic compounds in *A. halimus*, *L. crithmoides*, and *S. fruticosa*, respectively.

The antioxidant evaluation demonstrated that the three species possess remarkable antioxidant capacity, as evidenced by their free radical scavenging activity against DPPH and ABTS radicals and their ferric reducing antioxidant power (FRAP).

The insecticidal assessment demonstrated the effectiveness of the studied halophytes against *Tribolium confusum*. Contact bioassays showed significant insecticidal activity, whereas repellency assays indicated strong repellent effects after two hours of exposure. Likewise, the plant powders exhibited marked biocidal activity, with *S. fruticosa* powder inducing 100% mortality of *T. confusum* during the first days of application.

The wheat germination assay showed that all treated seeds maintained their germination capacity, with a germination rate of 100%, comparable to that of the untreated control, indicating the absence of adverse effects under the experimental conditions.

To support the experimental findings, an *in silico* molecular docking study was carried out using the phenolic compounds identified by HPLC-ESI-QTOF-MS against insect acetylcholinesterase (AChE). Among the identified compounds, feruloyltyramine from *A. halimus*, cynarine from *L. crithmoides*, and kaempferol 3-*O*-rutinoside 7-*O*-glucoside from *S. fruticosa* exhibited the highest binding affinities toward AChE, suggesting that these phenolic

compounds may contribute to the insecticidal potential observed in the *in vitro* biological assays.

Despite these promising findings, several inherent limitations of the present study must be acknowledged. First, the evaluation of acetylcholinesterase inhibition relies solely on theoretical molecular docking simulations, as direct *in vitro* or *in vivo* enzymatic assays were not performed to confirm the precise mechanism of action. Second, neither food toxicology nor ecotoxicological evaluations were conducted, meaning that no definitive conclusions can be drawn regarding environmental safety or suitability for human consumption. Finally, all biological evaluations were restricted to controlled laboratory settings, leaving real-world efficacy on stored grains, chemical stability, and practical formulation applicability unassessed.

To overcome these limitations and advance the practical utilization of these halophytes, future research should pursue several complementary avenues. Advanced phytochemical characterization using techniques such as LC–MS/MS, GC–MS, and NMR is required to isolate and quantify the main active constituents. Comprehensive *in vivo* toxicity, ecotoxicity, and safety evaluations must be conducted to establish biocompatibility prior to any agricultural application. In addition, efficacy studies under real grain-storage, greenhouse, and field conditions are essential to confirm performance in practical environments. Integrating dynamic bioinformatics approaches, such as molecular dynamics simulations, network pharmacology, and ADMET predictions alongside enzymatic validation, will further clarify the underlying mechanisms of action. Finally, the development of stable and environmentally friendly formulations will be an important step toward the practical application of these natural products as sustainable biopesticides and antioxidant agents.

References

Abbott, W. S. (1925). A Method of Computing the Effectiveness of an Insecticide. *Journal of Economic Entomology*, *18*(2), 265–267. https://doi.org/10.1093/jee/18.2.265a

Abdelaal. M.. Moustafa. E.. Alattar. A.. El-Sherbeny. G.. Mashaly. I.. & Yahia. A. (2024). Habitat preference. phytochemical constituents and biological potency of four Egyptian Mediterranean halophytes. *Catrina: The International Journal of Environmental Sciences*. *30*(1). 79–91. https://doi.org/10.21608/cat.2024.240869.1212

Adesina, J. M., & Aderibigbe, A. T. B. (2021). Seed preservatives properties of Secamone afzelii (Schult) K. Schum extracts on wheat grains damage and germination capability. *Bulletin of the National Research Centre*, *45*(1), 52. https://doi.org/10.1186/s42269-021-00507-z

Adorisio S., Giamperi L., Bucchini A. E. A., Delfino D. V., and Marcotullio M. C., (2020). Bioassay-Guided Isolation of Antiproliferative Compounds from *Limbarda crithmoides* (L.) Dumort. *Molecules*, *25*(8): 1893. https://doi.org/10.3390/molecules25081893

Ahmad, F., Iqbal, N., Zaka, S. M., Qureshi, M. K., Saeed, Q., Khan, K. A., Ghramh, H. A., Ansari, M. J., Jaleel, W., Aasim, M., & Awar, M. B. (2019). Comparative insecticidal activity of different plant materials from six common plant species against *Tribolium castaneum* (Herbst) (Coleoptera: Tenebrionidae). *Saudi Journal of Biological Sciences*, *26*(7), 1804–1808. https://doi.org/10.1016/j.sjbs.2018.02.018

Ahmad, I., Gul, H., Noureen, D.A., Ujjan, J.A., Manzoor, S., Muhammad, W., Saddozai, S., Jan, S. (2021). Antimicrobial, Antioxidant and Antidiabetic Potential of *Suaeda fruticosa* L. International Journal on Emerging Technologies 12(2): 155-160(2021).

Al Hawat, L., & Alallan, L. (2025). Estimation of antioxidant and hypolipidemic activities of extracts of *Citrus aurantium* leaves in vitro. *Phytomedicine Plus*, *5*(1), 100723. https://doi.org/10.1016/j.phyplu.2024.100723.

Al Mamari, H. (2022). Phenolic Compounds: Classification, Chemistry, and Updated Techniques of Analysis and Synthesis. In F. A. Badria (Ed.), *Biochemistry* (Vol. 26). IntechOpen. https://doi.org/10.5772/intechopen.98958

Ali, B., Musaddiq, S., Iqbal, S., Rehman, T., Shafiq, N., & Hussain, A. (2021). The Therapeutic Properties, Ethno pharmacology and Phytochemistry of Atriplex Species: A review. *Pakistan Journal of Biochemistry and Biotechnology*, 2(1), 49–64. https://doi.org/10.52700/pjbb.v2i1.38

Arya. P.. Vaidya. D.. Kaushal. M.. Devi. S.. Gupta. A.. & Chand. S. (2025). Effects of different solvents on phytochemical constituents. in-vitro antimicrobial activity. and volatile components of Boehmeria rugulosa Wedd. Wood extract. *Scientific Reports*. *15*(1). 29135. https://doi.org/10.1038/s41598-025-14506-x

Atta, B., Rizwan, M., Sabir, A. M., Gogi, M. D., Sabar, M., Bakhtawar, Ali, F., & Sarwar, M. (2020). Toxic and repellent characteristics of some plant extracts used against *Tribolium castaneum* (Herbst) (Coleoptera: Tenebrionidae) improve the grain quality of stored wheat. *Journal of Innovative Sciences*, *6*(1), 1–11. https://doi.org/10.17582/journal.jis/2020/6.1.1.11

Ayaz. A., Jamil. Q., Hussain. M., Anjum. F., Sarfraz. A.. Alqahtani. T.. Hussain. N.. Gahtani. R. M.. Dera. A. A.. Alharbi. H. M.. & Iqbal. S. M. (2022). Antioxidant and Gastroprotective Activity of *Suaeda fruticosa* Forssk. Ex J.F.Gmel. *Molecules*. *27*(14). 4368. https://doi.org/10.3390/molecules27144368.

Bakroune, N., Ouamane, A. T., Boultif, M., Bettiche, F., & Torki, S. T. (2024). Diversity of cereal pests (wheat and barley) grown in arid climate in Ziban region (provence of Biskra-southeastern Algeria). *Studia Universitatis Babeş-Bolyai Biologia*, *69*(2), 23–45. https://doi.org/10.24193/subbbiol.2024.2.02

Balachowsky, A. S. (1936). Les insectes nuisibles aux plantes cultivées et aux denrées stockées. Paris, France: Masson.

Benhamada, N., & Idoui, T. (2020). Traditional fermented wheat: nutritional quality and sensory evaluation of bread produced from composite fermented wheat flour. Carpathian *Journal of Food Science and Technology*, 12(2), 37- 46. https://doi.org/10.34302/crpjfst/2020.12.2.4

Benhamada, N., Benhamada, O., & Idoui, T. (2024). Study of the quality and loses of durum wheat (*Triticum durum*) during storage: An overview of traditional storage in Algeria. *Acta Scientiarum. Biological Sciences*, *46*, e70661. https://doi.org/10.4025/actascibiolsci.v46i1.70661

Benhammou. N.. Bekkara. F. A.. & Kadifkova Panovska. T. (2009). Antioxidant activity of methanolic extracts and some bioactive compounds of *Atriplex halimus*. *Comptes Rendus. Chimie*. *12*(12). 1259–1266. https://doi.org/10.1016/j.crci.2009.02.004

Bevan, A., Cutler, B., Hennig, C., & Yermeche, O. (2024). Cereal Silo-pits, Agro-pastoral Practices and Social Organisation in 19th Century Algeria. *Human Ecology*, 52(3), 497–513. https://doi.org/10.1007/s10745-024-00487-4

Bokri, H., Kahlaoui, S., Hcini, K., Dhoueibi, M., Harzallah-Skhiri, F., & Stambouli-Essassi, S. (2023). Induction of organogenesis and callogenesis in *Limbarda crithmoïdes* L. (Asteraceae) explants cultured on MS media supplemented with various concentrations of Na+ and K+. *Notulae Botanicae Horti Agrobotanici Cluj-Napoca*, *51*(2), 13147. https://doi.org/10.15835/nbha51213147

Bounouar. E.. Missoun. F.. Amari. N. O. Belabaci. F. Z.. Belabaci. S.. Sekkal. F. Z.. & Djebli. N. (2022). Antidiabetic effect of *Atriplex halimus* long and short term treatment against streptozotocin induced diabetes in rats. *Anales de Biología*. (44). 21–30. https://doi.org/10.6018/analesbio.44.03

Brodowska, K. M. (2017). Natural Flavonoids: Classification, Potential Role, And Application Of Flavonoid Analogues. https://doi.org/10.5281/ZENODO.545778

Brown, S. J., Shippy, T. D., Miller, S., Bolognesi, R., Beeman, R. W., Lorenzen, M. D., Bucher, G., Wimmer, E. A., & Klingler, M. (2009). The Red Flour Beetle, *Tribolium castaneum* (Coleoptera): A Model for Studies of Development and Pest Biology: Figure 1. *Cold Spring Harbor Protocols*, *2009*(8), pdb.emo126. https://doi.org/10.1101/pdb.emo126

Brzović, P., Radman, S., & Mekinić, I. G. (2025). Phenolic Antioxidants in the Adriatic Halophyte *Limbarda crithmoides*: Variation Across Phenological Stages. *Foods*, *14*(21), 3718. https://doi.org/10.3390/foods14213718

Castañeda-Loaiza. V.. Rodrigues. M. J.. Neng. N.. Quintas. C.. Ratão. I.. & Custódio. L. (2025). Optimizing germination and cultivation of edible halophytes using effluents from an IMTA system. *Journal of the Science of Food and Agriculture*. jsfa.70270. https://doi.org/10.1002/jsfa.70270

Castroviejo, S. (Coord. gen.), Buira, A., Quintanar, A., García, M. Á., Talavera, M., Fernández Piedra, M. P., & Aedo, C. (Eds.). (2017). *Flora Iberica. Plantas Vasculares de la Península Ibérica e Islas Baleares*. Vol. XVI (II): Compositae (partim). Madrid: Real Jardín Botánico, CSIC. XXIV. pp. 735–1450.

Chaouche, T. M., Haddouchi, F., Ksouri, R., & Atik-Bekkara, F. (2014). Evaluation of antioxidant activity of hydromethanolic extracts of some medicinal species from South Algeria. *Journal of the Chinese Medical Association*, *77*(6), 302–307. https://doi.org/10.1016/j.jcma.2014.01.009

Chapman,V.J. (1942). The new perspective in the halophytes. *Quarterly Review of Biology*, *17*(3), 291–311.

Chekroun-Bechlaghem, N., Belyagoubi-Benhammou, N., Belyagoubi, L., Gismondi, A., Nanni, V., Di Marco, G., Canuti, L., Canini, A., El Haci, I. A., & Atik Bekkara, F. (2019). Phytochemical analysis and antioxidant activity of *Tamarix africana*, *Arthrocnemum macrostachyum* and *Suaeda fruticosa*, three halophyte species from Algeria. *Plant Biosystems - An International Journal Dealing with All Aspects of Plant Biology*, *153*(6), 843–852. https://doi.org/10.1080/11263504.2018.1555191.

Chen, S., Wang, X., Cheng, Y., Gao, H., & Chen, X. (2023). A Review of Classification, Biosynthesis, Biological Activities and Potential Applications of Flavonoids. *Molecules*, *28*(13), 4982. https://doi.org/10.3390/molecules28134982

Clauser. M.. Dall'Acqua. S.. Loi. M. C.. & Innocenti. G. (2013). Phytochemical investigation on *Atriplex halimus* L. from Sardinia. *Natural Product Research*. *27*(20). 1940–1944. https://doi.org/10.1080/14786419.2013.793684

Cosme, F., Aires, A., Pinto, T., Oliveira, I., Vilela, A., & Gonçalves, B. (2025). A Comprehensive Review of Bioactive Tannins in Foods and Beverages: Functional Properties, Health Benefits, and Sensory Qualities. *Molecules*, *30*(4), 800. https://doi.org/10.3390/molecules30040800

Cruz, J. F., Troude, F., Griffon, D., & Hebert, J. P. (1988). Conservation des grains en régions chaudes. Paris: Ministère de la Coopération et du Développement. (Techniques rurales en Afrique), 545 pp.

Cutrim, C. S., & Cortez, M. A. S. (2018). A review on polyphenols: Classification, beneficial effects and their application in dairy products. *International Journal of Dairy Technology*, *71*(3), 564–578. https://doi.org/10.1111/1471-0307.12515

Dawson, P. S. (1977). Life history strategy and evolutionary history of *tribolium* flour beetles. *Evolution*, *31*(1), 226–229. https://doi.org/10.1111/j.1558-5646.1977.tb01001.x

Delobel, A., & Tran, M. (1993). Les Coléoptères des denrées alimentaires entreposées dans les régions chaudes. ORSTOM Éditions, Paris.

Dirar, A. I., Alsaadi, D. H. M., Wada, M., Mohamed, M. A., Watanabe, T., & Devkota, H. P. (2019). Effects of extraction solvents on total phenolic and flavonoid contents and biological activities of extracts from Sudanese medicinal plants. *South African Journal of Botany*, *120*, 261–267. https://doi.org/10.1016/j.sajb.2018.07.003.

Djidel, A., Daghbouche, S., Benrima, A., & Djazouli, Z.-E. (2018). Évaluation de l'activité insecticide de l'extrait aqueux brut de la Fabaceae *Cytisus triflorus* L'Hér. à l'égard de *Tribolium castaneum* (Herbst, 1797) (Coleoptera: Tenebrionidae). *Revue Agrobiologia*, *8*(2), 1093–1102.

Djillali, E. H., Souheyla, T., Nesrine, S., Sarah, H., & Louiza, T. (2018). Comparative phytochemical and in vitro bioactivity profiling of two Saharan halophytes: *Atriplex halimus* L. and *Atriplex nummularia* Lindl. *South African Journal of Botany*, *194*, 175–182. https://doi.org/10.1016/j.sajb.2026.04.038

Dorta, E., González, M., Lobo, M. G., Sánchez-Moreno, C., & De Ancos, B. (2014). Screening of phenolic compounds in by-product extracts from mangoes (*Mangifera indica* L.) by HPLC-ESI-QTOF-MS and multivariate analysis for use as a food ingredient. *Food Research International*, *57*, 51–60. https://doi.org/10.1016/j.foodres.2014.01.012

Douara. N.. Benzekri Benallou. M.. Termoul. M.. Mekibes. Z.. Bestani. B.. & Benderdouche. N. (2022). Removal of Textile Dyes on a Biosorbent Based on the Leaves of *Atriplex halimus*. *Iranian Journal of Chemistry and Chemical Engineering*. *41*(11). https://doi.org/10.30492/ijcce.2022.535090.4864

Dupont, F., & Guignard, J.-L. (2007). *Botanique : Systématique moléculaire*. 14e édition. Paris : Elsevier Masson, 285 p.

Easmin, S., Sarker, Md. Z. I., Ghafoor, K., Ferdosh, S., Jaffri, J., Ali, Md. E., Mirhosseini, H., Al-Juhaimi, F. Y., Perumal, V., & Khatib, A. (2017). Rapid investigation of α-glucosidase inhibitory activity of Phaleria macrocarpa extracts using FTIR-ATR based fingerprinting. *Journal of Food and Drug Analysis*, *25*(2), 306–315. https://doi.org/10.1016/j.jfda.2016.09.007

Elagdi, C., Bouaouda, K., Rahhal, R., Hsaine, M., Badri, W., Fougrach, H., & Hajjouji, H. E. (2023). Phenolic compounds, antioxidant and antibacterial activities of the methanolic extracts of *Euphorbia resinifera* and *Euphorbia echinus*. *Scientific African*, *21*, e01779. https://doi.org/10.1016/j.sciaf.2023.e01779.

Elhawary, E. A., Waheeb, H. O., Abdelhafiz, A. H. A., El-Waseif, A. A., & Shehata, A. Z. I. (2026). Phytochemical profiling, metabolomics, and molecular docking studies of *Atriplex halimus* aerial parts revealing potential insecticidal activity against the malaria vector *Anopheles pharoensis*. *Scientific Reports*, *16*(1), 15880. https://doi.org/10.1038/s41598-026-52695-1

FAO. (2026). FAO Cereal Supply and Demand Brief. Food and Agriculture Organization of the United Nations, Rome.

Feldman, M., & Levy, A. A. (2023). Wheat Evolution and Domestication. Springer International Publishing. https://doi.org/10.1007/978-3-031-30175-9

Ferreira, M. J., Pinto, D. C. G. A., Cunha, Â., & Silva, H. (2022). Halophytes as Medicinal Plants against Human Infectious Diseases. *Applied Sciences*, *12*(15), 7493. https://doi.org/10.3390/app12157493

Fields, P. G. (1992). The control of stored-product insects and mites with extreme temperatures. *Journal of Stored Products Research*, *28*(2), 89–118. https://doi.org/10.1016/0022-474X(92)90018-L

Finney, D. T. (1971). *Probit analysis* (3rd ed.). Cambridge University Press. London, 1971, 20–42.

Fleurat-Lessard, F. (2002). Qualitative reasoning and integrated management of the quality of stored grain: A promising new approach. *Journal of Stored Products Research*, *38*(3), 191–218. https://doi.org/10.1016/S0022-474X(01)00022-4

Fontana, G., Bruno, M., Senatore, F., & Formisano, C. (2014). Volatile constituents of aerial parts of two Mediterranean species of *Inula*: *Inula crithmoides* L. and *I. verbascifolia* (Willd.) Hausskn. (Asteraceae). *Natural Product Research*, *28*(13), 984–993. https://doi.org/10.1080/14786419.2014.902821

Food and Agriculture Organization of the United Nations. (2025). Global Information and Early Warning System on Food and Agriculture (GIEWS): Country Brief – Algeria. FAO. https://www.fao.org/giews/countrybrief/

Gheraissa. N.. Chemsa. A. E.. Cherrada. N.. Erol. E.. Elsharkawy. E. R.. Ghemam-Amara. D.. Zeghoud. S.. Rebiai. A.. Messaoudi. M.. Sawicka. B.. Atanassova. M.. & Abdel-Kader. M. S. (2023). Biochemical Profile and *In Vitro* Therapeutic Properties of Two Euhalophytes. *Halocnemum strobilaceum* Pall, And *Suaeda fruticosa* (L.) Forske.. Grown in the Sabkha Ecosystem in the Algerian Sahara. *Molecules*. *28*(8). 3580. https://doi.org/10.3390/molecules28083580

González-Sarrías, A., Tomás-Barberán, F. A., & García-Villalba, R. (2020). Structural Diversity of Polyphenols and Distribution in Foods. In F. A. Tomás-Barberán, A. González-Sarrías, & R. García-Villalba (Eds.), *Dietary Polyphenols* (1st ed., pp. 1–29). Wiley. https://doi.org/10.1002/9781119563754.ch1

Gooding, M. J., & Shewry, P. R. (2022). Wheat: Environment, Food and Health (1st ed.). *Wiley*. https://doi.org/10.1002/9781119652601

Gretia. (2009). État des lieux des connaissances sur les invertébrés continentaux des Pays de la Loire: bilan final. Rapport pour le Conseil régional des Pays de la Loire, 396 p.

Grigore M. N., & Toma C. (2010). A proposal for a new halophytes classification based on integrative anatomy observations. *Oltenia Journal for Studies in Natural Sciences*, *26*, 45–50.

Hameed, A., Hussain, S., Rasheed, A., Ahmed, M. Z., & Abbas, S. (2024). Exploring the Potentials of Halophytes in Addressing Climate Change-Related Issues: A Synthesis of Their Biological, Environmental, and Socioeconomic Aspects. *World*, *5*(1), 36–57. https://doi.org/10.3390/world5010003

Hatice Pekmez. (2016). Cereal Storage Techniques: A Review. *Journal of Agricultural Science and Technology B*, 6(2). https://doi.org/10.17265/2161-6264/2016.02.001

Hoornaert, H., Neng, N., Custódio, L., & Rodrigues, M. J. (2026). Physiological and biochemical tolerance responses of the estuarine saltmarsh plant *Limbarda crithmoides* L. under acetaminophen exposure: Insights into plant–pollutant interactions. *Estuarine, Coastal and Shelf Science*, *329*, 109640. https://doi.org/10.1016/j.ecss.2025.109640

Hu, W., Sarengaowa, Guan, Y., & Feng, K. (2022). Biosynthesis of Phenolic Compounds and Antioxidant Activity in Fresh-Cut Fruits and Vegetables. *Frontiers in Microbiology*, *13*, 906069. https://doi.org/10.3389/fmicb.2022.906069

Ileke, K. D., & Ogungbite, O. C. (2014). Entomocidal Activity of Powders and Extracts of Four Medicinal Plants Against *Sitophilus oryzae (L), Oryzaephilus mercator* (Faur) and *Ryzopertha dominica* (Fabr.). *7*(1). 57–62

Jallali. I.. Waffo Téguo. P.. Smaoui. A.. Mérillon. J.-M.. Abdelly. C.. & Ksouri. R. (2020). Bio-guided fractionation and characterization of powerful antioxidant compounds from the halophyte *Inula crithmoïdes*. *Arabian Journal of Chemistry*. *13*(1). 2680–2688. https://doi.org/10.1016/j.arabjc.2018.06.020

Joshi. A.. Rajput. V. D.. Verma. K. K.. Minkina. T.. Ghazaryan. K.. & Arora. J. (2023). Potential of *Suaeda nudiflora* and *Suaeda fruticosa* to Adapt to High Salinity Conditions. Horticulturae. 9(1). 74. https://doi.org/10.3390/horticulturae9010074

Katamadze, A., Vergara-Díaz, O., Uberegui, E., Yoldi-Achalandabaso, A., Araus, J. L., & Vicente, R. (2023). Evolution of wheat architecture, physiology, and metabolism during domestication and further cultivation: Lessons for crop improvement. *The Crop Journal*, 11(4), 1080–1096. https://doi.org/10.1016/j.cj.2023.06.006

Khalid, A., Hameed, A., & Tahir, M. F. (2023). Wheat quality: A review on chemical composition, nutritional attributes, grain anatomy, types, classification, and function of seed storage proteins in bread making quality. *Frontiers in Nutrition*, 10, 1053196. https://doi.org/10.3389/fnut.2023.1053196

Kumar, S., Singh, A., & Kumar, B. (2017). Identification and characterization of phenolics and terpenoids from ethanolic extracts of Phyllanthus species by HPLC-ESI-QTOF-MS/MS. *Journal of Pharmaceutical Analysis*, *7*(4), 214–222. https://doi.org/10.1016/j.jpha.2017.01.005

Lahlali, R., Barka, E. A., & Jemâa, J. M.-B. (Eds.). (2022). The Use of Plant Extracts and Essential Oils as Biopesticides. *Frontiers Media SA*. https://doi.org/10.3389/978-2-88976-513-3

Lepesme P. (1944). Les coléoptères des denrées alimentaires et des produits industriels entreposés, Ed. Encyclopédie Entomologique, Paris : 2-335.

Lopes, M., Sanches-Silva, A., Castilho, M., Cavaleiro, C., & Ramos, F. (2023). Halophytes as source of bioactive phenolic compounds and their potential applications. *Critical Reviews in Food Science and Nutrition*, *63*(8), 1078–1101. https://doi.org/10.1080/10408398.2021.1959295

Maheshwaran, L., Nadarajah, L., Senadeera, S. P. N. N., Ranaweera, C. B., Chandana, A. K., & Pathirana, R. N. (2024). Phytochemical Testing Methodologies and Principles for Preliminary Screening/ Qualitative Testing. *Asian Plant Research Journal*, *12*(5), 11–38. https://doi.org/10.9734/aprj/2024/v12i5267.

Mann, A., Lata, C., Kumar, N., Kumar, A., Kumar, A., & Sheoran, P. (2023). Halophytes as new model plant species for salt tolerance strategies. *Frontiers in Plant Science*, *14*, 1137211. https://doi.org/10.3389/fpls.2023.1137211

Mavric-Scholze, E., Simijonović, D., Avdović, E., Milenković, D., Šaćirović, S., Ćirić, A., & Marković, Z. (2025). Comparative analysis of antioxidant activity and content of (poly)phenolic compounds in cabernet sauvignon and merlot wines of Slovenian and Serbian vineyards. *Food Chemistry: X*, *25*, 102108. https://doi.org/10.1016/j.fochx.2024.102108

McDonald, L. L., Guy, R. H., & Speirs, R. D. (1970). *Preliminary evaluation of new candidate materials as toxicants, repellents and attractants against stored product insects* (Marketing Research Report No. 882). Agricultural Research Service, United States Department of Agriculture, 183p.

Miller, A. G., & Morris, M. (1988). Plants of Dhofar, the southern region of Oman: traditional, economic, and medicinal uses. Prepared and published by the Office of the Adviser for Conservation of the Environment, Diwan of Royal Court.

Moutassem, D., Boubellouta, T., Bellik, Y., Rouis, Z., Kucher, D. E., Utkina, A. O., Kucher, O. D., Mironova, O. A., Kavhiza, N. J., & Rebouh, N. Y. (2024). Insecticidal activity of *Thymus pallescens* de Noë and *Cymbogon citratus* essential oils against *Sitophilus zeamais* and *Tribolium castaneum*. *Scientific Reports*, *14*(1), 13951. https://doi.org/10.1038/s41598-024-64757-3

N'do, J. Y., Paré, D., Bondé, L., & Hilou, A. (2024). Comparative phytochemical profile and biological activity of three Terminalia species as alternative antimicrobial therapies. *Heliyon*, *10*(21), e40159. https://doi.org/10.1016/j.heliyon.2024.e40159

Naboulsi, I., El Fakhouri, K., Lamzira, R., Ramdani, C., Bitchagno, G. T. M., Boulamtat, R., Bakrim, W. B., Mahdi, I., Aboulmouhajir, A., Yasri, A., El Bouhssini, M., Ward, J. L., & Sobeh, M. (2022). Insecticidal Activities of *Atriplex halimus* L., Salvia rosmarinus Spenn. And Cuminum cyminum L. against Dactylopius opuntiae (Cockerell) under Laboratory and Greenhouse Conditions. *Insects*, *13*(10), 930. https://doi.org/10.3390/insects13100930

Nassrallah, A., & Abdel-Mobdy, A. (2021). Biochemical Investigation of Goat Milk Casein and Whey Protein Crude Methanol Extract. *Egyptian Journal of Chemistry*, *0*(0), 0–0. https://doi.org/10.21608/ejchem.2021.73844.3651.

Navarro, S. (2006). *Modified atmospheres for the control of stored-product insects and mites*. In J. W. Heaps (Ed.), Insect management for food storage and processing (2nd ed., pp. 105–146). AACC International. https://doi.org/10.1016/B978-1-891127-46-5.50016-7

Naville M. (2005). La biodiversité des espèces cultivées : Analyse dans le cas du blé, Paris: Université Paris XI, Paris, 20p.

Nikalje, G. C., Kumar, J., Nikam, T. D., & Suprasanna, P. (2019). FT-IR profiling reveals differential response of roots and leaves to salt stress in a halophyte *Sesuvium portulacastrum* (L.) L. *Biotechnology Reports*, *23*, e00352. https://doi.org/10.1016/j.btre.2019.e00352

Ould Kaddour. S.. Kouadria. R.. Bouzouina. M.. & Lotmani. B. (2019). Phytochemical identification and antioxidant activities of wild Algerian plant *Atriplex halimus* L. *International Food Research Journal*. *31*(6). 1494–1506. https://doi.org/10.47836/ifrj.31.6.10

Pandey, K. B., & Rizvi, S. I. (2009). Plant Polyphenols as Dietary Antioxidants in Human Health and Disease. *Oxidative Medicine and Cellular Longevity*, *2*(5), 270–278. https://doi.org/10.4161/oxim.2.5.9498

Pasqualone, A. (2025). Addressing Shortages with Storage: From Old Grain Pits to New Solutions for Underground Storage Systems. Agriculture, 15(3), 289. https://doi.org/10.3390/agriculture15030289

Pereira, V., Figueira, O., & Castilho, P. C. (2024). Flavonoids as Insecticides in Crop Protection—A Review of Current Research and Future Prospects. *Plants*, *13*(6), 776. https://doi.org/10.3390/plants13060776

Petit. T.. & Puskar. L. (2018). FTIR spectroscopy of nanodiamonds: Methods and interpretation. *Diamond and Related Materials*. *89*. 52–66. https://doi.org/10.1016/j.diamond.2018.08.005

Petropoulos, S. A., Karkanis, A., Martins, N., & Ferreira, I. C. F. R. (2018). Edible halophytes of the Mediterranean basin: Potential candidates for novel food products. *Trends in Food Science & Technology*, *74*, 69–84. https://doi.org/10.1016/j.tifs.2018.02.006

Prabhu, S., Molath, A., Choksi, H., Kumar, S., & Mehra, R. (2021). Classifications of polyphenols and their potential application in human health and diseases. *International Journal of Physiology, Nutrition and Physical Education*, *6*(1), 293–301. https://doi.org/10.22271/journalofsport.2021.v6.i1e.2236

Qasim, M., Aziz, I., Rasheed, M., Gul, B., & Khan, M. (2016). Effect of extraction solvents on polyphenols and antioxidant activity of medicinal halophytes. *Pakistan Journal of Botany*, *48*, 621–627.

Quézel, P., Santa S (1962). Nouvelle flore de l'Algérie et des régions désertiques méridionales. CNRS. Paris:1170 p.

Quirantes-Piné, R., Lozano-Sánchez, J., Herrero, M., Ibáñez, E., Segura-Carretero, A., & Fernández-Gutiérrez, A. (2013). HPLC–ESI–QTOF–MS as a Powerful Analytical Tool for Characterising Phenolic Compounds in Olive-leaf Extracts. *Phytochemical Analysis*, *24*(3), 213–223. https://doi.org/10.1002/pca.2401

Rajendran, S. (2003). Grain Storage: Perspectives and Problems. In H. Ramaswamy, G. Vijaya Raghavan, A. Chakraverty, & A. Mujumdar (Eds.), Handbook of Postharvest Technology (pp. 183–214). CRC Press. https://doi.org/10.1201/9780203911310.pt3

Rawat, A., Prakash, O., Nagarkoti, K., Kumar, R., Negi, M. S., Kumar, S., & Srivastava, R. M. (2024). Chemical profiling and bioactivity evaluation of thymol rich *Coleus aromaticus* Benth. Essential oil. *Medicinal Plant Biology*, *3*(1), 0–0. https://doi.org/10.48130/mpb-0024-0007

Righi, K., Assia Righi, F., Boubkeur, A., Boungab, K., Elouissi, A., & Djendara, A. C. (2018). Toxicity and repellency of three Algerian medicinal plants against pests of stored product: *Ryzopertha dominica* (Fabricius) (Coleoptera: Bostrichidae). *Banat's Journal of Biotechnology*, *IX*(17), 50–59. https://doi.org/10.7904/2068-4738-IX(17)-50

Rodrigues, M. J., Castañeda-Loaiza, V., Fernandes, E., & Custódio, L. (2023). A First Approach for the Micropropagation of the Edible and Medicinal Halophyte *Inula crithmoides* L. *Plants*, *12*(12), 2366. https://doi.org/10.3390/plants12122366

Roubi. M.. Elbouzidi. A.. Dalli. M.. Azizi. S.. Aherkou. M.. Taibi. M.. Guerrouj. B. E.. Addi. M.. & Gseyra. N. (2023). Phytochemical antioxidant and anticancer assessments of *Atriplex halimus* extracts: *In silico* and in *vitro* studies. *Scientific African*. *22*. e01959. https://doi.org/10.1016/j.sciaf.2023.e01959

Saïdana, D., Halima-Kamel, M. B., Mahjoub, M. A., Haouas, D., Mighri, Z., & Helal, A. N. (2007). Insecticidal Activities of Tunisian Halophytic Plant Extracts against Larvae and Adults of *Tribolium confusum*. *TROPICULTURA*, 25(4), 193-199.

Salah, S. (2023). Repellency and Phytoxicity Assessment of Plant Extracts, Essential Oils and Nanoparticles on *Tribolium castaneum* Herbst Beetles Infesting Wheat Grains (Triticum estivum L.). *BASRA JOURNAL OF SCIENCE*, *41*(2), 276–310. https://doi.org/10.29072/basjs.20230206

Saleem H, Khurshid U, Sarfraz M, Tousif MI, Alamri A, Anwar S, Alamri A, Ahmad I, Abdallah HH, Mahomoodally FM , Ahemad N. A comprehensive phytochemical, biological, toxicological and molecular docking evaluation of *Suaeda fruticosa* (L.) Forssk.: An edible halophyte medicinal plant.Food Chem. Toxic. 2021 Aug;154:112348. https://doi.org/10.1016/j.fct.2021.112348.

Salim, H. A., Mahdi, M. H., Zedan, D. A., & Rosok, B. O. (2019). Insecticidal and repellent activities of five plant extracts against stored grain pest *Tribolium confusum* (Jacquelin du Val, 1868) (Coleoptera: Tenebrionidae). *Journal of Physics: Conference Series*, *1294*(9), 092034. https://doi.org/10.1088/1742-6596/1294/9/092034

Schöller, M., Prozell, S., Al-Kirshi, A.-G., & Reichmuth, Ch. (1997). Towards biological control as a major component of integrated pest management in stored product protection. *Journal of Stored Products Research*, *33*(1), 81–97. https://doi.org/10.1016/S0022-474X(96)00048-3

Sekrane, F. Z.Y., Kada, R., FatiHa, R., Boukhari, Y., & Karaca, İ. (2022). Insecticidal Activity of Medicinal Plant, Schinus molle (Anacardiaceae) on *Tribolium confusum* (Coleoptera: Tenebrionidae). *Ziraat Fakültesi Dergisi*, *17*(2), 104–109. https://doi.org/10.54975/isubuzfd.1153369

Sha, H. C., Acharya, S., Sahu, B., & Barik, T. K. (2025). *In silico* investigation of acetylcholinesterase-insecticide interactions in *Anopheles stephensi* and *Anopheles culicifacies* using molecular docking. *Journal of Vector Borne Diseases*, *62*(1), 107–111. https://doi.org/10.4103/JVBD.JVBD_96_24.

Shaikh, J. R., & Patil, M. (2020). Qualitative tests for preliminary phytochemical screening: An overview. *International Journal of Chemical Studies*, *8*(2), 603–608. https://doi.org/10.22271/chemi.2020.v8.i2i.8834.

Shewry, P. R., & Hey, S. J. (2015). The contribution of wheat to human diet and health. *Food and Energy Security*, 4(3), 178–202. https://doi.org/10.1002/fes3.64

Shrestha, P., Adhikari, S., Lamichhane, B., & Shrestha, B. G. (2015). *Phytochemical Screening of the Medicinal Plants of Nepal*. *1*(6).

Shukla, J. N., & Palli, S. R. (2012). Sex determination in beetles: Production of all male progeny by Parental RNAi knockdown of transformer. *Scientific Reports*, *2*(1), 602. https://doi.org/10.1038/srep00602

Sivakumar, T., Devanathan, S., Ganesan, P., Duraisamy, K., Marimuthu, M., Sampathrajan, V., Adhimoolam, K., & Natesan, S. (2026). Flavonoids as bio-insecticides: Harnessing plant metabolites as a biochemical shield against insects. *Plant Protection Science*. https://doi.org/10.17221/56/2025-PPS

Soliman, M. M. M., Hassanein, A. A., & Abou-Yousef, H. M. (2005). Efficiency of Various Wild Plant Extracts Against the Cotton Aphid, *Aphis gossypii* Glov. (Aphididae: Homoptera). *Acta Phytopathologica et Entomologica Hungarica*, *40*(1–2), 185–196. https://doi.org/10.1556/APhyt.40.2005.1-2.15

Soummane, H., Larhsini, M., Naamani, K., & Coll, J. (2011). Studies of Larvicidal and Adulticidal Activities of Some Halophyte Plant Extracts Against Ceratitis capitata (Wiedemann). *Journal of Entomology*, *8*(6), 548–556. https://doi.org/10.3923/je.2011.548.556

Spochacz, M., Chowański, S., Walkowiak-Nowicka, K., Szymczak, M., & Adamski, Z. (2018). Plant-Derived Substances Used Against Beetles–Pests of Stored Crops and Food–and Their Mode of Action: A Review. *Comprehensive Reviews in Food Science and Food Safety*, *17*(5), 1339–1366. https://doi.org/10.1111/1541-4337.12377

Šramková, Z., Gregová, E., & Šturdík, E. (2009). Chemical composition and nutritional quality of wheat grain. *Acta Chimica Slovaca*, *2*(1), 115–138

Sridhar, A., Ponnuchamy, M., Kumar, P. S., Kapoor, A., Vo, D.-V. N., & Prabhakar, S. (2021). Techniques and modeling of polyphenol extraction from food: A review.

Environmental Chemistry Letters, *19*(4), 3409–3443. https://doi.org/10.1007/s10311-021-01217-8

Steffan, J. R. (1978). Description et biologie des insectes. In G. Scotti (Ed.), *Les insectes et les acariens des céréales stockées* (pp. 1–62). Paris, France: AFNOR & ITFC.

Suthar, R., & Solanki, H. (2022). Phytochemical screening of halophytic plant *Suaeda fruticosa* (l.) Forssk. Ex j.f.gmel. *International Association of Biologicals and Computational Digest*, *1*(2), 308–313. https://doi.org/10.56588/iabcd.v1i2.84

Tadj, A., Achir, M., Souana. K., Abderrahim. L. A., Boussaid. M., & Taïbi, K. (2024). Evaluation of the phytochemical composition. antioxidant. anti-inflammatory and antihemolytic activities of *Atriplex halimus* L. from the region of Tiaret. Algeria. *Studies in health sciences*. *5*(4). e12637. https://doi.org/10.54022/shsv5n4-047

Taia, W. K. (2020). Wide Scene on Halophytes. *International Journal of Contemporary Research and Review*, *11*(01), 20219–20232. https://doi.org/10.15520/ijcrr.v11i01.777

Thummajitsakul. S.. Samaikam. S.. Tacha. S.. & Silprasit. K. (2020). Study on FTIR spectroscopy. total phenolic content. antioxidant activity and anti-amylase activity of extracts and different tea forms of Garcinia schomburgkiana leaves. *LWT*. *134*. 110005. https://doi.org/10.1016/j.lwt.2020.110005

Tunaz, H., & Uygun, N. (2004). *Insect growth regulators for insect pest control*. *Turkish Journal of Agriculture and Forestry*, 28(6), 377–387. https://doi.org/10.3906/tar-0312-4

Tutin, T. G., Heywood, V. H., Burges, N. A., Moore, D. M., Valentine, D. H., Walters, S. M., & Webb, D. A. (Eds.). (1976). *Flora Europaea* (Vol. 4, *Plantaginaceae to Compositae (and Rubiaceae)*). Cambridge University Press. https://doi.org/10.5281/zenodo.29376

Verma, B., Karakoti, H., Kumar, R., Mahawer, S. K., Prakash, O., Srivastava, R. M., Kumar, S., Rawat, S., Rawat, D. S., & Oliveira, M. S. D. (2023). Phytochemical Screening and Evaluation of Pesticidal Efficacy in the Oleoresins of *Globba sessiliflora* Sims and *In Silico* Study. *Evidence-Based Complementary and Alternative Medicine*, *2023*(1), 5936513. https://doi.org/10.1155/2023/5936513

VonSengbusch, P. (2003). Halophytes Botanik Online; University of Hamburg: Hamburg, Germany.

Waisel, Y. (1972). The Biology of Halophytes; Elsevier: London, UK; Academic: Cambridge, MA, USA.

Walker, D. J., Lutts, S., Sánchez-García, M., & Correal, E. (2014). *Atriplex halimus* L.: Its biology and uses. *Journal of Arid Environments*, *100–101*, 111–121. https://doi.org/10.1016/j.jaridenv.2013.09.004

Wang, L., Yu, X., Zhang, Y., Wu, Y., & Xiong, F. (2021). Development of Caryopsis and Starch Physicochemical Properties in Different Grain Positions of Wheat Spikelets. In Review. https://doi.org/10.21203/rs.3.rs-763584/v1

Wulandari, R., Astuti, L. P., & Rahardjo, B. T. (2025). Population Growth of *Tribolium confusum* (Coleoptera: Tenebrionidae) on Various Commercial and Non-commercial Flour. Agro Bali : Agricultural Journal, 8(3), 1094–1105. https://doi.org/10.37637/ab.v8i3.2401

Yensen, N.P., Biel, K.Y. (2006). Soil remediation via salt-conduction and the hypotheses of halosynthesis and photoprotection. In M. A. Khan & D. J. Weber (Eds.), *Ecophysiology of high salinity tolerant plants* (Vol. 40, pp. 313–344).

Zagoskina, N. V., Zubova, M. Y., Nechaeva, T. L., Kazantseva, V. V., Goncharuk, E. A., Katanskaya, V. M., Baranova, E. N., & Aksenova, M. A. (2023). Polyphenols in Plants: Structure, Biosynthesis, Abiotic Stress Regulation, and Practical Applications (Review). *International Journal of Molecular Sciences*, *24*(18), 13874. https://doi.org/10.3390/ijms241813874

Zaier, M. M., Heleno, S. A., Mandim, F., Calhelha, R. C., Ferreira, I. C. F. R., Achour, L., Kacem, A., Dias, M. I., & Barros, L. (2022). Effects of the seasonal variation in the phytochemical composition and bioactivities of the wild halophyte *Suaeda fruticosa*. *Food Bioscience*, *50*, 102131. https://doi.org/10.1016/j.fbio.2022.102131

Zhou, W., Li, M., & Achal, V. (2025). A comprehensive review on environmental and human health impacts of chemical pesticide usage. Emerging Contaminants, 11(1), 100410. https://doi.org/10.1016/j.emcon.2024.100410

Zhuang, W.-B., Li, Y.-H., Shu, X.-C., Pu, Y.-T., Wang, X.-J., Wang, T., & Wang, Z. (2023). The Classification, Molecular Structure and Biological Biosynthesis of Flavonoids, and

Their Roles in Biotic and Abiotic Stresses. *Molecules*, *28*(8), 3599. https://doi.org/10.3390/molecules28083599

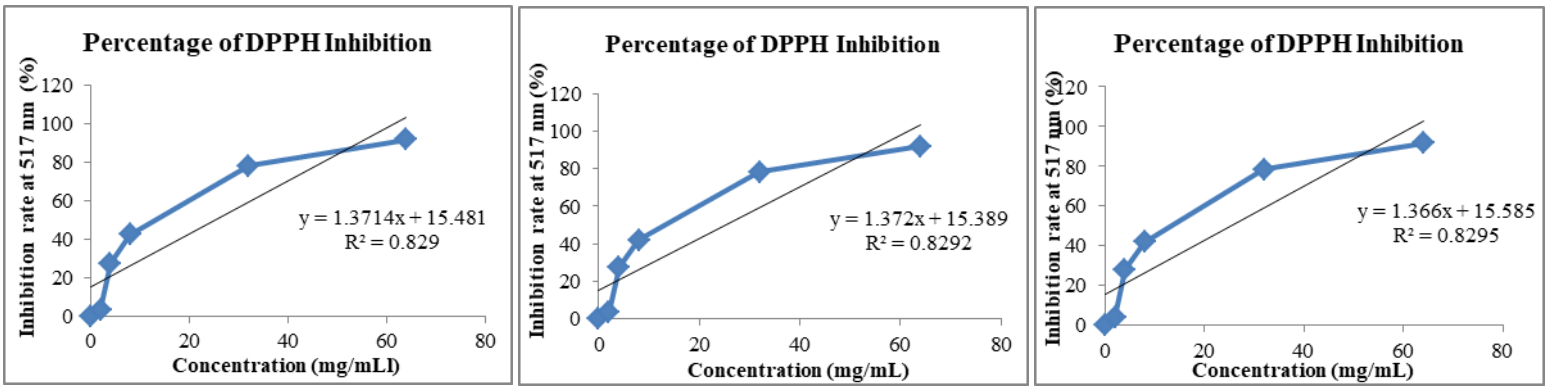
Ziaee, M., & Ganji, Z. (2016). Insecticidal efficacy of silica nanoparticles against Rhyzopertha dominica F. and *Tribolium confusum* Jacquelin du Val. *Journal of Plant Protection Research*, *56*(3), 250–256. https://doi.org/10.1515/jppr-2016-0037

Ziaee, M., & Moharramipour, S. (2013). Effectiveness of medicinal plant powders on *Sitophilus granarius* and *Tribolium confusum*. *2*.Zohry, N. M. H. (2017). Scanning electron morphological studies of Tribolium confusum Jacquelin du Val (Coleopteran: Tenebrionidae). The Journal of Basic and Applied Zoology, 78(1), 6. https://doi.org/10.1186/s41936-017-0008-0

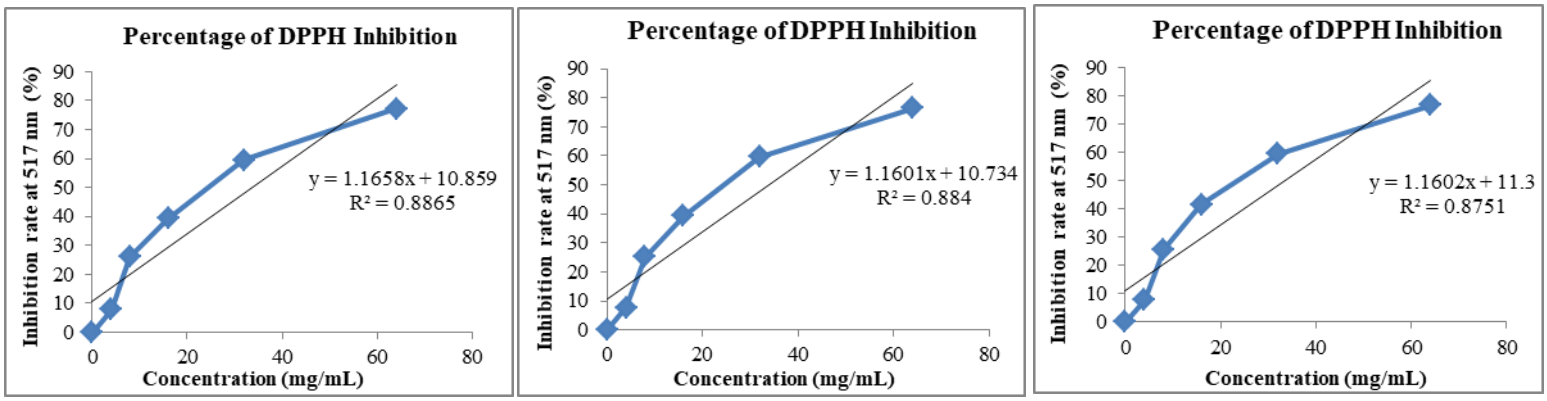
Annexes

Annexes

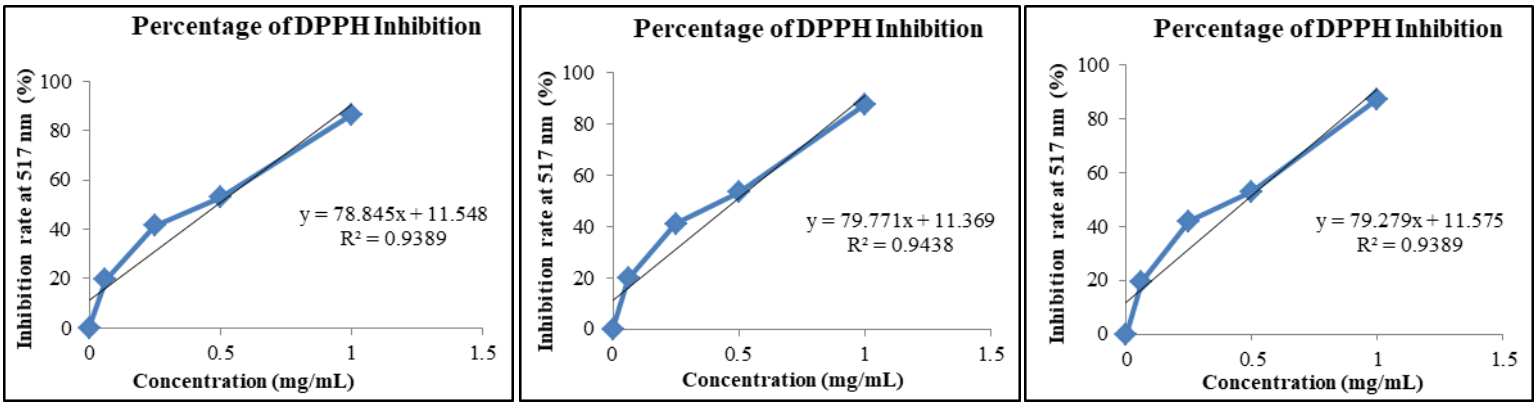
Annexe 01. DPPH radical scavenging activity of the different concentrations of plant extract and ascorbic acid



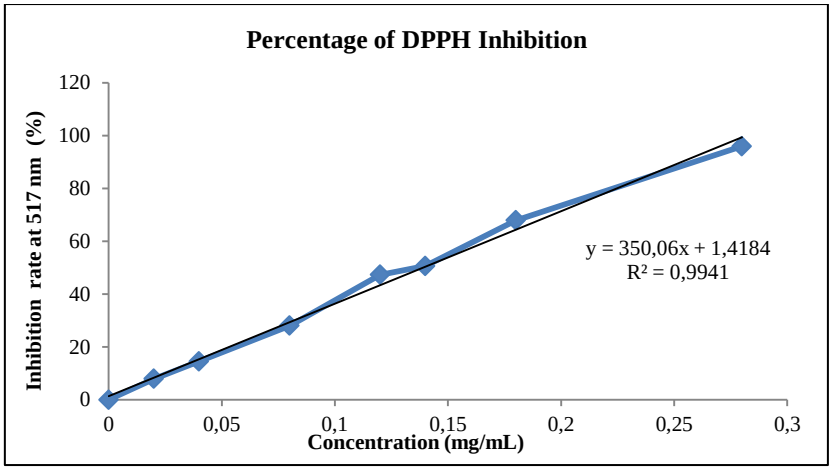
A. DPPH radical scavenging activity of the different concentrations of *A.halimus* (n=3).



B. DPPH radical scavenging activity of the different concentrations of *L.crithmoides* (n=3).

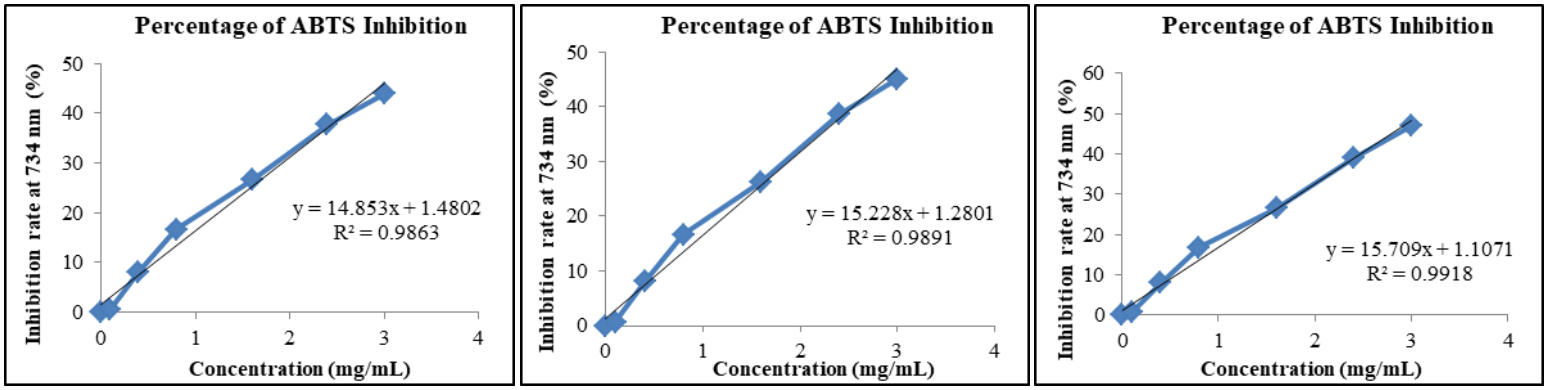


C. DPPH radical scavenging activity of the different concentrations of *S.fruticosa* (n=3).

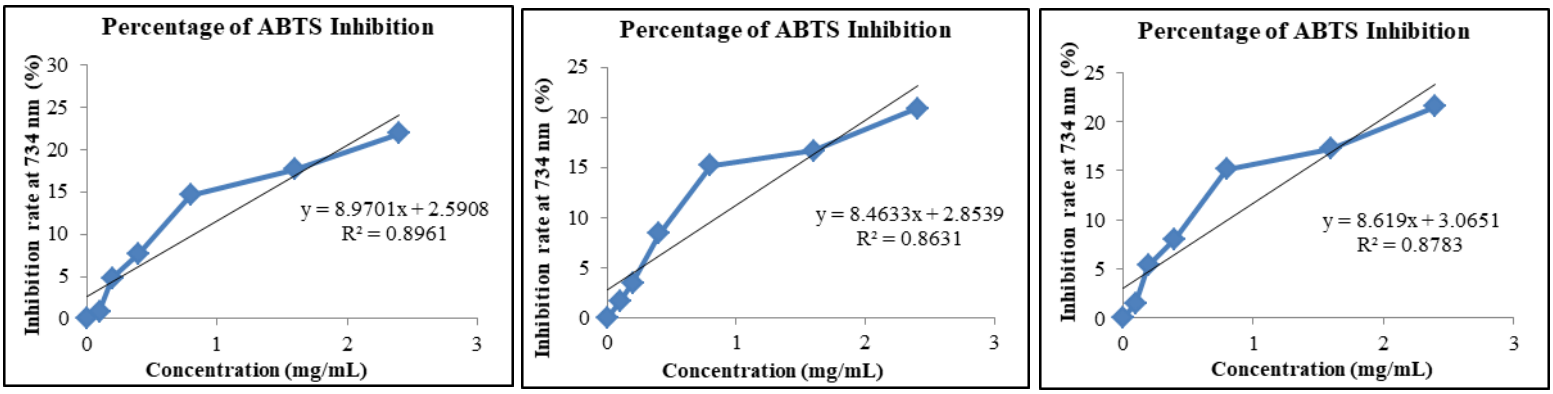


D. DPPH radical scavenging activity of the different concentrations of ascorbic acid.

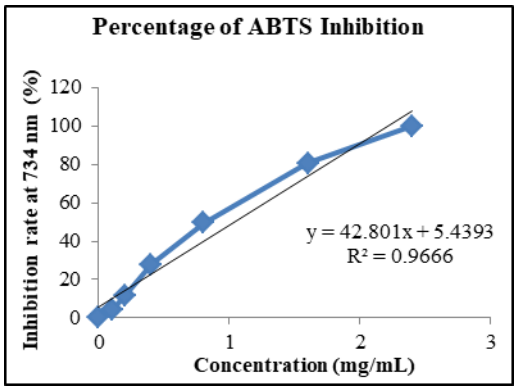
Annexe 02. ABTS radical scavenging activity of the different concentrations of plant extract and ascorbic acid

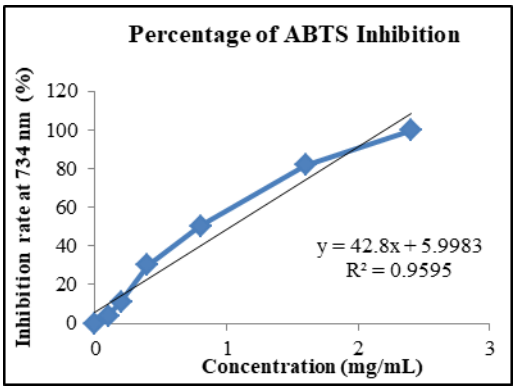


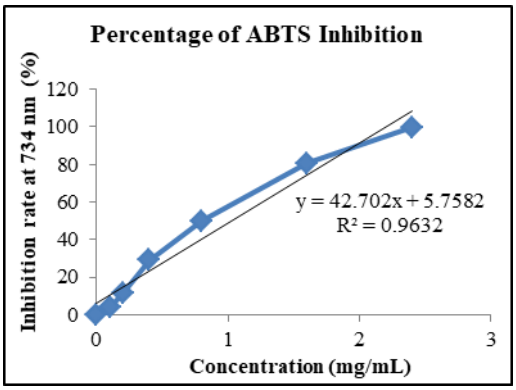
A. ABTS radical scavenging activity of the different concentrations of *A.halimus* (n=3).



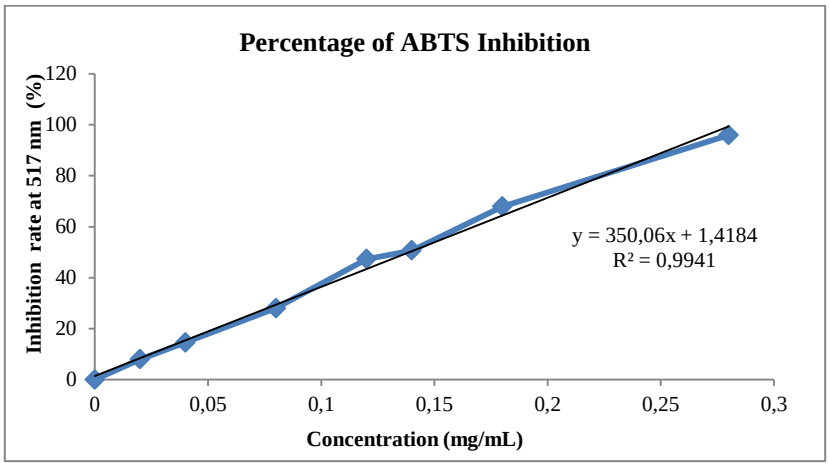
B. ABTS radical scavenging activity of the different concentrations of *L.crithmoides* (n=3).







C. ABTS radical scavenging activity of the different concentrations of *S.fruticosa* (n=3).



D. ABTS radical scavenging activity of the different concentrations of ascorbic acid

Annex 03. Communications and publications

A. National communications



Mounira TABOURI, Mustapha DJELLOULI, Khadidja BELKHEIR, Saïd NEMMICHE, Kamel BENOTMANE. Comparative study of polyphenols detection in *Artemisia herba alba* and *Suaeda vera* extracts using phytochemical screening and thin layer chromatography. 1er Séminaire National sur les enjeux de l'agriculture de demain, développement durable, autonomie alimentaire et changement climatique (EADDDAACC' 2024). L'Université Ahmed Zabana de Relizane, Algeria, 25/11/2024.



Mounira TABOURI, Mustapha DJELLOULI, Khadidja BELKHEIR, Saïd NEMMICHE, Kamel BENOTMANE. Phytochemical profile and antioxidant activity of Atriplex halimus methanolic extract. 2ème séminaire national de biodiversité, risques environnementaux et santé publique (SNBRESP 25). L'Université Chadli Bendjedid, El-Tarf, Algeria, 23 et 24 février 2025.

B. International communications



Mounira TABOURI, Mustapha DJELLOULI, Khadidja BELKHEIR, Saïd NEMMICHE, Kamel BENOTMANE. Phytochemical Screening and Thin Layer Chromatography for Qualitative identification of Phenolic Compounds in the Halophytic Plant "*Suaeda vera*". Mediterranean Conference on Environment, Risks and Health (MCERH). University of Mohamed Cherif Messaadia, Souk Ahras, Algeria, October, 15th & 16th, 2024.



Mounira TABOURI, Mustapha DJELLOULI, Khadidja BELKHEIR, Saïd NEMMICHE. Phytochemical composition and insecticidal activity of methanolic extract from two halophilic plants; *Atriplex halimus* and *Limbarda crithmoides*, Against *Tribolium confusum*. 1st International Seminar on Diversity, Valorization & Conservation of Phytodiversity (ISDVCP'25). Chlef University, Algeria, May 20th –22nd, 2025.

C. Puplication (Article): Tabouri, M., Djellouli, M., Belkheir, K., Benotmane, K., Dahoun, M., Mohammed, A. S., Nemmiche, S., Bendif, H., Alsalamah, S. A., Elfalleh, W., Boufahja, F., Moscoso-Ruiz, I., Cea-Pavez, I., Verardo, V., & Garzoli, S. (2026). Phytochemical Profile and Insecticidal Potential of Two Halophytes, *Atriplex halimus* and *Suaeda fruticosa* , Against *Tribolium confusum*: In Vitro and In Silico Approaches. *Chemistry & Biodiversity*, *23*(6), e71394. https://doi.org/10.1002/cbdv.71394

Chemistry & Biodiversity

CHEMISTRY & BIODIVERSITY

RESEARCH ARTICLE OPEN ACCESS

Phytochemical Profile and Insecticidal Potential of Two Halophytes, *Atriplex halimus* and *Suaeda fruticosa*, Against *Tribolium confusum*: In Vitro and In Silico Approaches

Mounira Tabouri[1,2] | Mustapha Djellouli[1,2] | Khadidja Belkheir[1] | Kamel Benotmane[1,2] | Meriem Dahoun[1] | Abdesselem Si Mohammed[1,2] | Saïd Nemmiche[2,3] | Hamdi Bendif[4] | Sulaiman A. Alsalamah[4] | Walid Elfalleh[4] | Fehmi Boufahja[4] | Inmaculada Moscoso-Ruiz[5] | Inés Cea-Pavez[5] | Vito Verardo[5,6] | Stefania Garzoli[7]

[1]Laboratory of Environment and Sustainable Development, Department of Biological Sciences, Faculty of Natural and Life Sciences, Ahmed Zabana University, Relizane, Algeria | [2]Laboratory of Biochemistry, Molecular Biology and Environmental Toxicology, Faculty of Medicine, Abdelhamid Ibn Badis University, Mostaganem, Algeria | [3]Department of Biological Sciences, Faculty of Natural and Life Sciences, Abdelhamid Ibn Badis University, Mostaganem, Algeria| [4]Department of Biology, College of Science, Imam Mohammad Ibn Saud Islamic University (IMSIU), Riyadh, Saudi Arabia| [5]Center For Research and Development of Functional Food (CIDAF), Granada, Spain | [6]Department of Nutrition and Food Science, University of Granada, Granada, Spain |[7]Department of Chemistry and Technologies of Drug, Sapienza University, Rome, Italy

Correspondence: Hamdi Bendif (hlbendif@imamu.edu.sa) |Stefania Garzoli (stefania.garzoli@uniroma1.it)

Received: 13 February 2026 | **Revised:** 14 May 2026 | **Accepted:** 18 May 2026

Keywords: *Atriplex halimus* | insecticidal activity | molecular docking | phytochemical profile | *Suaeda fruticosa* | *Tribolium confusum*

ABSTRACT

This study aimed to investigate the phytochemical profile and evaluate the in vitro and in silico insecticidal activities of methanolic extracts from two halophytes, *Atriplex halimus* (*A. halimus*) and *Suaeda fruticosa* (*S. fruticosa*). The investigations included phytochemical screening, determination of total phenolic, flavonoid, and tannin contents, as well as compound identification by high-performance liquid chromatography coupled with electrospray ionization quadrupole time-of-flight mass spectrometry (HPLC-ESI-QTOF-MS). The insecticidal activity was assessed through direct-contact bioassays against adults of *Tribolium confusum*. In addition, a molecular docking study was performed targeting the acetylcholinesterase enzyme (AChE). Phytochemical screening revealed the presence of several bioactive compounds in both plant extracts. *A. halimus* showed the highest flavonoid content, whereas *S. fruticosa* exhibited the highest levels of total phenolics and tannins, corresponding to superior insecticidal effect, as evidenced by its lower lethal concentration 50% (LC_{50}) value after 96 h of treatment. HPLC-ESI-QTOF-MS analysis in negative ion mode led to the identification of 24 bioactive constituents in *A. halimus* and 29 in *S. fruticosa*. The in silico study confirmed that most of the identified polyphenols exhibited binding affinity toward insect acetylcholinesterase, including kaempferol 3-O-rutinoside-7-O-glucoside, naringin, feruloyltyramine, and rutin.

1 | Introduction

In Algeria, cereal production in 2024 was estimated at approximately 4.1 million tonnes, close to the national average, reflecting the impact of uneven climatic conditions throughout the growing season [1]. Despite their economic importance, cereal crops remain highly vulnerable to numerous insect pests, which can cause substantial damage and yield losses [2]. Among the most destructive storage pests is *Tribolium confusum* (Duval) (Coleoptera: Tenebrionidae), commonly known as the confused

This is an open access article under the terms of the Creative Commons Attribution License, which permits use, distribution and reproduction in any medium, provided the original work is properly cited.
© 2026 The Author(s). *Chemistry & Biodiversity* published by Wiley-VHCA AG.